BIOELECTROCHEMICAL SYSTEMS POWERED BY CUSTOMIZABLE MICROBIAL CONSORTIA

By

Allison M. Speers

A DISSERTATION

Submitted to
Michigan State University
in partial fulfillment of the requirements
for the degree of

DOCTOR OF PHILOSOPHY

Microbiology and Molecular Genetics

2012

ABSTRACT

BIOELECTROCHEMICAL SYSTEMS POWERED BY CUSTOMIZABLE MICROBIAL CONSORTIA

By

Allison M. Speers

Bioelectrochemical systems (BESs) take advantage of the ability of organisms to catalyze electrochemical reactions for the production of electricity, biofuels and chemicals, or to perform valuable services such as wastewater treatment or the bioremediation toxic compounds. While many of these reactions occur naturally, increased reaction rates and product yields can be obtained by growing the organisms in BESs where a voltage difference between two electrodes provides additional thermodynamic impetus for the reactions by either accepting or donating electrons. Research to date has focused on the application of microbial fuel cells (MFCs) in which organisms oxidize organic matter and produce electricity, and on microbial electrolysis cells (MECs) in which a combination of organic matter oxidation and additional voltage inputs between the two electrodes catalyzes the production of H_2 for use as a biofuel. Many microorganisms have been shown to be capable of electron transfer reactions in BESs. Understanding these organisms will help to develop better-performing strains and is a major avenue of research for improving the performance of BESs.

Geobacter sulfurreducens is a dissimilatory iron-reducing bacterium that forms electrochemically active biofilms on anode electrodes of BESs and efficiently couples the oxidation of acetate to electricity production. I investigated additional electron donors for *G. sulfurreducens* current production. Formate and lactate were able to support the growth and electroactivity of *G. sulfurreducens* with electrodes as a terminal

electron acceptor, though with reduced efficiency compared with acetate. The anode biofilms grown with these substrates had different structural characteristics than those grown with acetate, which was suggestive of metabolic limitations. The addition of small amounts of acetate promoted formate carbon assimilation and improved current production, and pre-growing the biofilms with acetate enabled lactate to be oxidized as an electron donor.

Acetate, formate and lactate are often byproducts of ethanol fermentation so I sought to identify organisms capable of fermenting renewable substrates into ethanol and producing the electron donors for *G. sulfurreducens*. *Cellulomonas uda* was identified as a consolidated bioprocessing organism capable of degrading ammonia fiber expansion-pretreated corn stover. The two organisms were able to syntrophically interact, resulting in the simultaneous production of ethanol and H_2 in a MEC. Optimization of *C. uda* fermentation by nitrogen supplementation resulted in energy recoveries of ca. 56% from ethanologenesis, and the co-generation of H_2 in the MEC further increased the energy recoveries to ca. 73%.

Clostridium cellobioparum was identified as a species capable of fermenting glycerol, a major waste product of the biodiesel industry, into ethanol, 1,3-propanediol and electron donors for *G. sulfurreducens.* The two strains were improved by adaptive evolution for glycerol tolerance so growth could be sustained at 100 g/L glycerol loadings. Optimization of the coculture growth in MECs increased the consumption of glycerol to ca. 50 g/L. Decreases in pH due to the large amounts of fermentation products presented a challenge to MEC operation and opened avenues of further research for improvements of the BES configurations.

To my Mother

ACKNOWLEDGEMENTS

I would like to thank a great many friends, family and colleagues, without whom this research and my journey through graduate school would have never been possible.

First and foremost, I would like to thank Dr. Gemma Reguera for her guidance, mentorship and support to make this dissertation a reality. She was the reason I came to MSU even before I knew I would have the privilege of being a part of her lab, and she has provided me with many opportunities throughout graduate school to further my personal and professional development.

I owe a debt of gratitude to my guidance committee, Dr. Tom Schmidt, Dr. Robert Hausinger, and Dr. Bruce Dale for their advice, consultation, and guidance, and for helping to keep the projects on task and in perspective.

Thanks to all the past and present members of the Reguera lab. I especially want to thank Dena Cologgi, with whom I shared each step of the graduate school process, for her friendship, intellectual collaboration and for letting me tag along to Argonne National Lab for some of the most memorable experiences of the past six years. Thanks also to Jenna Young. I owe her a debt of gratitude for discussions about acid hydrolysis and the mysterious world of HPLC analysis. Chapter 4 of this dissertation is the result of a highly enjoyable and productive collaboration with her. I'd like to thank Becky Steidl for being a great source of information and guidance about genetics, and for making every holiday and birthday memorable with her excellent culinary skills. I would like to thank Mike Manzella for his energy, musical selection and always keeping the optimism high and the gas tanks full. I'd like to thank Sanela Lampa-Pastirk for always being

willing to explain physics, and electrochemistry concepts, slowly clearly and with a great deal of patience, and for the “Serbian Coffee” which kept me going many a long night. I would also like to thank the lab technicians Blair Bullard and Kwi Kim whose help and technical assistance throughout the early stages of this work laid the foundation for everything that came later. There would be no fuel cells or gas station without them. Kwi Kim also contributed to the research described in Appendix A. I am also grateful to Marvin Vann, Melissa Asher, Katie Boatman, Pablo Gutierez anyone who ever took a timepoint, washed a dish, or made media; the work I did would not have been possible without their help.

I am indebted to many collaborators for their intellectual contribution and technical assistance: Bryan Schindler and the Vieille Lab for letting us use and helping to troubleshoot the HPLC, Melinda Frame for teaching me how to use the Confocal Microscopes and suggesting the best way to image electrodes, Bruce Dale and Ming Lau for providing the AFEX-pretreated corn stover, Susan Leschine for providing a variety of cellulolytic strains, Kazem Kashefi for suggesting Tyndallization as the best way to sterilize reference electrodes, the Schmidt lab for guidance during my first lab rotation and use of their equipment, members of the GLBRC Hydrogenase team for advice on the microbial coculture of *Anabaena* and *Geobacter* as described in Appendix A, and Pappan Padmanab for printing every poster I ever made.

I would also like to acknowledge the following funding sources for their financial support: Michigan State’s College of Natural Science for a Marvin Hensley Endowed fellowship, a continuation fellowship and a dissertation completion fellowship, the

Michigan Economic Development Corporation, the Rackham Fund Foundation, the Great Lakes Bioenergy Research Center, and Michigan State's AgBioResearch center.

Lastly, I especially want to thank my family. I never would have made it this far without their support and sacrifices. The discussion around the dinner table when I was young made me want to be a scientist and the examples they set made it an easy dream to follow. Thanks also to Karl Hedderich for being at once my greatest source of inspiration and procrastination, and for making the time I spend out of the lab wonderful.

TABLE OF CONTENTS

LIST OF TABLES

LIST OF FIGURES

LIST OF SYMBOLS AND ABBREVIATIONS

A, acetate

AA, Allen and Arnon medium

AA/8, 8-fold dilution of Allen and Arnon medium

ACK, acetate kinase

AEM, anion exchange membrane

AFEX, ammonium fiber expansion

AFEX-CS, AFEX-pretreated corn stover

Ag/AgCl, silver/silver chloride reference electrode

ATP, adenosine triphosphate

BCA, bicinchoninic acid

BES, bioelectrochemical system

BLAST, basic local alignment search tool

BMFC, benthic microbial fuel cell

BSA, bovine serum albumin

C, cysteine

CB, cellobiose

CBP, consolidated bioprocessing

$CcelA_{10G}$, *C. cellobioparum* adapted for 10% (w/v) glycerol loading

CE, coulombic efficiency

CE, counter electrode

CEM, cation exchange membrane

CLSM, confocal laser scanning microscopy

CoA, coenzyme A

DB, Daniel Bond medium

DCMU, dichlorophenyldimethylurea

DMSO, dimethyl sulfoxide

E, voltage

E°, standard redox potential

e^{-}, electron

EAM, electrochemically active microorganism

EMF, electromotive force

EPS, exopolysaccharide

F, Faraday's constant

F, fumarate

FDH, formate dehydrogenase enzyme complex

FDH-N, nitrate-inducible formate dehydrogenase enzyme complex

FW, freshwater medium

G, glycerol

GASP, growth advantage in stationary phase

GC, gas chromatography

GO, glycolate oxidase

$GsulA_{5E}$, *G. sulfurreducens* adapted for 5% (v/v) ethanol loadings

H^{+}, proton

HEPES, 4-(2-hydroxyethyl)-1-piperazineethanesulfonic acid

HPLC, high pressure liquid chromatography

I, current

KM^{50}, kanamycin 50 μg/ml

LB, Luria-Bertani medium

LDH, lactate dehydrogenase

m, mass

MEC, microbial electrolysis cell

MFC, microbial fuel cell

MOPS, 3-(N-morpholino)propanesulfonic acid

MTT, 3-(4,5-dimethylthiazolyl-2-)2,5-diphenyltetrazolium bromide

η, energy recovery

N, nitrate

NA, numerical aperture

NB, nutrient broth medium

NTA, nitrilotriacetic acid

OCV, open circuit voltage

OD_{660}, optical density measured at 660 nm

oxt, oxygen-tolerant mutants of *G. sulfurreducens*

P, power

PBS, phosphate-buffered saline

PDH, pyruvate dehydrogenase

PFL, pyruvate formate lyase

PIPES, 1,4-piperazinediethanesulfonic acid

PMS, phenazine methosulfate

POR, pyruvate oxidoreductase

PTA, phosphotransacetylase

R, resistance

r_{CE}, maximum theoretical coulombic H_2 recovery

RE, reference electrode

SHE, standard hydrogen electrode

t, time

TBS, tris buffered saline

TCA, tricarboxylic acid

TW, terawatts

U, unit of activity

W, energy

WE, working electrode

W_E, energy recovered as ethanol

W_F, energy recovered from MFC

W_H, energy recovered as H_2 at the cathode

$W_{HA,}$ energy recovered as fermentative H_2 at the anode

W_P, energy input from potentiostat

WT, wild-type

YE, yeast extract

Chapter 1.
An introduction to bioelectrochemical systems.

THE GLOBAL ENERGY FUTURE

Energy production, water resources, and environmental degradation are three major challenges facing humanity in the 21st century (29, 42, 77). By 2050, the global population is expected to increase to approximately 9.4 billion people and the global power demand is expected to double to approximately 27 TW (42). Projections of non-renewable fuel resource supplies, though widely variable (16) suggest that oil resources will be depleted in 45-100 years (3). However, a massive transition away from the fossil-fuel dominated energy infrastructure to carbon neutral sources will be required long before fossil fuel resources are depleted if atmospheric CO_2 values are to stabilize at twice pre-industrial values (27). Targets of at least 10 TW of carbon-neutral power production by 2050 have been suggested (27). These targets may be reasonably met for electricity production, which makes up 17.2% of the global energy consumption, and 18.7% of which is already produced from renewable resources including hydro-electric, wind, and solar power (56). Transportation energy, on the other hand, makes up 27% of the energy consumption, produces 23% of global CO_2 emissions, and is expected to increase by 1.8% per year from 2005 to 2035 (3, 56). Presently only 2% of the transportation energy is derived from biofuels, primarily bioethanol and biodiesel (56).

For the past century, water use has been growing twice as fast as the population, however, 1.1 billion people in the developing world still do not have adequate access to clean water, and 2.6 billion people lack basic sanitation (77); as climate shifts occur, the availability of water resources will become increasingly uncertain. In the US, approximately 1.5% of our electricity is used for wastewater treatment at an annual cost

of $25 billion and this is expected to increase to $45 billion over the next 20 years (46). Industry will account for most of the projected increases in water usage until 2025 (77), and most of this water will need to be treated before being discharged into the environment or recycled for industrial uses. Thus, improving the water infrastructure in developing countries is an expensive and energy intensive prospect, requiring the cooperation of governments, businesses and communities. Nevertheless, it has the enormous societal benefits of improving quality of life, alleviating human health concerns, and stimulating the economy. Approximately 1.4 billion people live in river basins where the water usage exceeds water recharge rates (77), therefore, closing the loop on water resources through wastewater treatment and reuse may be the best way to reduce the strain on the dwindling natural water resources and ensure the availability of freshwater in the future.

The abundant solar energy radiation that falls on the earth is more than 3 orders of magnitude greater than global energy use, however, the ability to capture that energy depends on time, geographical location and climate (65). Plants and algae convert solar energy into sugars and oils that are potential feedstocks for transportation biofuels. A number of factors go into determining which feedstocks and biofuels are best for a given region including: the availability and fertility of land, the contribution of a given feedstock to biodiversity losses, greenhouse gas emissions and other pollutants, competition with food crops, the necessity of fossil fuel derived inputs such as pesticides, herbicides and fertilizers, the energy recovery, logistics of storage and transport, the economic value of coproducts and the economic impact on surrounding communities (3, 12). It is clear that there will not be one ideal feedstock choice as the world is a heterogeneous mixture of

resources, climates and cultures.

Because the move away from fossil fuels will affect all sectors of the energy economy, energy alternatives will need to be equally diverse and distributed, and address not only the replacement of non-renewable sources of electricity and transportation fuels but also the large chemicals industry currently based around petroleum refining (37). These energy alternatives will be increasingly decentralized as industries, especially in developing nations, look to be more self-sufficient. Biorefineries, for example, will have to specialize in processing the regional feedstocks into biofuels but also process a percentage of the feedstock into high-value chemicals to improve economic viability (79) often while also providing energy to run plant operations and attending to *in situ* wastewater recycling.

Microorganisms can degrade, produce, and transform a wide variety of chemicals and so can be used in almost every sector of the bioeconomy. Yeasts and bacteria can transform plant starches and lignocellulose into ethanol (25) and *n*-butanol (18), H_2 can be produced directly from photosynthesis or from fermentation of biomass (41), methane is a product of the anaerobic digestion of wastewater (67), and algae can be used to produce oil feedstocks for biodiesel production (75). In addition to biofuels, microbes can produce valuable chemical precursors for industry applications including succinate, lactate, acetate, citrate, 1,3-propanediol, 2,3-butanediol, and many others (38). The microbial biomass produced during many of these processes can be used as a source of protein for animal feed (59). Microbes also serve valuable roles in bioremediation of toxic compounds (15, 26) and wastewater treatment (55), and as described in more detail below, can even be a direct source of electricity production.

BIOELECTROCHEMICAL SYSTEMS

The ability of microbes to produce a current of electricity was first described approximately 100 years ago by M.C. Potter who measured electricity production in a modified galvanic cell by yeast and bacteria growing with glucose (64). However, the practical applications of this phenomenon were not appreciated until 1999 when experiments with *Shewanella oneidensis* showed that bacterial electricity production was possible without the addition of exogenous electron transfer mediators (39). Since that time, interest in microbially-mediated electricity production in devices known as microbial fuel cells (MFCs) has increased dramatically (Fig. 1.1). Furthermore, the number of electrochemical cell configurations and applications has expanded greatly to include microbial electrolysis cells (MECs) for H_2 production (43), plant-microbial and enzymatic fuel cells for power production and environmental sensing (35, 36), microbial desalination cells for water treatment (11), microbial carbon capture cells (61, 76), and microbial electrosynthesis cells for product formation or bioremediation (52, 78). The broad term bioelectrochemical system (BES) is often used to refer to these systems in which microbes, plants or enzymes catalyze electrochemical reactions (9). Due to their wide diversity of applications and carbon neutral operation, BESs can be applied at the nexus of water, energy and climate, and their potential to contribute meaningful solutions to the crisis is being widely studied.

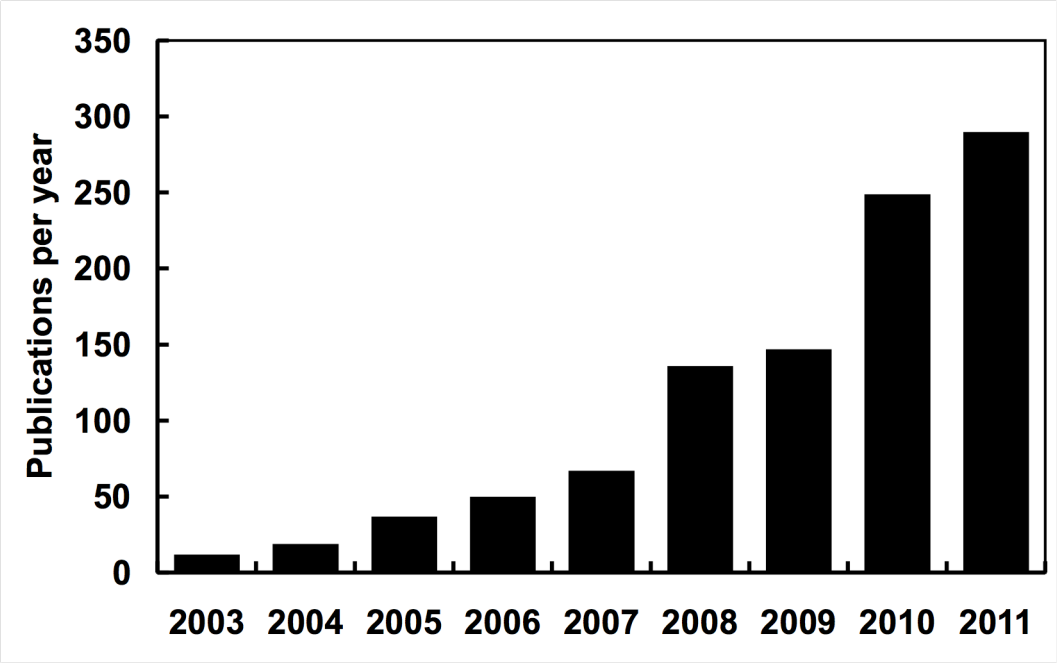

Fig. 1.1: The number of publications per year from 2003 to 2011 including the term "microbial fuel cells". From ISI Web of Knowledge database search.

The general configuration of a MFC (Fig. 1.2) consists of two chambers (anode and cathode), each containing an electrode (termed the anode and cathode electrode, respectively), and separated by a membrane that is permeable to either anions (anion exchange membrane, AEM) or cations (cation exchange membrane, CEM) (46). The anode electrode can be any conductive, non-corrosive material, but usually consists of inexpensive, high surface-area graphite or carbon. The cathode electrode is usually made of the same material as the anode but is often doped with a catalyst such as platinum. The basic principle of operation of a MFC is that microorganisms grown in the anode chamber, often as biofilms on the anode electrode, oxidize organic matter and transfer the electrons through a series of redox-active enzymes and molecules (electron

transport chain) to the anode electrode, which serves as the terminal electron acceptor for the organism. The difference in oxidation potential between the substrate and the electrode provides the thermodynamic impetus for the redox reactions, and allows the organism to produce adenosine triphosphate (ATP) as the energy source for the cell (21). The electrons (e^-) and protons (H^+) liberated during the oxidation of the organic matter travel from the anode electrode to the cathode electrode through an external circuit or through the membrane, respectively, where they are consumed by chemical reduction of an electron acceptor, generally O_2, forming either water ($O_2 + 4H^+ + 4e^- \rightarrow 2H_2O$) or hydrogen peroxide ($O_2 + 2H^+ + 2e^- \rightarrow H_2O_2$). The primary function of the membrane is to allow protons to travel from the anode to the cathode. In addition, cathodic O_2 is prevented from permeating into the anode, which would consume some of the electrons produced during respiration. The device to be powered by the MFC is placed in the external electrical circuit between the anode and cathode electrodes (Fig. 1.2). The voltage drop across the device (*E*) can be measured. By dividing *E* by the resistance of the device (*R*), the current (*I*) produced in the MFC can be determined (*I* = *E/R).* The power production (*P*) of the MFC is the useful energy provided to run the device, and is a product of the amount of electrical current flowing through the external circuit and the potential difference measured between the anode and cathode electrode (*P* = *IE*).

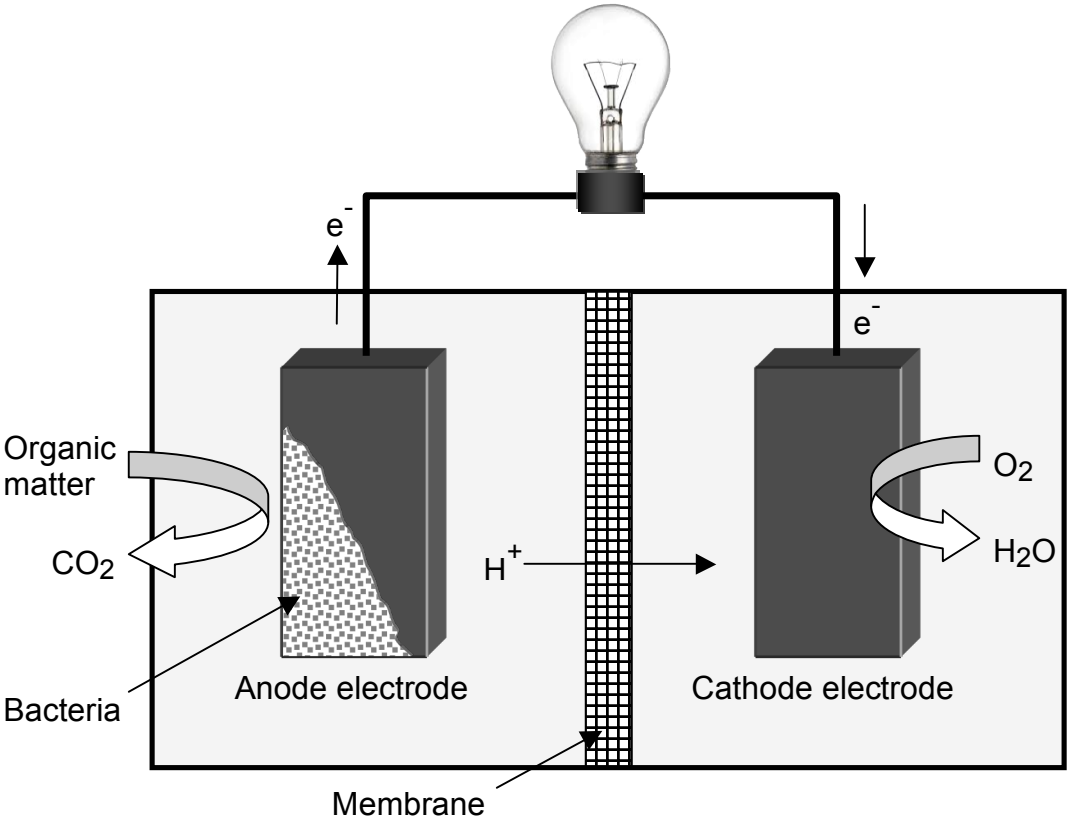

Fig. 1.2: A schematic of a 2-chamber MFC showing anode and cathode chamber separated by a membrane. A bacterial biofilm grows on the anode electrode by oxidizing organic material to CO_2. At the cathode, O_2 reacts with electrons (e^-) and protons (H^+) to form H_2O. The load being powered, shown here as a light bulb, is placed in the external electrical circuit and connected to the anode and cathode electrodes with a conductive wire. Adapted from (46).

Several parameters are often used to assess the performance of MFCs. Current is often given per surface area of the anode electrode (current density, mA/m^2), which describes the electron transfer rates from the bacteria to the electrode. Current density can be improved by increasing the amount of biomass growing on the anode, and the metabolic rate or electron transfer capabilities of the bacteria (30). Alternatively, current density can be calculated relative to the cathode surface area; in this case the current density can be improved by using an efficient catalyst at the cathode to increase the reaction rate. Power is also most often expressed with respect to the anode surface area (power density, mW/m^2). This is a measure of the capacity of the MFC architecture for power generation and is influenced by the internal resistance of the MFC (30). Increasing the ionic strength of the electrolyte, increasing the size of the membrane and permeability to ion flow, and increasing the size and conductivity of the electrodes and connections can decrease internal resistance and maximize power density (19, 60). Power can also be expressed in relation to the volume of the reactor (mW/m^3); this is the standard way to measure power production per liter of wastewater treated. Volumetric power densities have been improved by increasing the total surface area of the electrodes with respect to the volume of the reactor (47). Coulombic efficiency (CE) is the percent of the electrons available in the substrate are transferred to the anode electrode and recovered as electricity (46). The CE will generally be lower if the bacteria in the anode are actively growing and storing some of the electrons in cell biomass, or if the electrons are diverted to alternative electron acceptors such as any cathodic O_2 permeating into the anode.

The voltage of the MFC is a representation of the electrochemical potential energy between the two electrodes. The theoretical maximum voltage, or electromotive force (EMF) is determined by the thermodynamics of the reduction and oxidation reactions in the anode and cathode electrodes and is affected by the concentration of the reactants and products, pH, and temperature (46). The maximum theoretical voltage of a MFC is approximately 1.2 V where organic matter is oxidized at the anode and O_2 is reduced at the cathode (51), however, the typical working voltage is closer to 0.3-0.7 V due to energy losses (46). For example, the standard reduction potential of O_2 at atmospheric concentrations (pO_2 = 0.2) and neutral pH (pH = 7) is 0.805 V vs. a standard H_2 electrode (SHE), however, the measured potential of a cathode with O_2 as the oxidant is closer to 0.2 V, resulting in an energy loss (or overpotential) that is 0.605 V (50). This energy loss is due to the high energy of activation of the reaction. For this reason, efficient catalysts such as platinum are often required as cathode electrodes. Other cathode configurations and catholytes are commonly used to decrease this energy loss (Table 1.1). In some cases, especially in MFCs used for wastewater treatment, a biocathode is used in place of the catalyst. In this case the wastewater usually flows first into the anode where most of the organic matter is removed and then, into the cathode (32). The native microbes capable of accepting electrons colonize the cathode electrode and subsequently catalyze the reduction of dissolved O_2 (83). Air cathodes are sometimes used in which the cathode is exposed to the air on one side and connected to the anode chamber on the other, thus eliminating the need to sparge the cathode chamber with air. This is beneficial because the partial pressure of O_2 in

the air is much higher than the concentration of dissolved O_2 in water, although a catalyst is still needed on the cathode (44). Alternatively, the catholyte can be a strong chemical oxidizer such as ferricyanide or permanganate (66, 81). These chemicals provide a lower theoretical EMF to the MFC compared to O_2, but, in practice, perform better than O_2 because of the lower energy of activation of the reaction (50). The overpotentials are low enough that catalysts are no longer required, and power outputs from the MFC are greatly increased (46, 66). However, as the oxidizers need to be chemically regenerated, they are not practical for scaled up applications (46). Finally, just as with traditional H_2 fuel cells (working voltage ~0.7 V), MFCs can be stacked together and connected in series, to produce sufficient voltage to power a device (46).

Table 1.1: Common materials and configurations used in MFC and MECs.

	Cathode	Catholyte	Configuration	Inputs	Outputs	Anode
MFC	Catalyst (e.g. platinum)	O_2	Two-chamber or air cathode	Organic matter	Electricity	Conductive, noncorrosive, high surface area (e.g carbon or graphite)
	Carbon or graphite	Ferricyanide, Permanganate	Two-chamber			
	Carbon or graphite with biocathode	O_2	Two-chamber			
MEC	Carbon or graphite with or without catalyst, or biocathode	H^+	One- or two-chamber	Organic matter, electricity	H_2	

Optimization of the materials and cell configurations of MFCs has resulted in the performance of these systems increasing five to six orders-of-magnitude in the past decade (47), reaching power densities of 1,010 mW/m^3 (20) or 6,860 mW/m^2 (anode surface area) (19). For the most part, the highest power densities have been achieved in small, bench-scale MFC devices less than a few liters in volume and only a few large-scale MFCs have been tested. In scaled-up reactors, cost minimization becomes extremely important. Many larger MFCs (> 1 L) do not use a membrane between the anode and cathode, using inexpensive separators such as cloth instead (47). Cost reductions can also be achieved through the use of anode materials such as carbon mesh, which is 20-100 times less expensive than carbon cloth or felt (47). The use of air cathodes also reduces operational costs (44). Progress has also been made in the development of non-precious metal catalysts (1, 13, 54) or air cathodes with activated carbon (22, 71, 82). Lastly, the anode and cathode electrodes are typically spaced close together and the ratio of the anode surface area to the reactor volume is maximized to decrease diffusion distances between the two electrodes (33, 84).

Two pilot scale MFCs have been started for wastewater treatment, one at the Foster's brewery in Queensland, Australia, by a group of researchers at the University of Queensland, and the other in the U.S. by University of Connecticut researchers (47). Unfortunately, few data have been made publicly available so the performance of these MFCs is not known. A startup company, Emefcy Bioenergy Systems, has publicized plans to commercialize MFC technology for low-strength wastewater treatment from the food, drink, pharmaceutical and chemical industries (www.emefcy.com). Logan (2005) estimated that a town of 100,000 people producing 16.4 billion gallons of wastewater

annually could result in theoretical electricity recoveries from wastewater as high as 2.3 MW (48). When the amount of power produced by the MFC was set at a practical value of 1 W/m^2, estimates of electricity production decreased to 0.5 MW, which is enough electricity to power approximately 330 homes (not including heating costs), and could be sold for the equivalent of US $1 million per year (48).

Another pilot scale MFC strategy that has been successfully implemented is called a Benthic MFC (BMFC), which is deployed in seawater (73, 74). The anode electrode is buried in the anoxic sediment and the cathode remains in the overlying oxygenated water. The electrodes are colonized by the natural microflora and the substrate is the organic matter naturally present in the sediment, generally detritus from phytoplankton. Because a biofilm naturally grows on the cathode electrode that catalyzes the reduction of O_2, BMFCs do not require precious metal catalysts. These types of MFCs have been reported to produce approximately 28 mW/m^2 at 0.27 V for over a year and without decreases in performance (74). More recently, BMFCs with improved design and deployment were reportedly able to power a meteorological buoy that was measuring air and water temperature, atmospheric pressure, and humidity (73). Similarly, a BMFC was used to monitor the movements of acoustically-tagged green sea turtles in San Diego Bay, CA (73). Other promising reports of this technology have been reported elsewhere (2, 23, 58).

Despite these rapid achievements in the past years, challenges still remain that limit the application of MFC to wide scale electricity production. A MFC for use in wastewater treatment, for example, would need to have a reactor volume of hundreds of

cubic meters and the costs of electrode materials are still prohibitively high at this scale (50). In general, the cathodic reaction is the rate-limiting step that reduces the performance of the MFC (46). Oxygen is generally the preferred oxidant at the cathode because it is freely available, but the overpotentials, slow reaction rate, and the need for catalysts, decrease fuel cell performance and increase the cost (50). Additionally, the high power densities observed with small electrode surface areas cannot be assumed to scale linearly as the anode size is increased, so the electrodes used in practical applications will have to be larger than the power density of lab-scale MFCs would suggest (17). The internal resistance of the MFC is high which also limits power production (19, 60). MECs, which do not produce power and therefore are not subject to the same limitations, have been investigated as viable alternatives to MFCs (Table 1.1).

As MECs are designed for the production of H_2 at the cathode, rather than electricity production, they are not subjected to the same limitations as MFCs and have thus been investigated as viable alternatives to MFCs (Table 1.1). H_2 production in a MEC is also advantageous over H_2 production from traditional microbial fermentation because theoretical H_2 yields are higher for respiration than fermentation. For example, the stoichiometric production of H_2 from the complete oxidation of glucose to CO_2 is 12 mol/mol glucose, whereas H_2 production from glucose fermented to acetate results in a maximum of 4 mol H_2/mol glucose (43). The potential required to produce H_2 at the cathode is -0.414 V (at a pH of 7). If acetate, for example, is used as the substrate in the anode (-0.3 V), the EMF (i.e. potential difference) between the anode and cathode

electrodes is -0.114 V. The negative value for the EMF suggests that the reaction is not spontaneous, so a theoretical cell voltage greater than 0.114 V must be added to MEC from an external power supply and oxygen must be eliminated from the cathode chamber (46). Due to overpotentials at the cathode, the amount of additional voltage needed in practice is approximately 0.25 V (46). While this is an endothermic process, requiring the input of energy, the cell voltage required is much lower than that of electrolysis from water (1.8-2.0 V) because the anode bacteria act as catalysts to degrade organic matter into protons and electrons, which is a thermodynamically favorable process with an adequate electron acceptor (46).

The additional voltage can be applied to the system by either a DC power source or by using a potentiostat to set the voltage of the anode electrode with respect to a reference electrode placed into the anode chamber (57). In the case of the DC power source, the potential of the anode electrode will vary depending on the oxidation potential of the substrate, substrate concentration, the applied voltage, and the microbe(s) used (57). When a potentiostat is used, the anode potential remains constant and the cathode potential varies to overcome the overpotentials needed to sustain the current at the anode (57). The more positive the anode potential, the more energy is theoretically available for the bacteria. In fact, poising the potential of the anode electrode of a BMFC during the initial phase of deployment decreased the startup time required for microbes to colonize the electrode (23). The use of a potentiostat also allows for more control over the anode potential, and therefore the metabolism of the bacteria, which increases the reproducibility of experiments. For these reasons, most of the experiments described in this dissertation were performed

under potentiostatic control and a voltage of 0.24 V vs. an Ag/AgCl reference electrode was used (Fig. 1.3).

The components and design of a MEC can be similar to that of MFCs (Table 1.1). The anode electrode is generally made of carbon or graphite and the cathode can be graphite or carbon usually impregnated with an inorganic catalyst or a biocatalyst (46, 49). Often, methanogenic organisms can dominate the biocathode and the production of methane is observed in addition to H_2 (14). Because O_2 is not required at the cathode, the electrodes can be separated into two chambers using a membrane or they can be combined into a single chamber. One problem associated with single chambered MECs is that the H_2 produced at the cathode can easily reach the anode electrode and be used as an electron donor by the anode biofilm, thereby artificially increasing the measured CE of the system. To prevent this, most of the research described in this dissertation was carried out in two-chambered MECs (depicted in Fig. 1.3). A Nafion membrane was used to separate the two chambers, and the anode and cathode electrodes were 12 cm^2 graphite rods. Both chambers were continually sparged with sterile anaerobic gasses to maintain anaerobiosis. The MEC setup was chosen because it was easy to set up, could be easily sterilized in an autoclave (except the reference electrodes), and 4 MEC experiments could be run simultaneously using the same potentiostat. More details about the operation of the MECs are provided in Chapter 1.

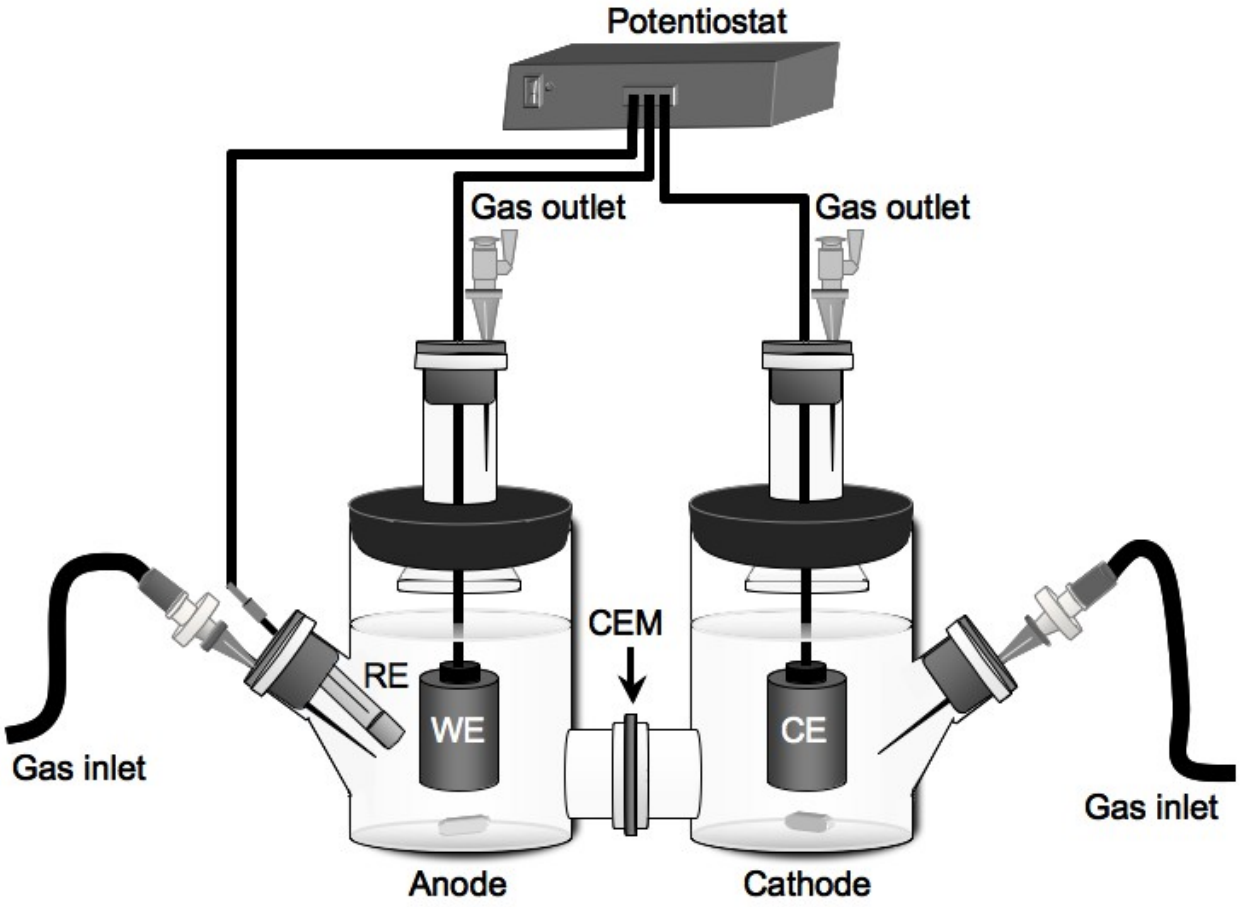

Fig. 1.3: Schematic of the MEC reactor used for most of the research described in this dissertation. A potentiostat was used to apply a voltage across the cell that was sufficient to produce H_2 at the cathode (counter electrode, CE). The potential of the anode electrode (working electrode, WE) was set to 0.24 V vs an Ag/AgCl reference electrode (RE) that was placed in the anode chamber. A Nafion cation exchange membrane (CEM) was used to separate the two chambers. Both chambers were sparged with sterile anaerobic gasses (N_2 or N_2:CO_2 [80:20]), to maintain anaerobiosis.

ELECTROCHEMICALLY ACTIVE MICROORGANISMS

Electrochemically active microorganisms (EAMs) are the microbes that catalyze the electrochemical reactions in BESs (7). These organisms can be present on the anode or cathode electrode, either donating or accepting electrons, respectively. The organisms can grow planktonically or as electroactive biofilms, and they can be either a monoculture of one species or a mixed species community, sometimes including organisms that are not electrically active (7). Planktonic organisms can transfer electrons to the electrode using soluble electron carrier molecules called mediators. Some organisms such as *Pseudomonas* spp. (63) and *Shewanella* spp. (53) make their own mediators, while others such as *Proteus vulgaris* (40), *Clostridium cellulolyticum* (72), *Escherichia coli* and *Actinobacillus succinogenes* (62), require the addition of exogenous mediators. By contrast, some organisms can grow as electro-active biofilms on the electrode and can transfer electrons across the biofilm thickness and to the electrode interface using outer membrane cytochromes (8) or conductive appendages (i.e. pili nanowires) (68), or by mediators released into the extracellular matrix (7).

Geobacter sulfurreducens and *Shewanella oneidensis* are two of the most commonly studied bacteria that produce electricity in MFCs. *G. sulfurreducens* is a dissimilatory iron-reducing bacterium (10) that forms thick multi-layered biofilms on the anode electrode (69). They cannot produce electricity when growing planktonically, instead requiring direct contact with the electrode surface (5). They transfer electrons by means of cytochromes and conductive pili (6, 68). *S. oneidensis*, on the other hand, is a facultative anaerobe that can grow either planktonically, transferring electrons by means

of secreted flavins as endogenous mediators (53), or as biofilms through direct contact with the electrode by means of cytochromes (24).

Wastewater treatment MFC applications often result in the anode, and often the cathode, electrode being colonized by a diverse community of native microorganisms. Genetic characterization of the anode community enriched from sludge often identifies members of the *Bacteroidetes* class and members of the δ-Proteobacteria including *Geobacter*-like species (34). Other species are also detected, including fermentative organisms, and sulfate- and nitrate-reducing organisms, which are often not electrically active and therefore tend to decrease the performance of the MFC (7). Molecular analysis of the anode community in BMFCs showed great variability as a function of the sediment source (4, 70), though δ-Proteobacteria especially from the family Geobacteraceae are often enriched (28). The genus *Desulfuromonas* within the *Geobacteraceae* family are abundant in saltwater BMFCs, whereas freshwater BMFCs are often enriched in fresh water representatives of the family such as the genera *Geobacter* and *Pelobacter* as well as the acidobacterial genus *Geothrix* (28). Furthermore, the family Desulfobulbaceae dominated the BMFC community from estuarine sediments (28).

In general, one of the most important parameters affecting MFCs performance is the source of inoculum and the type of microorganism (e.g. Gram-positive or negative) (7). MFCs powered by mixed communities generated from a diverse inoculum such as wastewater or sludge tend to perform better than those powered by single species (45). For example, the per-biomass rate of electron transfer was lower for a pure culture of *G. sulfurreducens* [178 μmol electron (g protein)$^{-1}$ min^{-1}] than for a mixed community

containing *Geobacter*-like strains [374 μmol electron (g protein)$^{-1}$ min^{-1}] (30, 31). Despite this, the increase of *Geobacter*-like strains from 32%-70% of the anode biofilm community correlated well with increases in the current generation of MFCs from 0.12 mA/cm^2 to 1.12 mA/cm^2 (30), suggesting that a balance exists between the number of high-current-producing organisms and community diversity. Gram-negative organisms such as *G. sulfurreducens* produce more current on average than Gram-positive organisms; however, mixing the two results in better performance still (7). One of the challenges to using mixed species communities in BESs is that strain improvements through genetic manipulation are difficult. Identifying single species capable of high current production is therefore important for future work. *G. sulfurreducens* remains one of the best performing species in BESs in pure culture and has become a model organism for understanding electron transport in electronically active biofilms. For example, adaptive evolution of *G. sulfurreducens* over a period of approximately 5 months in the presence of a poised anode electrode resulted in a strain that produced significantly more current than the wild-type strain (80). For these reasons, *G. sulfurreducens* was selected as the organism of choice for the research presented in this dissertation.

REFERENCES

REFERENCES

1. **Ahmed, J., Y. Yuan, L. H. Zhou, and S. Kim.** 2012. Carbon supported cobalt oxide nanoparticles-iron phthalocyanine as alternative cathode catalyst for oxygen reduction in microbial fuel cells. J. Power Sources **208:**170-175.

2. **An, J., H. Moon, and I. S. Chang.** 2010. Multiphase electrode microbial fuel cell system that simultaneously converts organics coexisting in water and sediment phases into electricity. Environ. Sci. Technol. **44:**7145-7150.

3. **Atabani, A. E., A. S. Silitonga, I. A. Badruddin, T. M. I. Mahlia, H. H. Masjuki, and S. Mekhilef.** 2012. A comprehensive review on biodiesel as an alternative energy resource and its characteristics. Renew. Sust. Energ. Rev. **16:**2070-2093.

4. **Bond, D. R., D. E. Holmes, L. M. Tender, and D. R. Lovley.** 2002. Electrode-reducing microorganisms that harvest energy from marine sediments. Science **295:**483-485.

5. **Bond, D. R., and D. R. Lovley.** 2003. Electricity production by *Geobacter sulfurreducens* attached to electrodes. Appl. Environ. Microbiol. **69:**1548-55.

6. **Bond, D. R., S. M. Strycharz-Glaven, L. M. Tender, and C. I. Torres.** 2012. On electron transport through *Geobacter* biofilms. ChemSusChem **5:**1099-1105.

7. **Borole, A. P., G. Reguera, B. Ringeisen, Z.-W. Wang, Y. Feng, and B. H. Kim.** 2011. Electroactive biofilms: Current status and future research needs. Energy Environ. Sci. **4**:4813-4834

8. **Bouhenni, R. A., G. J. Vora, J. C. Biffinger, S. Shirodkar, K. Brockman, R. Ray, P. Wu, B. J. Johnson, E. M. Biddle, M. J. Marshall, L. A. Fitzgerald, B. J. Little, J. K. Fredrickson, A. S. Beliaev, B. R. Ringeisen, and D. A. Saffarini.** 2010. The role of *Shewanella oneidensis* MR-1 outer surface structures in extracellular electron transfer. Electroanalysis **22:**856-864.

9. **Bullen, R. A., T. C. Arnot, J. B. Lakeman, and F. C. Walsh.** 2006. Biofuel cells and their development. Biosens. Bioelectron. **21:**2015-2045.

10. **Caccavo, F., Jr., D. J. Lonergan, D. R. Lovley, M. Davis, J. F. Stolz, and M. J. McInerney.** 1994. *Geobacter sulfurreducens* sp. nov., a hydrogen- and acetate-oxidizing dissimilatory metal-reducing microorganism. Appl. Environ. Microbiol. **60:**3752-9.

11. **Cao, X. X., X. Huang, P. Liang, K. Xiao, Y. J. Zhou, X. Y. Zhang, and B. E. Logan.** 2009. A new method for water desalination using microbial desalination cells. Environ. Sci. Technol. **43:**7148-7152.

12. **Carolan, J. E., S. V. Joshi, and B. E. Dale.** 2007. Technical and financial feasibility analysis of distributed bioprocessing using regional biomass pre-processing centers. JAFIO **5:**1-27.

13. **Chen, Y. F., Z. S. Lv, J. M. Xu, D. Q. Peng, Y. X. Liu, J. X. Chen, X. B. Sun, C. H. Feng, and C. H. Wei.** 2012. Stainless steel mesh coated with MnO_2/carbon nanotube and polymethylphenyl siloxane as low-cost and high-performance microbial fuel cell cathode materials. J. Power Sources **201:**136-141.

14. **Cheng, S., D. Xing, D. F. Call, and B. E. Logan.** 2009. Direct biological conversion of electrical current into methane by electromethanogenesis. Environ. Sci. Technol. **43:**3953-3958.

15. **Cologgi, D. L., S. Lampa-Pastirk, A. M. Speers, S. D. Kelly, and G. Reguera.** 2011. Extracellular reduction of uranium via *Geobacter* conductive pili as a protective cellular mechanism. Proc. Natl. Acad. Sci. USA **108:**15248-52.

16. **Dale, M.** 2012. Meta-analysis of non-renewable energy resource estimates. Energy Policy **43:**102-122.

17. **Dewan, A., H. Beyenal, and Z. Lewandowski.** 2008. Scaling up microbial fuel cells. Environ. Sci. Technol. **42:**7643-7648.

18. **Ezeji, T. C., N. Qureshi, and H. P. Blaschek.** 2007. Bioproduction of butanol from biomass: from genes to bioreactors. Curr. Op. Biotechnol. **18:**220-227.

19. **Fan, Y., E. Sharbrough, and H. Liu.** 2008. Quantification of the internal resistance distribution of microbial fuel cells. Environ. Sci. Technol. **42:**8101-8107.

20. **Fan, Y. Z., H. Q. Hu, and H. Liu.** 2007. Enhanced coulombic efficiency and power density of air-cathode microbial fuel cells with an improved cell configuration. J. Power Sources **171:**348-354.

21. **Finkelstein, D. A., L. M. Tender, and J. G. Zeikus.** 2006. Effect of electrode potential on electrode-reducing microbiota. Environ. Sci. Technol. **40:**6990-6995.

22. **Ghasemi, M., S. Shahgaldi, M. Ismail, B. H. Kim, Z. Yaakob, and W. R. W. Daud.** 2011. Activated carbon nanofibers as an alternative cathode catalyst to platinum in a two-chamber microbial fuel cell. Int. J. Hydrogen Energy **36:**13746-13752.

23. **Gong, Y. M., S. E. Radachowsky, M. Wolf, M. E. Nielsen, P. R. Girguis, and C. E. Reimers.** 2011. Benthic microbial fuel cell as direct power source for an acoustic modem and seawater oxygen/temperature sensor system. Environ. Sci. Technol. **45:**5047-5053.

24. **Gorby, Y. A., S. Yanina, J. S. McLean, K. M. Rosso, D. Moyles, A. Dohnalkova, T. J. Beveridge, I. S. Chang, B. H. Kim, K. S. Kim, D. E. Culley, S. B. Reed, M. F. Romine, D. A. Saffarini, E. A. Hill, L. Shi, D. A. Elias, D. W. Kennedy, G. Pinchuk, K. Watanabe, S. i. Ishii, B. Logan, K. H. Nealson, and J. K. Fredrickson.** 2006. Electrically conductive bacterial nanowires produced by *Shewanella oneidensis* strain MR-1 and other microorganisms. Proc. Natl. Acad. Sci. USA **103:**11358-11363.

25. **Gray, K. A., L. Zhao, and M. Empage.** 2006. Bioethanol. Curr. Opin. Chem. Biol. **10:**141-146.

26. **Guimaraes, B. C. M., J. B. A. Arends, D. van der Ha, T. Van de Wiele, N. Boon, and W. Verstraete.** 2010. Microbial services and their management: Recent progresses in soil bioremediation technology. Appl. Soil Ecol. **46:**157-167.

27. **Hoffert, M. I., K. Caldeira, A. K. Jain, E. F. Haites, L. D. D. Harvey, S. D. Potter, M. E. Schlesinger, S. H. Schneider, R. G. Watts, T. M. L. Wigley, and D. J. Wuebbles.** 1998. Energy implications of future stabilization of atmospheric CO_2 content. Nature **395:**881-884.

28. **Holmes, D. E., D. R. Bond, R. A. O'Neill, C. E. Reimers, L. R. Tender, and D. R. Lovley.** 2004. Microbial communities associated with electrodes harvesting electricity from a variety of aquatic sediments. Microbial Ecol. **48:**178-190.

29. **Intergovernmental Panel on Climate Change.** 2001. Climate Change 2001: Synthesis report, summary for policymakers. IGPCC.

30. **Ishii, S., B. E. Logan, and Y. Sekiguchi.** 2012. Enhanced electrode-reducing rate during the enrichment process in an air-cathode microbial fuel cell. Appl. Microbiol. Biotechnol. **94:**1087-94.

31. **Ishii, S., K. Watanabe, S. Yabuki, B. E. Logan, and Y. Sekiguchi.** 2008. Comparison of electrode reduction activities of *Geobacter sulfurreducens* and an enriched consortium in an air-cathode microbial fuel cell. Appl. Environ. Microbiol. **74:**7348-55.

32. **Jang, J. K., T. H. Pham, I. S. Chang, K. H. Kang, H. Moon, K. S. Cho, and B. H. Kim.** 2004. Construction and operation of a novel mediator- and membrane-less microbial fuel cell. Process Biochem. **39:**1007-1012.

33. **Jiang, D. Q., X. A. Li, D. Raymond, J. Mooradain, and B. K. Li.** 2010. Power recovery with multi-anode/cathode microbial fuel cells suitable for future large-scale applications. Int. J. Hydrogen Energy **35:**8683-8689.

34. **Jung, S., and J. M. Regan.** 2007. Comparison of anode bacterial communities and performance in microbial fuel cells with different electron donors. Appl. Microbiol. Biotechnol. **77:**393-402.

35. **Kakehi, N., T. Yamazaki, W. Tsugawa, and K. Sode.** 2007. A novel wireless glucose sensor employing direct electron transfer principle based enzyme fuel cell. Biosens. Bioelectron. **22:**2250-2255.

36. **Kaku, N., N. Yonezawa, Y. Kodama, and K. Watanabe.** 2008. Plant/microbe cooperation for electricity generation in a rice paddy field. Appl. Microbiol. Biotechnol. **79:**43-49.

37. **Kamm, B., and M. Kamm.** 2007. Biorefineries - Multi product processes, p. 175-204. *In* R. Ulber and D. Sell (ed.), White Biotechnology, vol. 105.

38. **Kamm, B., and M. Kamm.** 2004. Principles of biorefineries. Appl. Microbiol. Biotechnol. **64:**137-145.

39. **Kim, B. H., T. Ikeda, H. S. Park, H. J. Kim, M. S. Hyun, K. Kano, K. Takagi, and H. Tatsumi.** 1999. Electrochemical activity of an Fe(III)-reducing bacterium, *Shewanella putrefaciens* IR-1, in the presence of alternative electron acceptors. Biotechnol. Tech. **13:**475-478.

40. **Kim, N., Y. Choi, S. Jung, and S. Kim.** 2000. Effect of initial carbon sources on the performance of microbial fuel cells containing *Proteus vulgaris*. Biotechnol. Bioeng. **70:**109-114.

41. **Lee, H. S., W. F. J. Vermaas, and B. E. Rittmann.** 2010. Biological hydrogen production: prospects and challenges. Trends Biotechnol. **28:**262-271.

42. **Lewis, N. S., and D. G. Nocera.** 2006. Powering the planet: Chemical challenges in solar energy utilization. Proc. Natl. Acad. Sci. USA **103:**15729-15735.

43. **Liu, H., S. Grot, and B. E. Logan.** 2005. Electrochemically assisted microbial production of hydrogen from acetate. Environ. Sci. Technol. **39:**4317-4320.

44. **Liu, H., R. Ramnarayanan, and B. E. Logan.** 2004. Production of electricity during wastewater treatment using a single chamber microbial fuel cell. Environ. Sci. Technol. **38:**2281-2285.

45. **Logan, B. E.** 2009. Exoelectrogenic bacteria that power microbial fuel cells. Nat. Rev. Microbiol. **7:**375-381.

46. **Logan, B. E.** 2008. Microbial fuel cells. Wiley-Interscience, Hoboken, N.J.

47. **Logan, B. E.** 2010. Scaling up microbial fuel cells and other bioelectrochemical systems. Appl. Microbiol. Biotechnol. **85:**1665-71.

48. **Logan, B. E.** 2005. Simultaneous wastewater treatment and biological electricity generation. Water Sci. Technol. **52:**31-37.

49. **Logan, B. E., D. Call, S. Cheng, H. V. M. Hamelers, T. Sleutels, A. W. Jeremiasse, and R. A. Rozendal.** 2008. Microbial electrolysis cells for high yield hydrogen gas production from organic matter. Environ. Sci. Technol. **42:**8630-8640.

50. **Logan, B. E., B. Hamelers, R. Rozendal, U. Schroder, J. Keller, S. Freguia, P. Aelterman, W. Verstraete, and K. Rabaey.** 2006. Microbial fuel cells: methodology and technology. Environ. Sci. Technol. **40:**5181-92.

51. **Logan, B. E., and J. M. Regan.** 2006. Microbial fuel cells - challenges and applications. Environ. Sci. & Technol. **40:**5172-5180.

52. **Lovley, D. R., and K. P. Nevin.** 2011. A shift in the current: New applications and concepts for microbe-electrode electron exchange. Curr. Opin. Biotechnol. **22:**441-448.

53. **Marsili, E., D. B. Baron, I. D. Shikhare, D. Coursolle, J. A. Gralnick, and D. R. Bond.** 2008. *Shewanella* secretes flavins that mediate extracellular electron transfer. Proc. Natl. Acad. Sci. USA **105:**3968-3973.

54. **Martin, E., B. Tartakovsky, and O. Savadogo.** 2011. Cathode materials evaluation in microbial fuel cells: A comparison of carbon, Mn_2O_3, Fe_2O_3 and platinum materials. Electrochimica Acta **58:**58-66.

55. **Maszenan, A. M., Y. Liu, and W. J. Ng.** 2011. Bioremediation of wastewaters with recalcitrant organic compounds and metals by aerobic granules. Biotechnol. Adv. **29:**111-123.

56. **Murphy, J. D., and T. Thamsiriroj.** 2011. What will fuel transport systems of the future? Mater. Today **14:**518-524.

57. **Nam, J. Y., J. C. Tokash, and B. E. Logan.** 2011. Comparison of microbial electrolysis cells operated with added voltage or by setting the anode potential. Int. J. Hydrogen Energy **36:**10550-10556.

58. **Nielsen, M. E., C. E. Reimers, and H. A. Stecher.** 2007. Enhanced power from chambered benthic microbial fuel cells. Environ. Sci. Technol. **41:**7895-7900.

59. **Nitayavardhana, S., and S. K. Khanal.** 2012. Biofuel residues/wastes: Ban or boon? Crit. Rev. Env. Sci. Tec. **42:**1-43.

60. **Oh, S. E., and B. E. Logan.** 2006. Proton exchange membrane and electrode surface areas as factors that affect power generation in microbial fuel cells. Appl. Microbiol. Biotechnol. **70:**162-169.

61. **Pandit, S., B. K. Nayak, and D. Das.** 2012. Microbial carbon capture cell using cyanobacteria for simultaneous power generation, carbon dioxide sequestration and wastewater treatment. Bioresour. Technol. **107:**97-102.

62. **Park, D. H., and J. G. Zeikus.** 2000. Electricity generation in microbial fuel cells using neutral red as an electronophore. Appl. Environ. Microbiol. **66:**1292-1297.

63. **Pham, T. H., N. Boon, P. Aelterman, P. Clauwaert, L. De Schamphelaire, L. Vanhaecke, K. De Maeyer, M. Hoefte, W. Verstraete, and K. Rabaey.** 2008. Metabolites produced by *Pseudomonas* sp. enable a Gram-positive bacterium to achieve extracellular electron transfer. Appl. Microbiol. Biotechnol. **77:**1119-1129.

64. **Potter, M. C.** 1911. Electrical effects accompanying the decomposition of organic compounds. Proc. R. Soc. London, Ser. B **84:**260-276.

65. **United Nations Development Programme.** 2000. World energy assessment: Energy and the challenge of sustainability. United Nations, New York.

66. **Rabaey, K., G. Lissens, S. D. Siciliano, and W. Verstraete.** 2003. A microbial fuel cell capable of converting glucose to electricity at high rate and efficiency. Biotechnol. Lett. **25:**1531-1535.

67. **Rao, P. V., S. S. Baral, R. Dey, and S. Mutnuri.** 2010. Biogas generation potential by anaerobic digestion for sustainable energy development in India. Renewable Sustainable Energy Rev. **14:**2086-2094.

68. **Reguera, G., K. D. McCarthy, T. Mehta, J. S. Nicoll, M. T. Tuominen, and D. R. Lovley.** 2005. Extracellular electron transfer via microbial nanowires. Nature **435:**1098-101.

69. **Reguera, G., K. P. Nevin, J. S. Nicoll, S. F. Covalla, T. L. Woodard, and D. R. Lovley.** 2006. Biofilm and nanowire production lead to increased current in microbial fuel cells. Appl. Environ. Microbiol. **72:**7345-7348.

70. **Reimers, C. E., P. Girguis, H. A. Stecher, L. M. Tender, N. Ryckelynck, and P. Whaling.** 2006. Microbial fuel cell energy from an ocean cold seep. Geobiology **4:**123-136.

71. **Shi, X. X., Y. J. Feng, X. Wang, H. Lee, J. Liu, Y. P. Qu, W. H. He, S. M. S. Kumar, and N. Q. Ren.** 2012. Application of nitrogen-doped carbon powders as low-cost and durable cathodic catalyst to air-cathode microbial fuel cells. Bioresour. Technol. **108:**89-93.

72. **Sund, C. J., S. McMasters, S. R. Crittenden, L. E. Harrell, and J. J. Sumner.** 2007. Effect of electron mediators on current generation and fermentation in a microbial fuel cell. Appl. Microbiol. Biotechnol. **76:**561-568.

73. **Tender, L. M., S. A. Gray, E. Groveman, D. A. Lowy, P. Kauffman, J. Melhado, R. C. Tyce, D. Flynn, R. Petrecca, and J. Dobarro.** 2008. The first demonstration of a microbial fuel cell as a viable power supply: Powering a meteorological buoy. J. Power Sources **179:**571-575.

74. **Tender, L. M., C. E. Reimers, H. A. Stecher, 3rd, D. E. Holmes, D. R. Bond, D. A. Lowy, K. Pilobello, S. J. Fertig, and D. R. Lovley.** 2002. Harnessing microbially generated power on the seafloor. Nat. Biotechnol. **20:**821-5.

75. **Verma, N. M., S. Mehrotra, A. Shukla, and B. N. Mishra.** 2010. Prospective of biodiesel production utilizing microalgae as the cell factories: A comprehensive discussion. Afr. J. Biotechnol. **9:**1402-1411.

76. **Wang, X., Y. Feng, J. Liu, H. Lee, C. Li, N. Li, and N. Ren.** 2010. Sequestration of CO_2 discharged from anode by algal cathode in microbial carbon capture cells (MCCs). Biosens. Bioelectron. **25:**2639-43.

77. **Watkins, K.** Human Development Report 2006. Beyond scarcity: Power, poverty and the global water crisis. United Nations Development Programme.

78. **Yan, H., T. Saito, and J. M. Regan.** 2012. Nitrogen removal in a single-chamber microbial fuel cell with nitrifying biofilm enriched at the air cathode. Water Res. **46:**2215-2224.

79. **Yazdani, S. S., and R. Gonzalez.** 2007. Anaerobic fermentation of glycerol: a path to economic viability for the biofuels industry. Curr. Opin. Biotechnol. **18:**213-9.

80. **Yi, H., K. P. Nevin, B.-C. Kim, A. E. Franks, A. Klimes, L. M. Tender, and D. R. Lovley.** 2009. Selection of a variant of *Geobacter sulfurreducens* with enhanced capacity for current production in microbial fuel cells. Biosens. Bioelectron. **24:**3498-3503.

81. **You, S., Q. Zhao, J. Zhang, J. Jiang, and S. Zhao.** 2006. A microbial fuel cell using permanganate as the cathodic electron acceptor. J. Power Sources **162:**1409-1415.

82. **Zhang, F., D. Pant, and B. E. Logan.** 2011. Long-term performance of activated carbon air cathodes with different diffusion layer porosities in microbial fuel cells. Biosens. Bioelectron. **30:**49-55.

83. **Zhang, G. D., Q. L. Zhao, Y. Jiao, K. Wang, D. J. Lee, and N. Q. Ren.** 2012. Efficient electricity generation from sewage sludge using biocathode microbial fuel cell. Water Res. **46:**43-52.

84. **Zhang, X. Y., S. A. Cheng, P. Liang, X. Huang, and B. E. Logan.** 2011. Scalable air cathode microbial fuel cells using glass fiber separators, plastic mesh supporters, and graphite fiber brush anodes. Bioresour. Technol. **102:**372-375.

Chapter 2.
Electron donors supporting the growth and electroactivity of *Geobacter sulfurreducens* anode biofilms.

This chapter was published previously and has been reprinted with permission.

ABSTRACT

Geobacter bacteria efficiently oxidize acetate into electricity in bioelectrochemical systems, yet the range of fermentation products that supports the growth of anode biofilms and electricity production has not been thoroughly investigated. Here we show that *Geobacter sulfurreducens* oxidized formate and lactate with electrodes and Fe(III) as terminal electron acceptors, though with reduced efficiency compared to acetate. The structure of the formate and lactate biofilms increased in roughness, and the substratum coverage decreased, to alleviate the metabolic constraints derived from the assimilation of carbon from the substrates. Low levels of acetate promoted formate carbon assimilation and biofilm growth and increased the system's performance to levels comparable to those with acetate only. Lactate carbon assimilation also limited biofilm growth and led to the partial oxidization of lactate to acetate. However, lactate was fully oxidized in the presence of fumarate, which redirected carbon fluxes into the tricarboxylic acid cycle, and by acetate-grown biofilms. These results expand the known ranges of electron donors for *Geobacter*-driven fuel cells and identify microbial constraints that can be targeted to develop better-performing strains and increase the performance of bioelectrochemical systems.

INTRODUCTION

The ability of microorganisms to completely oxidize organic compounds to carbon dioxide with an electrode serving as the sole electron acceptor shows promise for the conversion of complex substrates, such as organic wastes and renewable biomass, to electricity and/or biofuels in bioelectrochemical systems (BESs) (19, 20, 26). The degradation of complex substrates in BESs is a multistep process initiated by a fermentative partner, which can be a defined microbial catalyst (34) or a consortium of microorganisms with synergistic activities (19). The activities of the fermentative partner(s) generate complex mixtures of organic acids, such as acetate, lactate and formate, which accumulate and acidify the fermentation broth, thus inhibiting microbial growth. H_2 is also a major product of the fermentation of organic matter and its accumulation negatively controls the rate of decomposition (40). Because fermentation end products serve as electron donors for the electrogenic partner, interspecies metabolite transfer contributes greatly to the coulombic efficiencies and electrochemical performance of BESs (6, 14, 30). For this reason, the efficient conversion of fermentation end products to electricity is critical for the efficient processing of complex substrates in BESs.

BESs fed with fermentation products often enrich for exoelectrogens in the *Geobacteraceae* family (16, 26). Key to this enrichment is the ability of *Geobacter* bacteria to grow on the anode electrode as an electroactive biofilm (32). This process requires energy expenditure and sufficient carbon for cell biomass (41) and synthesis of the structural and electronic components of the biofilm matrix, such as electrically

conductive pili (31-33) and *c*-type cytochromes associated with an exopolysaccharide (EPS) matrix (36). *Geobacter* bacteria also need to divert some of the electron donor carbon for gluconeogenesis, biomass synthesis, and other anabolic reactions. Thus, electron donor oxidation and assimilation for carbon by *Geobacter* bacteria is ultimately responsible for the electrochemical performance of *Geobacter*-driven BESs. This, in turn, modulates parameters such as biofilm structure and resistance, current density, and mass transfer that limit power production in BESs (39).

Most studies thus far have focused on investigating the electron transfer mechanisms that enable *Geobacter* biofilms to reduce the electrode (25, 32, 35). In contrast, little is known about how electron donors affect the growth and electrochemical performance of *Geobacter* anode biofilms, which is fundamental for design optimization in BESs as well as for the development of better-performing strains. Acetate is the preferred electron donor for *Geobacter* bacteria; it can be oxidized in the tricarboxylic acid (TCA) cycle to produce energy for growth and electrons for electrode reduction while also providing carbon, via its conversion to pyruvate, for gluconeogenesis, biomass synthesis and other anabolic reactions (41). H_2 also supports current generation in BESs driven by acetate-grown biofilms of the model organism *Geobacter sulfurreducens* (2). However, *G. sulfurreducens* cannot grow autotrophically with CO_2 (9) and needs organic carbon for cell growth (41). For this reason, carbon-containing electron donors are, in principle, necessary to support the growth of anode biofilms in BESs.

The role of formate and lactate as electron donors in BESs is less understood.

Both were originally reported not to serve as electron donors for the reduction of Fe(III) (4). However, recent studies demonstrated that lactate could support current generation in a microbial electrolysis cell and could also be oxidized with Fe(III) as an electron acceptor (5). *Geobacter*-like sequences are in fact detected in formate- and lactate-fed BESs (16). Formate and lactate can theoretically produce more negative cell voltages (-0.403 and -0.325 *V* versus standard hydrogen electrode [SHE], respectively) than acetate (-0.277 *V* versus SHE) (14). However, the performance of formate- and lactate-fed BESs is often reduced compared to acetate. For example, power densities in BESs operated under identical conditions but fed different substrates were reportedly higher with acetate (835 ± 20.5 mW/m^2) than with lactate (739 ± 32.2 mW/m^2) and significantly lower with formate (62 ± 0.1 mW/m^2) (15). Furthermore, the power densities matched well with the numerical abundance of *Deltaproteobacteria*, a phylum dominated by *Geobacter* exoelectrogens, in the anode biofilms (acetate, 63%; lactate, 43%; formate, 14%) (15). These results suggested that metabolic constraints associated with the use of formate and lactate by *Geobacter* exoelectrogens limited the performance of the BESs.

Because formate and lactate are often end products of the fermentation of complex substrates and can also theoretically produce higher cell voltages than acetate, we investigated their use as electron donors in BESs driven by the model representative *G. sulfurreducens*. Here, we show that both formate and lactate supported current production in BESs and were oxidized with Fe(III), though with reduced efficiency compared to acetate controls. The reduced performance with formate was due to growth limitations during formate carbon assimilation but could be alleviated by

chemical complementation with low levels of acetate. In contrast, lactate carbon assimilation was suboptimal, and cells generated energy for growth through its partial oxidation to acetate. However, providing fumarate as the electron acceptor, which also serves as a carbon source and mobilizes carbon fluxes to the TCA cycle, or sufficient acetate to build the anode biofilms promoted the complete oxidation of lactate and increased BES performance. This expands the known range of electron donors that support the growth and activity of electroactive biofilms of *G. sulfurreducens* in BESs and provides the knowledge necessary to develop strains with improved performance and enrichment protocols that maximize the growth and reductive capabilities of *Geobacter* anode biofilms.

MATERIALS AND METHODS

Bacterial strains and culture conditions. *G. sulfurreducens* PCA was routinely cultured anaerobically in modified fresh water (FW) medium (7) supplemented with 1 μM Na_2SeO_4 to promote growth and with acetate (15 mM) and fumarate (40 mM) as electron donor and acceptor, respectively. Growth with other electrons donors was tested by replacing acetate with 10 mM D,L-lactate, 30 mM formate or 60 mM formate and measuring the culture's turbidity spectrophotometrically at 600 nm. When indicated, fumarate was replaced with 56 mM Fe(III)-citrate as the electron acceptor, and growth was monitored by measuring the amount of HCl-extractable Fe(II) resulting from the reduction of Fe(III) (21). *Shewanella oneidensis* MR-1, which was used as a control for lactate dehydrogenase activity, was routinely cultured in tryptic soy broth (30 g/L). All cultures were incubated at 30°C.

BESs. Cultures used as inoculum for BESs were grown in anaerobic mineral medium (38) supplemented with 10 ml/L vitamin mix (1) (herein referred to as DB media) with acetate (20 mM) and fumarate (40 mM) serving as electron donor and acceptor, respectively. The BESs consisted of dual-chambered, H-type fuel cells with the anode and cathode chambers separated by a Nafion membrane (Ion Power, Inc., New Castle, DE) and each containing 90 ml of DB medium and an electron donor (1 mM acetate, 4 mM formate, 0.67 mM D,L-lactate). For BESs with H_2, 8.8 ml of sterile H_2 gas was added to the headspace of the anode chamber to provide 0.36 mmol H_2 or the same number of electrons (0.72 mmol) as in 90 ml of 1 mM acetate. When indicated, BESs were also supplemented with 0.1 mM acetate. Alternatively, anode biofilms were

grown with 1 mM acetate until depleted, and then the medium of the anode chamber was replaced inside a glove box chamber (Coy Laboratory Products, Inc., Grass Lake, MI) with fresh medium containing 0.67 mM lactate. Graphite rod electrodes (Alfa Aesar, 1.27 cm diameter, 99% metals basis, 12 cm^2) served as the working (anode) and counter (cathode) electrodes. A VSP potentiostat (BioLogic, Claix, France) was used to set a 0.24-V potential at the anode electrode versus a 3 M Ag/AgCl reference electrode (Bioanalytical systems, Inc., West Lafayette, IN). Both chambers were made anoxic and buffered to pH 7 by continuous sparging with N_2-CO_2 (80:20). A 40% (vol/vol) inoculum of early-stationary-phase cells grown at 30°C in DB medium with acetate and fumarate was harvested by centrifugation (4,000 x *g*, 8 min, 25°C), washed once, and resuspended in 10 ml of DB medium before inoculating into the 90 ml of sterile DB media contained in the anode chamber. Supernatant samples were periodically removed to monitor electron donor removal and formation of metabolic intermediates, as described in detail in the "Analytical Techniques" section.

CLSM and COMSTAT analyses. The anode biofilms were examined microscopically using a FluoView FV1000 inverted microscope system (Olympus, Center Valley, PA) equipped with a UPLFLN 40X oil immersion objective (Olympus; numerical aperture [NA], 1.30). For these analyses, the anode electrodes were removed from the BESs once current had dropped to zero, and the biofilm cells were differentially stained live (green) and dead (red) with the BacLight viability kit (Invitrogen, Carlsbad, CA) by following the manufacturer's recommendations. The anode electrode was placed on a Lab-Tek coverglass chamber (Nunc, Rochester, NY) filled with 3 ml 1X phosphate-buffered saline (PBS) and imaged by confocal laser scanning microscopy

(CLSM) at excitation wavelengths of 488 nm (SYTO 9, live cells) and 543 nm (propidium iodide, dead cells). Emission from SYTO 9 was detected with a BA505-525 bandpass filter and from propidium iodide with a BA560IF longpass filter. Image stacks were collected every 1 μm and three-dimensional image projections were produced using the FV10-ASW 3.0 software (Olympus). Image stacks were taken from approximately 8 random fields (1,024 x 1,024 pixels, 0.31 μm/pixel) per electrode, and a minimum of two BES replicates was examined for each electron donor tested. The structure of the anode biofilm was analyzed using COMSTAT image analysis software, as previously described (13). Connected volume filtration was used to remove noise in the data from cells not attached to the substratum.

Lactate dehydrogenase and protein assays. *G. sulfurreducens* cells were grown in 100 ml of DB media supplemented with 10 mM D,L-lactate. *S. oneidensis* MR-1 was also grown in 100 ml of DB media but prepared aerobically, buffered with 1,4-piperazinediethanesulfonic acid (PIPES) rather than bicarbonate, and supplemented with 45 mM D,L-lactate. Mid-exponential-phase cells (optical density at 600 nm [OD_{600}] of 0.3 to 0.5) were harvested by centrifugation (4,000 x *g*, 20 min, 4°C), washed twice, and resuspended in 20 mM 4-(2-hydroxyethyl)-1-piperazineethanesulfonic acid (HEPES) buffer (pH 7, 100 mM NaCl, 2 mM β-mercaptoethanol), as described before (29). The cells were then lysed by sonication using a Branson Sonifier 450 (5 times, 1 min, 50% duty cycle, in an ice water bath). The rate of D- and L-lactate-oxidizing activity coupled to the reduction of phenazine methosulfate (PMS) and 3-(4,5-dimethylthiazolyl-2-)2,5-diphenyltetrazolium bromide (MTT) was measured spectrophotometrically at 570 nm, as previously described (29). A unit (U) of lactate dehydrogenase activity was

defined as the amount of enzyme that reduces 1 nmol of MTT per min. The enzyme activity was normalized to the total cell protein, which was measured by solubilizing the sonicated cell extracts with 1/2 vol of 2 N NaOH at 100°C for 1 h, neutralizing with 1/2 vol of 2 N HCl, and measuring the protein concentration with the reducing agent-compatible Pierce bicinchoninic acid (BCA) protein assay kit (Thermo Scientific, Rockford, IL) and bovine serum albumin (BSA) as the standard.

Analytical techniques. Culture supernatant fluids were filtered (0.45-μm-syringe filters; National Scientific, Rockwood, TN) and analyzed by high performance liquid chromatography (HPLC) (Waters, Milford, MA) at 30°C, as previously described (23).

RESULTS AND DISCUSSION

Current generation from formate and lactate. The electrical conversion of formate and lactate by *G. sulfurreducens* in BESs was investigated in reference to acetate. The electron donors were provided as equimolar supplies of electrons (1 mM acetate, 4 mM formate, and 0.67 mM lactate). The anode was poised at a constant potential of 240 mV versus Ag/AgCl to maintain consistency between different fuel cells, remove any potential limitations from electron transfer at the cathode, and eliminate the possibility of oxygen intrusions into the anode chamber (2) that might support aerobic growth (18). Current production with acetate increased linearly after a short lag phase (Fig. 2.1A), as the planktonic cells from the inoculum attached to the electrode and grew with constant doubling times while oxidizing acetate and producing electricity (22). The rate of current increase, which correlates with the exponential phase of biofilm growth (22), averaged 0.12 mA h^{-1} in triplicate BESs and reached a maximum of ca. 0.81 mA (Table 2.1) before declining as the acetate was depleted (Fig. 2.1A). Coulombic efficiencies were ca. 80% (Table 2.1), indicating that on average 80% of the acetate was converted into current, while the remaining substrate was used for cell biomass. In contrast, negative controls with H_2 or without electron donor failed to support biofilm growth and current generation (Fig. 2.1B).

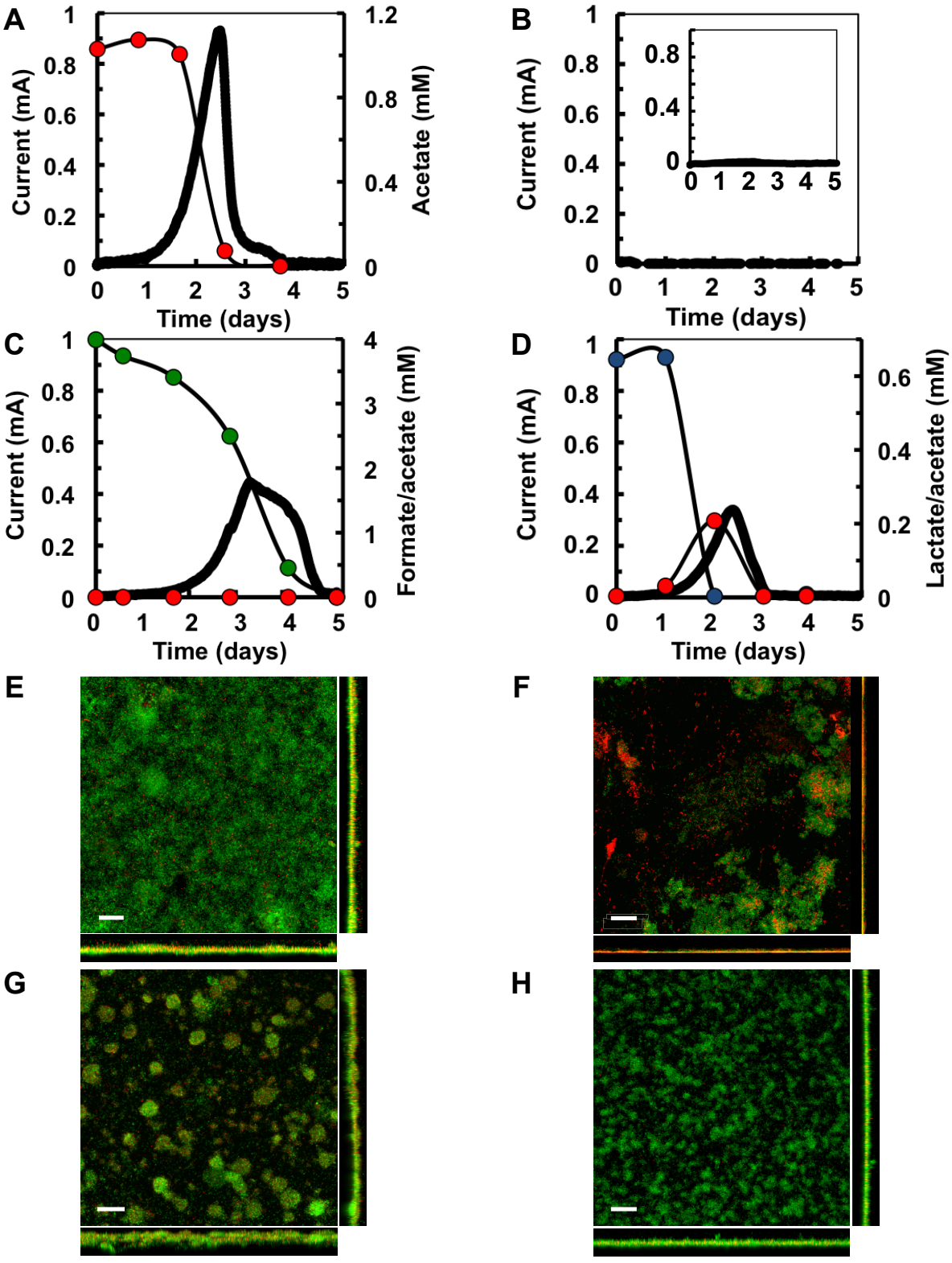

Fig. 2.1: Current generation (solid line) and electron donor uptake (circles [red, acetate; green, formate; blue, lactate]) (A to D) and CLSM micrographs of anode biofilms (E to

H) in fuel cells fed with acetate (A and E), H_2 (B and F), formate (C and G) or lactate (D and H). The inset in B shows controls with no electron donor. The biofilms in E to H were stained with the BacLight viability dyes (green, live cells; red, dead cells). Top views and the corresponding projections in the *x* (bottom) and *y* (right) axes are shown. Scale bar, 20 μm. For interpretation of the references to color in this and all other figures, the reader is referred to the electronic version of this dissertation.

Table 2.1. Performance of BESs of *G. sulfurreducens* fed with different electron donors

Electron donor	Rate of current increase ($mA\ h^{-1}$)	Maximum current (mA)	CE [a] (%)
Acetate	0.12 ± 0.01	0.81 ± 0.05	80 ± 3
Formate	0.12 ± 0.01	0.48 ± 0.04	93 ± 1
Lactate	0.12 ± 0.01	0.33 ± 0.01	38 ± 1
Formate [b]	0.12 ± 0.01	0.90 ± 0.03	75 ± 1
Lactate [b]	0.13 ± 0.01	0.37 ± 0.02	44 ± 1
Lactate [c]	0.09 ± 0.01	0.81 ± 0.01	90 ± 1

[a] CE, Coulombic efficiency.

[b] Supplemented with 0.1 mM acetate.

[c] Biofilms grown with 1 mM acetate before addition of media containing 0.67 mM lactate.

The rates of current increase in formate-fed BESs were similar to the acetate-fed systems (Fig. 2.1C and Table 2.1), suggesting that the growth rates of the biofilms were similar to acetate biofilms. However, the maximum current was almost half of that obtained with acetate (Table 2.1), and current production declined slowly while the formate was consumed (Fig. 2.1C). Coulombic efficiencies (93%) were higher in formate-fed than in acetate-fed systems (Table 2.1), indicating that over time the anode biofilms converted more formate to electricity than acetate yet at a lower rate. These results suggested that formate carbon assimilation, rather than oxidation, limited BES performance.

Lactate also supported similar rates of current increase (Fig. 2.1D and Table 2.1). Although all the lactate was removed from the culture broth (Fig. 2.1D), the maximum current and coulombic efficiencies were lower with lactate than with acetate and formate (Table 2.1). Interestingly, lactate uptake was coupled to the accumulation of acetate in the culture broth, which was used to support current production once all the lactate had been exhausted (Fig. 2.1D). This suggests that lactate was partially oxidized to acetate. This is similar to what has been reported for *S. oneidensis* grown anaerobically in MFCs (17). As lactate has three carbons and acetate has two, the maximum theoretical lactate-acetate ratio is 1:1.5. However, we measured 0.4 mol of acetate for every mol of lactate consumed. This suggests that most of the lactate was diverted to cell biomass, rather than electricity production, during growth on the anode. This is consistent with the coulombic efficiencies calculated for the lactate-fed BESs, which indicated that on average only 38% of the lactate was converted into electricity (Table 2.1).

Biofilm biomass and structure in formate- and lactate-fed BESs. Current generation by *G. sulfurreducens* is directly proportional to the growth of the anode biofilms on the electrode (32). This requires energy from the oxidation of electron donors as well as from the assimilation of some of the electron donor carbon through gluconeogenesis, biomass synthesis, and other anabolic activities (41). Because the structural organization of the biofilm is highly responsive to carbon use efficiency (13), we used the COMSTAT statistic software (13) to quantitatively analyze the structure of the anode biofilms as a function of the electron donor. Figs. 2.1E to H show representative fields obtained by CLSM. Changes in biofilm structure were readily apparent in the CLSM micrographs. The acetate biofilms had confluent growth and very few dead cells (Fig. 2.1E), whereas the H_2 biofilms had many dead cells and cell aggregates with no defined structure (Fig. 2.1F). In contrast, the formate and lactate biofilms were porous and patchy and composed of small microcolonies, which were smaller and denser in the lactate biofilms (Fig. 2.1G and H). Table 2.2 shows the structural parameters analyzed in the biofilms: total biomass (calculated as biovolume per surface area), mean biofilm thickness, roughness coefficient (variations in the biofilm thickness and, therefore, an indicator of biofilm heterogeneity), surface-to-biovolume ratio (portion of the biofilm that is exposed to nutrient flow), and substratum coverage (the area of the electrode occupied by the biofilm biomass). Because acetate-fed biofilms had the best performance (Fig. 2.1A), their structural parameters were used as a reference. The anode biofilms formed in the H_2 BESs (Fig. 2.1B) were used as negative controls. The most notable variations were decreases in total biofilm biomass and thickness from systems fed with the different substrates, which correlated well with

the observed decreases in maximum current (R^2 = 0.973 and R^2 = 0.977, respectively). Coulombic efficiencies for formate were higher than for any other electron donor, including acetate (Table 2.1). Thus, less formate was used for cell biomass and the biofilm biomass and thickness were reduced compared to acetate biofilms (Table 2.2). Lactate biofilms also had reduced biomass and thickness (Table 2.2) and low coulombic efficiencies (Table 2.1). This suggests that both lactate oxidation and assimilation for carbon limited biofilm growth and current generation.

Table 2.2. Anode biofilm structure as a function of the electron donor.

Electron donor	Total biomass ($\mu m^3/\mu m^2$)	Average Thickness (μm)	Roughness coefficient (0 to ∞)	Surface to volume ratio ($\mu m^2/\mu m^3$)	Substratum coverage (%)
Acetate	25.8 ± 3.2	26.7 ± 3.9	0.1 ± 0.1	0.8 ± 0.3	99.9 ± 0.1
Formate	13.7 ± 1.9	21.7 ± 4.1	0.3 ± 0.1	1.9 ± 0.4	75.0 ± 12.2
Lactate	13.0 ± 3.8	16.0 ± 3.6	0.2 ± 0.1	1.6 ± 0.7	91.0 ± 7.6
H_2	2.9 ± 0.6	10.2 ± 3.3	1.0 ± 0.2	2.0 ± 0.4	37.2 ± 9.2
Formate [a]	25.5 ± 8.4	26.9 ± 9.4	0.2 ± 0.1	0.9 ± 0.3	99.3 ± 0.6
Lactate [a]	17.9 ± 3.6	18.9 ± 2.7	0.1 ± 0.1	1.2 ± 0.7	97.2 ± 3.9

[a] Supplemented with 0.1 mM acetate.

The roughness and the surface-to-volume ratio increased, and the substratum coverage decreased, in the formate and lactate biofilms (Table 2.2). The biofilm heterogeneity (measured as roughness) was inversely proportional to the substratum coverage (R^2 =0.966). This shows that the structural organization of the anode biofilms was highly responsive to the electron donor. The preferred electron donor, acetate, supported the highest yields of biofilm growth and allowed for the formation of thicker, relatively uniform, confluent biofilms. This maximized electrode coverage and cell stacking per electrode surface area. In contrast, metabolic constraints associated with the use of formate or lactate prevented optimal biofilm growth. As a result, the biofilms were more porous and heterogeneous, which increased nutrient flow and minimized diffusion limitations but reduced the electrode coverage. This is in agreement with mathematical models of biofilm growth that support the notion that the biofilm structure adapts to the availability of nutrients. For example, biofilm growth is predicted to be slower at lower concentrations of nutrients due to diffusion limitations. Models show that low concentrations of nutrients, and, therefore slow growth, result in porous biofilms composed of channels and interstitial voids, whereas saturating concentrations of nutrients and rapid growth result in the formation of thick, compact and uniform biofilms (27, 28). Hence, the increases in roughness and surface-to-volume ratios measured with formate and lactate reflected the lower biofilm growth yields compared to acetate.

Formate and lactate as electron donors with Fe(III) and fumarate. As the standard redox potential ($E°$) of the half reaction of $Fe^{3+} + e^- \rightarrow Fe^{2+}$ ($E°$ = 771 mV versus SHE) is more positive than the potential (450 mV versus SHE or 240 mV versus 3 M Ag/AgCl) used in the BES experiments (Fig. 2.1), a higher electromotive force ($\Delta E°$)

and, therefore, more energy for growth and more electrons available for reductive reactions are theoretically possible for the electron donor/Fe(III) coupling than for the electron donor/electrode pair. Thus, we investigated if formate and lactate could support cell growth in cultures with Fe(III) citrate as sole electron acceptor. For these experiments, cells were harvested by centrifugation and washed prior to inoculation to prevent any nutrient carryover. As shown in Fig. 2.2A, cultures supplemented with 30 mM formate (concentrations like those previously tested [4]) grew and reduced all the Fe(III), though doubling times (17.3 ± 7.9 h) were longer than those supplemented with equimolar concentrations of carbon in the 15 mM acetate controls (9.7 ± 0.2 h). Increasing the concentration of formate to 60 mM to provide the same amount of electrons as in 15 mM acetate did not improve growth but rather slowed it down, with generation times in triplicate cultures averaging 45.1 (± 6.1) h. These results demonstrate that, in contrast to early reports (4), the coupling of formate oxidation to Fe(III) is possible, yet growth with formate is slower than with acetate. In contrast, formate (30 mM) did not support growth with the intracellular electron acceptor fumarate (Fig. 2.2B). Higher concentrations of formate (60 mM) also failed to support growth (data not shown). Furthermore, less than 10% of the formate was removed from the supernatants of the 30 mM and 60 mM formate cultures. The standard redox potential of the $fumarate^{2-} + 2\ e^{-} + 2H^{+} \rightarrow succinate^{2-}$ (E° = 31 mV versus SHE) is significantly lower than the Fe(III)/Fe(II) pair and the electrode potential that supported the formate-to-current BES reaction (Fig. 2.1). As a result, the formate/fumarate coupling did not generate as much energy for cell growth as the formate/Fe(III) coupling.

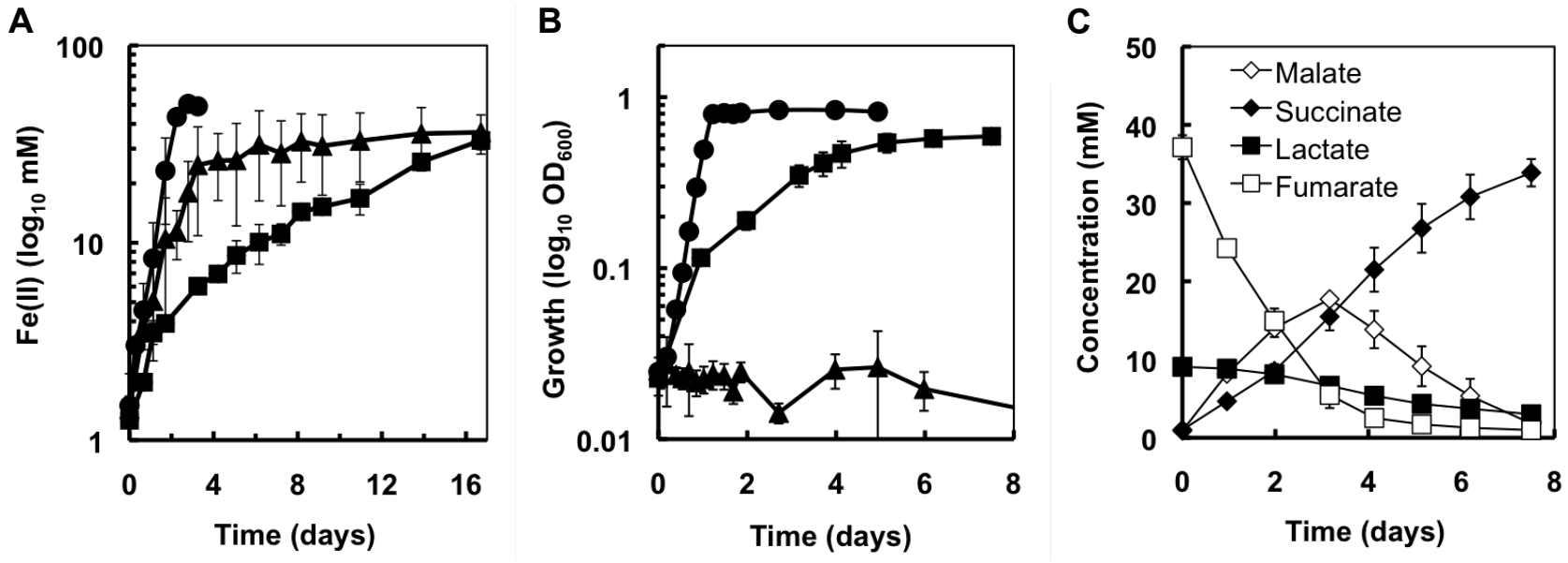

Fig. 2.2: Iron reduction (A) and growth (B) of *G. sulfurreducens* with acetate (circles), formate (triangles) or lactate (squares) as electron donors and Fe(III) citrate (A) or fumarate (B) as electron acceptor. (C) Lactate oxidation coupled to fumarate reduction and generation of malate and succinate in lactate-fumarate cultures shown in panel B.

As with the formate studies, we investigated if the more energetically favorable lactate/Fe(III) coupling was possible. After an extended lag phase (ca. 2 days), cells started to grow exponentially and reduced the available Fe(III) citrate (Fig. 2.2A). However, average doubling times with lactate (90 ± 12 h) were ca. 5- and 9-times longer than with formate and acetate, respectively. Hence, although at high-enough redox potential *G. sulfurreducens* can also use lactate as an electron donor, growth is slower than with acetate or formate. Interestingly, lactate also supported growth in cultures with fumarate (Fig. 2.2B). Fumarate has a lower redox potential than Fe(III) and, theoretically, less energy for growth, and fewer electrons for reductive reactions are expected for the lactate/fumarate coupling. Yet, growth was stimulated (doubling time, 35 ± 2 h) in the fumarate cultures (Fig. 2.2B) compared to the Fe(III) cultures (Fig. 2.2A). Furthermore, lactate oxidation was coupled to the reduction of fumarate to succinate, but acetate was not detected (Fig. 2.2C). These results suggested that lactate was completely oxidized to CO_2. Approximately 90% of the electrons in the lactate consumed (73 ± 2) were recovered as succinate (66 ± 2) consistent with the reduction of most of the fumarate, and malate was also detected (Fig. 2.2C). Only 7% (± 3%) of the fumarate was not recovered as succinate (Fig. 2.2C). This is in agreement with metabolic flux analyses of acetate-fumarate cultures that indicate that less than 10% of the fumarate is used as a source of carbon (41). Fumarate enters the TCA cycle to generate malate, which can then be converted into oxaloacetate and phosphoenolpyruvate for gluconeogenesis. Malate and oxaloacetate intermediates can also generate pyruvate to replenish acetyl coenzyme A (acetyl-CoA) for oxidation in the TCA cycle (41). In fact, some low levels of pyruvate (<1 mM) also accumulated in the

culture over time. Oxaloacetate can also be condensed with acetyl-CoA to produce citric acid, a reaction catalyzed by the citrate synthase enzyme of the TCA cycle (3). This provides a route for lactate-derived acetyl-CoA to be fully oxidized in the TCA cycle when fumarate is the electron acceptor.

Metabolic constraints associated with the assimilation of formate carbon. Acetate and formate are oxidized and assimilated for carbon using different metabolic pathways. As shown in Fig. 2.3, most of the energy derived from acetate comes from its oxidation through the TCA cycle, while its assimilation as carbon is derived from gluconeogenesis via pyruvate (41). In contrast, formate oxidation in *G. sulfurreducens* is predicted to be catalyzed by a periplasmically-oriented, membrane-bound formate dehydrogenase (FDH) enzyme complex (24), which shows similarity to the nitrate-inducible formate dehydrogenase (FDH-N) that couples formate oxidation and nitrate reduction in *Escherichia coli* (8). Genome analyses also predict that formate carbon can be assimilated in the reaction of the pyruvate formate lyase (PFL) (24), which uses formate and acetyl-CoA as substrates to produce pyruvate and CoA (Fig. 2.3). Previous studies (37) suggested that the PFL reaction may not be functional in the direction towards formate synthesis. Yet, whether this reaction can function in the opposite direction for formate carbon assimilation has never been investigated. As acetate can provide acetyl-CoA for the PFL reaction, we investigated the efficiency of formate carbon assimilation as pyruvate by supplementing formate-fed BESs with low concentrations (0.1 mM) of acetate, which were previously shown to provide sufficient amount of carbon for cell growth with H_2 as an electron donor (9). The small amount of acetate rescued the growth defect with formate (Fig. 2.4A) and supported similar rates

of current increase and maximum current as in acetate-fed BESs (Table 2.1). Furthermore, formate and acetate were removed from the culture broth concomitantly (Fig. 2.4B), consistent with formate carbon being co-assimilated with acetyl-CoA in the PFL reaction. Coulombic efficiencies in formate-fed BESs supplemented with acetate (75%) were also lower than those measured with formate only (Table 2.1). Thus, less formate was being used as an electron donor for electricity generation, and more was being diverted for cell biomass. The addition of acetate also promoted the confluent growth of the anode biofilms, whose height and biomass increased to levels comparable to the acetate controls (Fig. 2.4C and Table 2.2). The biofilms were more uniform and did not increase the surface area exposed to nutrient flow, as indicated by the lower roughness coefficient and surface-to-biovolume ratio (Table 2.2). Substrate coverage also increased and was saturating. As the thickness of the biofilm is directly proportional to the maximum current (32), alleviating the metabolic constraints associated with the assimilation of formate carbon promoted the growth of confluent biofilms (Fig. 2.4C) and maximized electrode coverage (Table 2.2) and BES performance (Fig. 2.4A).

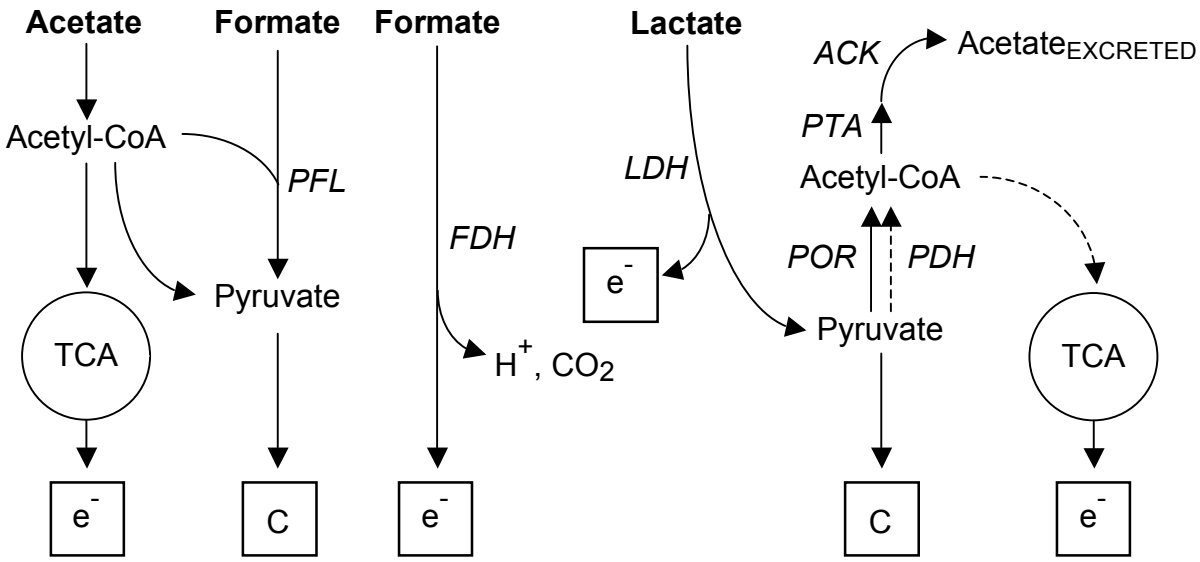

Fig. 2.3: Metabolic routes for the oxidation (e^-) and carbon assimilation (C) of acetate, formate and lactate (in bold). Alternative routes predicted to also be operative when fumarate serves as the electron acceptor are shown with dashed lines. Enzyme abbreviations: *PFL*, pyruvate formate lyase; *FDH*, formate dehydrogenase; *ACK*, acetate kinase; *PTA*, phosphotransacetylase; *PDH*, pyruvate dehydrogenase; *POR*, pyruvate oxidoreductase; *LDH*, lactate dehydrogenase.

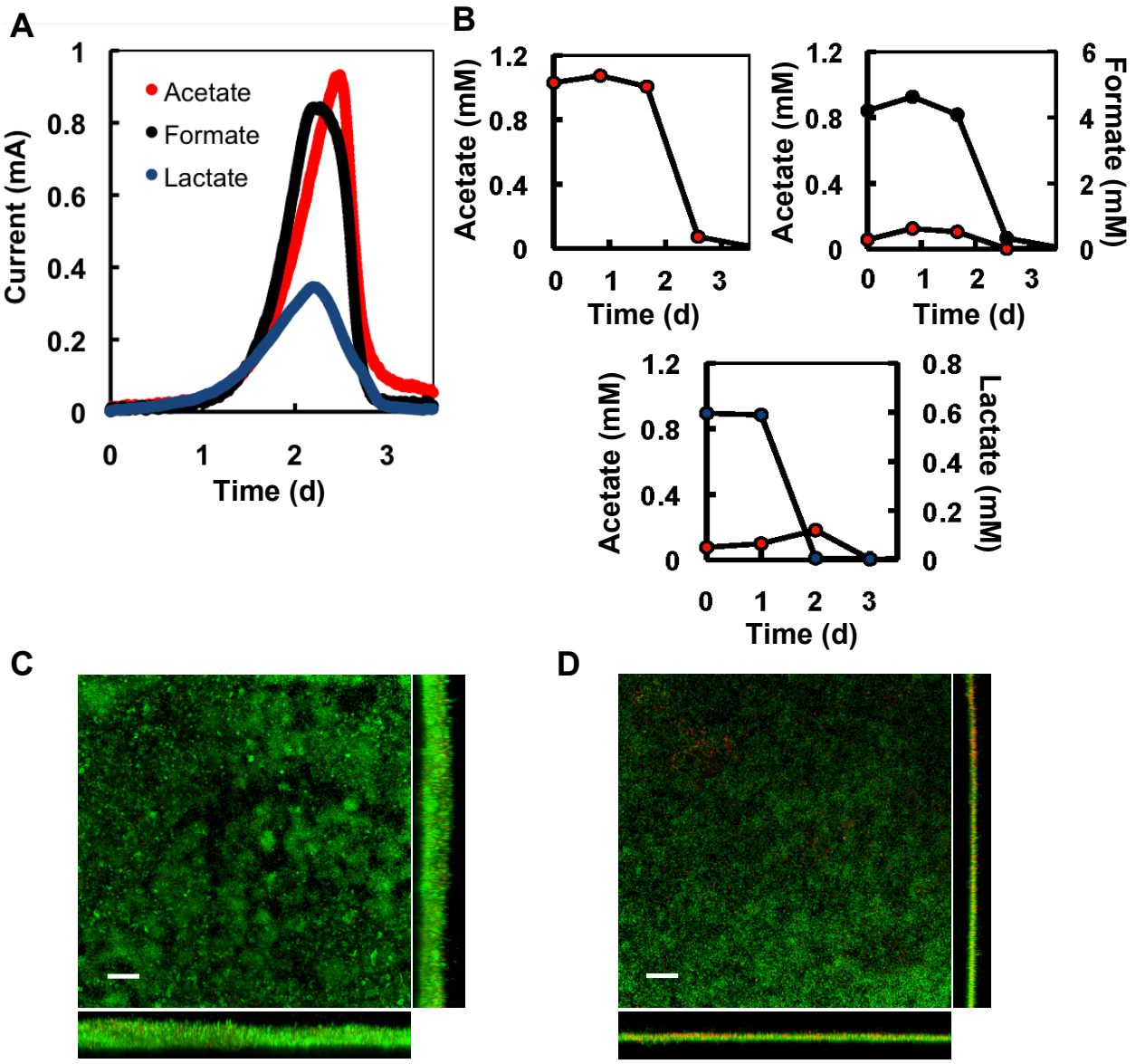

Fig. 2.4: (A and B) Effect of acetate supplementation (0.1 mM) on current generation (A) and substrate uptake (B) in fuel cells with acetate (red), formate (black), and lactate (blue). (C and D) CLSM micrographs of the anode biofilms from formate (C) and lactate (D) fuel cells supplemented with 0.1 mM acetate. The biofilms were stained with the BacLight viability dyes (green, live cells; red, dead cells). Top views and the corresponding projections in the *x* (bottom) and *y* (right) axes are shown. Scale bar, 20 μm.

Lactate oxidation and assimilation for carbon in *G. sulfurreducens*. Lactate is oxidized and assimilated independently of acetate (Fig. 2.3). Consistent with this, supplementing the BESs with small amounts of acetate (0.1 mM) had no significant effects on performance (Fig. 2.4A) or in lactate-acetate stochiometry (Fig. 2.4B) but improved coulombic efficiencies (Table 2.1), as current was also generated from the oxidation of acetate. Biofilm structural parameters, such as roughness and surface-to-biovolume ratio, were also similar to the acetate-fed biofilms (Table 2.2). Substrate coverage increased as well and was mostly saturating (Table 2.2). However, the biofilm biomass and thickness, though greater than in lactate-only BESs, were lower than those in acetate biofilms (Table 2.2). In contrast, lactate was fully oxidized by acetate-grown anode biofilms (Fig. 2.5A). Furthermore, maximum current and coulombic efficiencies increased to levels comparable to acetate biofilms (Table 2.1). The biofilms maintained the confluent growth and maximum substrate coverage of acetate biofilms (Fig. 2.5B). Thus, lactate can be fully oxidized by the anode biofilms once the carbon demands are satisfied.

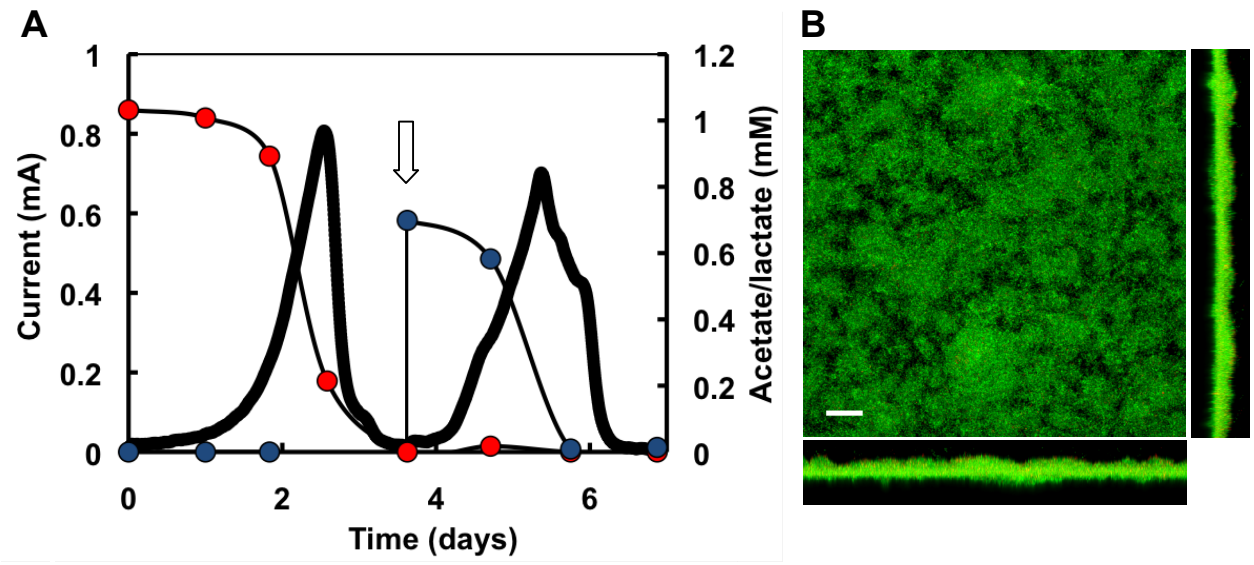

Fig. 2.5: Lactate oxidation by acetate-grown biofilms in BESs. (A) Current generation coupled to acetate and then lactate use as electron donors. The addition of lactate to the anode chamber is shown with an arrow. (B) CLSM micrograph of lactate-oxidizing anode biofilms previously grown with acetate. The biofilms were stained with the BacLight viability dyes (green, live cells; red, dead cells). Top view and the corresponding projections in the *x* (bottom) and *y* (right) axes are shown. Scale bar, 20 μm.

Lactate oxidation and assimilation for carbon are initiated in the reaction catalyzed by the lactate dehydrogenase (LDH) enzyme (Fig. 2.3). Although the genome of *G. sulfurreducens* does not contain an annotated LDH gene (24), comparative genomic analyses identified an operon (*ldhEFG*) encoding proteins homologous to the multisubunit lactate oxidase of *S. oneidensis* MR-1 (29). We identified a homologous region in the *G. sulfurreducens* genome in genome-wide comparisons of the *ldhEFG*

region of *S. oneidensis* using the tools available at the Comprehensive Microbial Resource website (http://cmr.jcvi.org/tigr-scripts/CMR/CmrHomePage.cgi). The region includes genes (*GSU1622* to *GSU1624*) encoding an L-lactose permease, a GlcD flavoprotein, and the Fe-S subunit of a putative glycolate oxidase (GO) enzyme, and it is conserved in other *Geobacter* genomes such as *Geobacter uraniireducens* and *Geobacter metallireducens*. GO is a peroxisomal enzyme of plants and cyanobacteria that shares remarkable structural homology with LDH and other flavoproteins that catalyze dehydrogenation reactions (11). As a result, GO can catalyze the oxidation of lactate yet at a lower rate (12). Consistent with this, D-LDH and L-LDH activities (99 ± 16 and 128 ± 10 U/mg protein, respectively) in cell extracts of *G. sulfurreducens* grown with lactate and fumarate were significantly lower than in cell extracts of *S. oneidensis* MR-1 (848 ± 95 and 331 ± 42 U/mg protein, respectively).

The activity of the LDH enzyme converts lactate into pyruvate, which can then be converted into acetyl-CoA by the pyruvate ferredoxin oxidoreductase (POR) enzyme (Fig. 2.3). However, the POR reaction is slow in the pyruvate-to-acetyl-CoA direction (37) and lactate-derived pyruvate is predicted to accumulate inside the cell, thereby creating an excess flux of carbon and limiting growth. *E. coli* balances excess fluxes of carbon and generates energy for growth by diverting the excess carbon as acetyl-CoA substrate for the acetate kinase (ACK)/phosphotransacetylase (PTA) pathway, which results in the excretion of acetate and the generation of ATP (10). The ACK/PTA pathway is also present in *G. sulfurreducens* (37) and provides a two-step reaction to partially oxidize lactate to acetate and gain energy for growth (Fig. 2.3). In contrast to the partial oxidation of lactate in BESs (Fig. 2.1D), lactate was fully oxidized in cultures

with fumarate (Fig. 2.2C). This is because fumarate carbons are used through alternative pathways (Fig. 2.3), such as the reaction catalyzed by the pyruvate dehydrogenase (PDH), which replenishes acetyl-CoA, and the generation of oxaloacetate from fumarate-derived malate (41). Acetyl-CoA and oxaloacetate are then condensed in the reaction catalyzed by the citrate synthase enzyme of the TCA cycle. This allows lactate to be completely oxidized when fumarate is the electron acceptor.

Implications. The results presented herein demonstrate that *G. sulfurreducens* has a broader range of electron donors than originally reported (4). They also provide insights into the limitations reported for *Geobacter*-driven BESs fed with fermentation end products such as acetate, lactate and formate (16). Although higher voltages are predicted for formate and lactate than acetate (14), acetate-fed fuel cells produce higher power densities than lactate-fed fuel cells and significantly higher than formate-fed fuel cells operated under identical conditions (15). This is because acetate supports optimal biofilm growth and current production in *Geobacter* bacteria. Lactate oxidation to pyruvate, which is a poor electron donor for *G. sulfurreducens* (37), creates an excess flux of carbon inside the cells and limits growth. As a result, lactate is partially oxidized to acetate in BESs. Thus, slower growth is predicted for *G. sulfurreducens*-like organisms during enrichments with lactate. However, the performance of BESs can be improved by adding carbon sources that alleviate the excess carbon fluxes and promote the complete oxidation of lactate in the TCA cycle. Formate oxidation was also coupled to current production, yet BES performance was limited by formate carbon assimilation in the PFL reaction. This provides a plausible explanation for the finding that anode biofilms from formate-fed BESs are dominated by low-power-producing *Paracoccus*

species and only harbor a small percentage (14%) of high-power-producing *Geobacter*-like members (15). *Paracoccus* spp. can efficiently oxidize formate to CO_2 and H_2 (15). Although H_2 can be used as an electron donor by exoelectrogens like *G. sulfurreducens*, a carbon source is required to build the biofilm cell biomass. Formate can provide carbon for biofilm growth, yet its assimilation is limited by acetate availability. As a result, *Geobacter* spp. are out-competed on the anode electrode by low-power producing, formate-oxidizing organisms (15). However, the growth of *Geobacter* spp. with formate could be stimulated by providing small amounts of acetate in the inoculum to promote the assimilation of formate carbon to support biofilm growth on the anode electrode.

Taken together, these results highlight the importance of selecting combinations of electron donors that promote the growth and establishment of *Geobacter* anode biofilms. This information can be applied to develop better-performing strains and to manipulate the microbial and metabolic diversity of anode biofilms for increased power production from defined substrates in BESs.

REFERENCES

REFERENCES

1. **Balch, W. E., G. E. Fox, L. J. Magrum, C. R. Woese, and R. S. Wolfe.** 1979. Methanogens: reevaluation of a unique biological group. Microbiol. Rev. **43:**260-96.

2. **Bond, D. R., and D. R. Lovley.** 2003. Electricity production by *Geobacter sulfurreducens* attached to electrodes. Appl. Environ. Microbiol. **69:**1548-55.

3. **Bond, D. R., T. Mester, C. L. Nesbo, A. V. Izquierdo-Lopez, F. L. Collart, and D. R. Lovley.** 2005. Characterization of citrate synthase from *Geobacter sulfurreducens* and evidence for a family of citrate synthases similar to those of eukaryotes throughout the Geobacteraceae. Appl. Environ. Microbiol. **71:**3858-65.

4. **Caccavo, F., Jr., D. J. Lonergan, D. R. Lovley, M. Davis, J. F. Stolz, and M. J. McInerney.** 1994. *Geobacter sulfurreducens* sp. nov., a hydrogen- and acetate-oxidizing dissimilatory metal-reducing microorganism. Appl. Environ. Microbiol. **60:**3752-9.

5. **Call, D. F., and B. E. Logan.** 2011. Lactate oxidation coupled to iron or electrode reduction by *Geobacter sulfurreducens* PCA. Appl. Environ. Microbiol. **77:**8791-4.

6. **Call, D. F., R. C. Wagner, and B. E. Logan.** 2009. Hydrogen production by *Geobacter* species and a mixed consortium in a microbial electrolysis cell. Appl. Environ. Microbiol. **75:**7579-87.

7. **Cologgi, D. L., S. Lampa-Pastirk, A. M. Speers, S. D. Kelly, and G. Reguera.** 2011. Extracellular reduction of uranium via *Geobacter* conductive pili as a protective cellular mechanism. Proc. Natl. Acad. Sci. USA **108:**15248-52.

8. **Coppi, M. V.** 2005. The hydrogenases of *Geobacter sulfurreducens*: a comparative genomic perspective. Microbiology **151:**1239-1254.

9. **Coppi, M. V., R. A. O'Neil, and D. R. Lovley.** 2004. Identification of an uptake hydrogenase required for hydrogen-dependent reduction of Fe(III) and other electron acceptors by *Geobacter sulfurreducens*. J. Bacteriol. **186:**3022-8.

10. **el-Mansi, E. M., and W. H. Holms.** 1989. Control of carbon flux to acetate excretion during growth of *Escherichia coli* in batch and continuous cultures. J. Gen. Microbiol. **135:**2875-83.

11. **Fraaije, M. W., and A. Mattevi.** 2000. Flavoenzymes: diverse catalysts with recurrent features. Trends Biochem. Sci. **25:**126-32.

12. **Frederick, S. E., P. J. Gruber, and N. E. Tolbert.** 1973. The occurrence of glycolate dehydrogenase and glycolate oxidase in green plants: an evolutionary survey. Plant Physiol. **52:**318-23.

13. **Heydorn, A., A. T. Nielsen, M. Hentzer, C. Sternberg, M. Givskov, B. K. Ersboll, and S. Molin.** 2000. Quantification of biofilm structures by the novel computer program COMSTAT. Microbiology **146:**2395-407.

14. **Kiely, P. D., D. F. Call, M. D. Yates, J. M. Regan, and B. E. Logan.** 2010. Anodic biofilms in microbial fuel cells harbor low numbers of higher-power-producing bacteria than abundant genera. Appl. Microbiol. Biotechnol. **88:**371-80.

15. **Kiely, P. D., G. Rader, J. M. Regan, and B. E. Logan.** 2011. Long-term cathode performance and the microbial communities that develop in microbial fuel cells fed different fermentation endproducts. Bioresour. Technol. **102:**361-6.

16. **Kiely, P. D., J. M. Regan, and B. E. Logan.** 2011. The electric picnic: synergistic requirements for exoelectrogenic microbial communities. Curr. Opin. Biotechnol. **22:**378-85.

17. **Lanthier, M., K. B. Gregory, and D. R. Lovley.** 2008. Growth with high planktonic biomass in *Shewanella oneidensis* fuel cells. FEMS Microbiol. Lett. **278:**29-35.

18. **Lin, W. C., M. V. Coppi, and D. R. Lovley.** 2004. *Geobacter sulfurreducens* can grow with oxygen as a terminal electron acceptor. Appl. Environ. Microbiol. **70:**2525-8.

19. **Logan, B. E., and J. M. Regan.** 2006. Electricity-producing bacterial communities in microbial fuel cells. Trends Microbiol. **14:**512-8.

20. **Lovley, D. R.** 2008. The microbe electric: conversion of organic matter to electricity. Curr. Opin. Biotechnol. **19:**1-8.

21. **Lovley, D. R., and E. J. Phillips.** 1987. Rapid assay for microbially reducible ferric iron in aquatic sediments. Appl. Environ. Microbiol. **53:**1536-1540.

22. **Marsili, E., J. Sun, and D. R. Bond.** 2010. Voltammetry and growth physiology of *Geobacter sulfurreducens* biofilms as a function of growth stage and imposed electrode potential. Electroanalysis **22**.

23. **McKinlay, J. B., J. G. Zeikus, and C. Vieille.** 2005. Insights into *Actinobacillus succinogenes* fermentative metabolism in a chemically defined growth medium. Appl. Environ. Microbiol. **71:**6651-6.

24. **Methé, B. A., K. E. Nelson, J. A. Eisen, I. T. Paulsen, W. Nelson, J. F. Heidelberg, D. Wu, M. Wu, N. Ward, M. J. Beanan, R. J. Dodson, R. Madupu, L. M. Brinkac, S. C. Daugherty, R. T. DeBoy, A. S. Durkin, M. Gwinn, J. F. Kolonay, S. A. Sullivan, D. H. Haft, J. Selengut, T. M. Davidsen, N. Zafar, O. White, B. Tran, C. Romero, H. A. Forberger, J. Weidman, H. Khouri, T. V. Feldblyum, T. R. Utterback, S. E. Van Aken, D. R. Lovley, and C. M. Fraser.** 2003. Genome of *Geobacter sulfurreducens*: metal reduction in subsurface environments. Science **302:**1967-1969.

25. **Nevin, K. P., B. C. Kim, R. H. Glaven, J. P. Johnson, T. L. Woodard, B. A. Methe, R. J. Didonato, S. F. Covalla, A. E. Franks, A. Liu, and D. R. Lovley.** 2009. Anode biofilm transcriptomics reveals outer surface components essential for high density current production in *Geobacter sulfurreducens* fuel cells. PLoS One **4:**e5628.

26. **Pant, D., G. Van Bogaert, L. Diels, and K. Vanbroekhoven.** 2010. A review of the substrates used in microbial fuel cells (MFCs) for sustainable energy production. Bioresour. Technol. **101:**1533-1543.

27. **Picioreanu, C., M. C. van Loosdrecht, and J. J. Heijnen.** 1998. A new combined differential-discrete cellular automaton approach for biofilm modeling: application for growth in gel beads. Biotechnol. Bioeng. **57:**718-31.

28. **Picioreanu, C., M. C. van Loosdrecht, and J. J. Heijnen.** 1998. Mathematical modeling of biofilm structure with a hybrid differential-discrete cellular automaton approach. Biotechnol. Bioeng. **58:**101-16.

29. **Pinchuk, G. E., D. A. Rodionov, C. Yang, X. Li, A. L. Osterman, E. Dervyn, O. V. Geydebrekht, S. B. Reed, M. F. Romine, F. R. Collart, J. H. Scott, J. K. Fredrickson, and A. S. Beliaev.** 2009. Genomic reconstruction of *Shewanella oneidensis* MR-1 metabolism reveals a previously uncharacterized machinery for lactate utilization. Proc. Natl. Acad. Sci. USA **106:**2874-9.

30. **Rabaey, K., N. Boon, S. D. Siciliano, M. Verhaege, and W. Verstraete.** 2004. Biofuel cells select for microbial consortia that self-mediate electron transfer. Appl. Environ. Microbiol. **70:**5373-5382.

31. **Reguera, G., K. D. McCarthy, T. Mehta, J. S. Nicoll, M. T. Tuominen, and D. R. Lovley.** 2005. Extracellular electron transfer via microbial nanowires. Nature **435:**1098-101.

32. **Reguera, G., K. P. Nevin, J. S. Nicoll, S. F. Covalla, T. L. Woodard, and D. R. Lovley.** 2006. Biofilm and nanowire production lead to increased current in microbial fuel cells. Appl. Environ. Microbiol. **72:**7345-7348.

33. **Reguera, G., R. B. Pollina, J. S. Nicoll, and D. R. Lovley.** 2007. Possible nonconductive role of *Geobacter sulfurreducens* pilus nanowires in biofilm formation. J. Bacteriol. **189:**2125-7.

34. **Ren, Z., T. E. Ward, and J. M. Regan.** 2007. Electricity production from cellulose in a microbial fuel cell using a defined binary culture. Environ. Sci. Technol. **41:**4781-6.

35. **Richter, H., K. P. Nevin, H. F. Jia, D. A. Lowy, D. R. Lovley, and L. M. Tender.** 2009. Cyclic voltammetry of biofilms of wild type and mutant *Geobacter sulfurreducens* on fuel cell anodes indicates possible roles of OmcB, OmcZ, type IV pili, and protons in extracellular electron transfer. Energy Environ. Sci. **2:**506-516.

36. **Rollefson, J. B., C. S. Stephen, M. Tien, and D. R. Bond.** 2011. Identification of an extracellular polysaccharide network essential for cytochrome anchoring and biofilm formation in *Geobacter sulfurreducens*. J. Bacteriol. **193:**1023-33.

37. **Segura, D., R. Mahadevan, K. Juarez, and D. R. Lovley.** 2008. Computational and experimental analysis of redundancy in the central metabolism of *Geobacter sulfurreducens*. PLoS Comput. Biol. **4:**e36.

38. **Srikanth, S., E. Marsili, M. C. Flickinger, and D. R. Bond.** 2008. Electrochemical characterization of *Geobacter sulfurreducens* cells immobilized on graphite paper electrodes. Biotechnol. Bioeng. Symp. **99:**1065-73.

39. **Torres, C. I., A. K. Marcus, H. S. Lee, P. Parameswaran, R. Krajmalnik-Brown, and B. E. Rittmann.** 2010. A kinetic perspective on extracellular electron transfer by anode-respiring bacteria. FEMS Microbiol. Rev. **34:**3-17.

40. **Wolin, M. J.** 1982. Hydrogen transfer in microbial communities. *In* A. T. Bull and J. H. Slater (ed.), Microbial interactions and communities, vol. 1. Academic Press, London.

41. **Yang, T. H., M. V. Coppi, D. R. Lovley, and J. Sun.** 2010. Metabolic response of *Geobacter sulfurreducens* towards electron donor/acceptor variation. Microb. Cell Fact. **9:**90.

Chapter 3.
Consolidated bioprocessing of AFEX-pretreated corn stover to ethanol and hydrogen in a microbial electrolysis cell.

This chapter was published previously and has been reprinted with permission from:

Speers, A. M., and G. Reguera, Consolidated bioprocessing of AFEX-pretreated corn stover to ethanol and hydrogen in a microbial electrolysis cell, Environ. Sci. Technol. Published online June14, 2012. DOI 10.1021/es3008497.

ABSTRACT

The consolidated bioprocessing (CBP) of corn stover pretreated via ammonia fiber expansion (AFEX-CS) into ethanol was investigated in a microbial electrolysis cell (MEC) driven by the exoelectrogen *Geobacter sulfurreducens* and the CBP bacterium *Cellulomonas uda*. *C. uda* was identified in a screening for its ethanologenic potential from AFEX-CS and for producing electron donors for *G. sulfurreducens* fermentatively. *C. uda* produced ethanol from AFEX-CS in MECs inoculated simultaneously or sequentially, with the concomitant conversion of the fermentation byproducts into electricity by *G. sulfurreducens*. The fermentation and electrical conversion efficiencies were high, but much of the AFEX-CS remained unhydrolyzed as nitrogen availability limited the growth of the CBP partner. Nitrogen supplementation stimulated the growth of *C. uda*, AFEX-CS hydrolysis and ethanologenesis. As a result, the synergistic activities of the CBP and exoelectrogen catalysts resulted in substantial energy recoveries from ethanologenesis alone (ca. 56%). The co-generation of cathodic H_2 in the MEC further increased the energy recoveries to ca. 73%. This, and the potential to optimize the activities of the microbial catalysts via culturing approaches and genetic engineering or adaptive evolution, makes this platform attractive for the processing of agricultural wastes.

INTRODUCTION

Ethanol is a promising biofuel that can be manufactured from lignocellulosic feedstocks by microbial fermentation of biomass sugars (4). Because food crops such as corn and sugarcane are readily processable feedstocks, they have been grown as the first-generation of energy crops for bioethanol in the US and Brazil, respectively (20). However, the long-term production of bioethanol from food crops faces limitations due to the expected increasing demand for arable land and price increases of crop-derived food products used for human and animal consumption (48). Lignocellulose substrates such as agricultural wastes, forestry residues, and dedicated bioenergy crops could provide enough sustainable feedstock supplies to displace one-third or more of the current demand for transportation fuels in the U.S. (35, 50), with minimum environmental impact (17). However, the high lignin content in these substrates limits their enzymatic digestibility and potential use in ethanol fermentations at costs and scales competitive with corn ethanol (17, 57).

Several pretreatment options have been proposed to improve enzymatic hydrolysis (21, 56, 57). One of them, the ammonia fiber expansion (AFEX) process (24), shows promise as a cost-effective, scaled-up pretreatment of lignocellulose substrates because it recycles the pretreatment chemical (ammonia) (56), improves the enzymatic digestibility of the substrate (24), and generates a highly fermentable hydrolysate (2, 23, 49). AFEX modifies the structure of lignin so as to permit enzyme access, partially depolymerizes hemicellulose, and promotes cellulose decrystallinization, while minimizing the formation of toxic degradation products that could inhibit subsequent hydrolysis and fermentation reactions (13, 27, 33). In addition, it is an effective

pretreatment for a wide range of lignocellulosic substrates (3, 24) and leaves small amounts of ammonia in the pretreated substrate that serve as nutritional supplements in subsequent fermentations (24). In a recent study, high yields of ethanol were obtained using an enzymatic hydrolysate derived from AFEX-treated corn stover and a recombinant yeast strain without the need for biomass washing, detoxification or nutrient supplementation (23). However, the enzymatic hydrolysis step and the inefficient fermentation of hemicellulose sugars remain major bottlenecks (23).

Consolidated bioprocessing (CBP) technologies (28), i.e., those in which a single microbe hydrolyzes the substrate and ferments the hexose and pentose sugars, have been proposed as the most cost-efficient industrial configuration for ethanol production (29). While significant advances have been made to engineer CBP yeasts, challenges still remain to produce industrial strains that heterologously express saccharolytic enzymes and coferment cellulose and hemicellulose sugars (30, 52). Native lignocellulose degraders show promise as CBP catalysts (22, 29) because their hydrolysis and fermentation efficiencies are naturally evolved to maximize cell growth yields from biomass (25). However, these microorganisms are adapted to growing within specialized, synergistic consortia (30), where fermentation products are rapidly removed to prevent feedback inhibition of biomass decomposition and fermentation using various electron acceptors as final electron sinks (55). Because Fe(III) oxides can be abundant electron acceptors in soils and sediments, iron reduction is an influential and rate-limiting step in the recycling of organic matter in the biosphere (16). The possibility of mimicking CBP consortia in bioelectrochemical cells is attractive because an electrode can be used to replace the natural electron acceptors and model Fe(III)-

reducing exoelectrogens such as *Geobacter sulfurreducens* are available that conserve energy for growth by transferring electrons from waste fermentation products such as acetate, formate, lactate and H_2 to electrodes (6, 7, 9, 46). Furthermore, with sufficient electrical input, the current generated in the anode can be converted into H_2 in the cathode chamber in a microbial electrolysis cell (MEC), thus producing H_2 fuel as a co-product (19).

Previous studies (40) with cocultures of *G. sulfurreducens* and the CBP bacterium, *Clostridium cellulolyticum*, demonstrated that cellulose degradation can be coupled to electricity generation in a microbial fuel cell (MFC). However, this platform was limited by the rates of the cathodic reaction, the use of purified forms of cellulose, low ethanol yields, and the inefficient electrical conversion of the fermentation byproducts, which accumulated in the medium (40). The direct coupling of cellulose to electricity was also demonstrated in MFCs driven by strains of *Enterobacter cloacae* and mixed cultures (41). Fermentation inhibitors derived from the pretreatment of lignocellulose substrates can also be converted into electricity in a MFC powered by a microbial consortium enriched on the anode (8). Additionally, untreated and steam-exploded corn stover supported current in a MFC driven by a CBP consortia enriched from soil samples (54). However, energy recovery from corn stover or from cellulose in MFCs is much lower than that of cellulosic bioethanol production, suggesting that considerably more power needs to be produced to make the platform competitive (54). This will require significant increases in the efficiency of corn stover saccharification and electricity generation.

MECs are attractive as CBP platforms for ethanol because the electrical input can be used to simultaneously produce H_2 in the cathode at much higher yields than those achieved fermentatively (19). Furthermore, the applied potential removes cathodic limitations (39, 41, 54) and promotes the growth of exoelectrogenic biofilms on the anode electrode (37). This maximizes the conversion of fermentation byproducts to cathodic H_2 while preventing the accumulation of feedback inhibitors. However, it is important to minimize electron losses by selecting CBP strains that produce fermentation byproducts that serve as electron donors for the exoelectrogen. Here we describe the identification of a CBP strain, *Cellulomonas uda*, which hydrolyzed and fermented AFEX-pretreated corn stover (AFEX-CS) to ethanol, and produced fermentation byproducts that served as electron donors for *G. sulfurreducens* in a MEC. The synergistic interactions between the CBP catalyst and the exoelectrogen stimulated ethanol production and minimized electron losses through the conversion of all the fermentative byproducts into H_2 in the cathode, thereby increasing the total energy recovery from the AFEX-CS up to 73%. This provides a competitive CBP platform for bioenergy production from lignocellulosic substrates.

MATERIALS AND METHODS

Bacterial strains and culture conditions. *G. sulfurreducens* PCA was routinely cultured at 30°C in anaerobic DB medium (46) with 20 mM acetate and 40 mM fumarate. Native CBP strains (Table 3.1) were cultured at 35°C in anaerobic GS2 media (10) supplemented with 0.2% cellobiose (GS2-CB). When indicated, 0.2% (w/v) corn stover (processed and pretreated with the AFEX method (23) and ground and sieved (0.75 mm pore size) to a homogenous powder with ca. 8% moisture content) (AFEX-CS) was used as a carbon source. Growth of the CBP strains with AFEX-CS was evaluated by inoculating late exponential-phase GS2-CB cultures into anaerobic DB medium with AFEX-CS to a final optical density at 660 nm (OD_{660}) of 0.04. The cultures were incubated at 35°C and spectrophotometric readings (OD_{660}) were taken every 12 h after resuspending the cultures by inversion and allowing the solids to settle for 20 min.

Batch cultures with fumarate. Late-exponential phase cultures of *C. uda* ATCC 21399 and *G. sulfurreducens* grown at 30°C in DB medium with cellobiose (0.2%) or acetate (20 mM) and fumarate (40 mM), respectively, were inoculated to an OD_{660} of 0.02 in the same (coculture) or separate (monoculture) tubes containing anaerobic DB medium with 0.2% (w/v) AFEX-CS and 40 mM fumarate. Control monocultures of *G. sulfurreducens* contained AFEX-CS and 40 mM fumarate or 20 mM acetate. When indicated, *G. sulfurreducens* was also grown with or without AFEX-CS in the presence of acetate (20 mM) and fumarate (40 mM). All cultures were incubated at 30°C and the planktonic growth (OD_{660}) of the undisturbed cultures was monitored periodically. Three

replicates were sacrificed every 48 h for pH measurements of the fermentation broth and for GC and HPLC analyses, as described in detail in the “Analytical techniques” section. Cells in the cocultures were differentially stained with the SYTO 9 (green, Gram-negative, *G. sulfurreducens*) and hexidium iodide (red, Gram-positive, *C. uda*) dyes in the BacLight Gram Stain kit (Invitrogen), as recommended by the manufacturer. The stained cells were adsorbed onto glass slides, imaged at random locations using a fluorescence microscope, and counted to calculate the relative percentage of each strain in the sample.

MECs. Dual-chambered, H-type MECs, set up as previously described (46), were autoclaved before adding 90 ml of sterile, anaerobic DB medium to the anode and cathode chambers. The reference electrodes (3 M Ag/AgCl, Bioanalytical systems Inc.) were sterilized by Tyndallization in anaerobic Luria Bertani medium (four cycles, each comprising 30 min in boiling medium and 24 h at 30°C) and then in 70% ethanol for 1 min before rinsing with sterile water. The anode electrode was poised to 0.24 V with a VSP potentiostat (BioLogic) and the MEC chambers were sparged with filter-sterilized N_2:CO_2 (80:20) gas until the current stabilized. Cells were harvested by centrifugation (6,000 x *g*, 6 min, 25°C) from a 40% (v/v) inoculum of an early stationary-phase culture of *C. uda* or *G. sulfurreducens* grown at 30°C in DB medium with cellobiose or acetate and fumarate, respectively. The cells were washed once, and resuspended in 10 ml of DB medium before inoculating them separately (monocultures) or together (coculture) into an anode chamber containing 0.2% (w/v) AFEX-CS.

Alternatively, a sequential inoculation strategy was followed in which *G. sulfurreducens* anode biofilms were first grown with 1 mM acetate until the acetate was

depleted and the current declined. The medium of the anode chamber was then replaced with fresh DB-AFEX-CS medium with or without 35 mM NH_4Cl supplementation inside a glove bag (Coy Laboratory Products, Inc.). When indicated, the anode chamber was also inoculated with *C. uda* cells. All MECs were incubated at 30°C with stirring and without sparging of the anode chamber. The cathode chamber was sparged continuously to prevent crossover of H_2 into the anode chamber. The percent of cathodic H_2 recovered in our system was determined by discontinuing the sparging of the cathode chamber, sampling the headspace and analyzing the gas composition by GC, as described below. Fermentation products in the anode broth were analyzed by HPLC and the AFEX-CS was also collected and used to estimate the hydrolysis efficiency, fermentation efficiency, and energy recovery, as described below. When indicated, nitrogen assimilation was also monitored over time by determining the concentration of NH_4^+ in the fermentation broth. Briefly, 60 µl of diluted culture supernatant fluids were mixed with 120 µl of Nessler's reagent (Fluka) and the optical density of the solution at 425 nm was measured and compared to a standard curve generated with NH_4Cl as a standard.

AFEX-CS hydrolysis and fermentation efficiencies. The AFEX-CS was harvested by centrifugation, washed four times with sterile water, and resuspended in 500 µL 0.2 N NaOH. The suspension was neutralized with 500 µL 0.2 N HCl, and dried in pre-weighed microcentrifuge tubes using a SpeedVac Plus SC110A centrifugal evaporator (Savant Instruments Inc., Holbrook, NY). The difference between the weight of the tube with the dry material and the initial weight of the tube was used to calculate

the dry weight of the AFEX-CS material. The glucose and xylose content of the AFEX-CS was then estimated after solubilizing the dry AFEX-CS with a modified acid hydrolysis procedure (45). Briefly, ca. 20 mg of dry AFEX-CS were resuspended in 200 µl 72% (v/v) H_2SO_4 and incubated for 1 h at 30°C. The samples were periodically (ca. every 15 min) vortexed at high speed for 10 s during incubation before transferring them to 17-ml glass pressure tubes and diluting them with 5.6 ml deionized water. The tubes were sealed with butyl rubber stoppers, crimped, and autoclaved for 30 min at 121°C (dry cycle). After cooling to room temperature, the hydrolysate was transferred to 15-ml centrifuge tubes, centrifuged (4000 rpm, 20 min, 25°C) to remove any remaining solids, and the supernatant was collected and neutralized with 0.3 g $CaCO_3$. The samples were centrifuged briefly to remove any insoluble material before HPLC analysis of the sugar content. The glucan and xylan content of the AFEX-CS (glucose and xylose equivalents, respectively, in acid hydrolysates) was estimated to be 28% (± 2) glucose and 18% (± 1) xylose, respectively, which is in the ranges previously reported (18). The xylose content of the AFEX-CS remaining at the end of the incubation period was also used to estimate the efficiency of the hydrolysis in reference to uninoculated controls. Glucose was not an accurate proxy because of interference from the abundant curdlan exopolysaccharide (β-1,3 glucose) produced by *C. uda* biofilms (59).

The glucan and xylan content of the AFEX-CS (28% glucose and 18% xylose equivalents, respectively) was used to estimate the amount of glucose and xylose solubilized by the CBP strain and, therefore, available for fermentation. Glucose and xylose were also measured in the fermentation broth at the end of the incubation period

by HPLC, and these values were used to estimate the amount of sugars that had not been fermented and the fermentation efficiency.

Energy Recovery. Energy recovery η (%) for the simultaneously inoculated MECs was calculated by dividing the energy outputs by energy inputs (54), as described in the following equation:

$$\eta = \frac{W_E + W_H}{(W_{CS} + W_{AFEX})m + W_P} \quad (1)$$

The energy outputs in eq. 1 included the amount of energy recovered as ethanol (W_E), which was calculated as the heat of combustion of the ethanol produced (upper heating value 23.4 MJ/L; (44)), and the energy recovered as H_2 at the cathode (W_H in eq. 1), which was estimated using the heat of combustion of the H_2 (upper heating value 285.83 kJ/mol; (11)). The cathodic H_2 recovery of the system was calculated as the number of moles of H_2 measured in the headspace of the cathode chamber at the end of the experiment divided by the maximum theoretical coulombic H_2 recovery (r_{CE}), which was obtained from the amount of current (I) produced in the MEC as follows:

$$r_{CE} = \frac{\int_0^t I\,dt}{2F} \quad (2)$$

Where F is Faraday's constant and 2 represents the number of moles of electrons per mol of H_2 (11). The energy inputs in eq. 1 included the energy input from AFEX-CS [$(W_{CS} + W_{AFEX})m$], which was determined by the heat of combustion of raw corn stover

(W_{CS}; 10,000 J/g; (54)), and from the AFEX pretreatment process (W_{AFEX}; 300 J/g; B.E. Dale personal communication), and the mass of AFEX-CS (m) consumed over the duration of the experiment. The electricity input from the potentiostat to maintain the cell voltage (W_P in eq. 1) over the duration of the experiment (t) was calculated as

$$W_P = \int_{t=0}^{t} I\ E\ dt \qquad (3)$$

Where I is the measured current and E is the cell voltage (26). The applied potential of the cathode was measured with respect to a reference electrode (3 M Ag/AgCl, Bioanalytical Systems Inc.) inserted into the cathode chamber. The cell voltage was calculated as the difference between the measured cathodic potential and the applied potential at the anode electrode.

Energy recovery for the sequentially inoculated MECs was calculated in a similar way, except that the heat of combustion of the acetate provided (870.28 kJ/mol; (11)) was included to account for the energy input from acetate (W_A), as follows:

$$\eta = \frac{W_E + W_H}{(W_{CS} + W_{AFEX})m + W_P + W_A} \qquad (4)$$

Confocal laser scanning microscopy (CLSM). At the end of the MEC experiments, the anode biofilms were examined by CLSM as previously described (46), except that *G. sulfurreducens* and *C. uda* cells were differentially stained with the BacLight Gram Stain kit (Invitrogen) by following the manufacturer's recommendations. Cells on the AFEX-CS solids were also stained by mixing 200 µl of the resuspended culture with 500 µl of the dye mix prepared in tris buffered saline (TBS). After 15 min of

incubation at room temperature, the supernatant was removed by aspiration and the solids were resuspended in 100 µl TBS, transferred to a Lab-Tek coverglass chamber (Nunc) and imaged with an Olympus FluoView FV1000 inverted microscope equipped with a UPLFLN 10X objective (Olympus, NA 0.30). The excitation wavelength was 488 nm for both dyes. The emission spectra were detected with a BA505-525 band pass filter (SYTO 9, green) and a BA650IF long pass filter (hexidium iodide, red). Image stacks were collected every 2 µm, and image projections were generated using the FV10-ASW 3.0 software (Olympus).

Analytical techniques. The gas composition in the headspace of the culture vessels and of the anode and cathode chambers of the MECs was routinely sampled and analyzed by gas chromatography (GC) using a Varian CP-4900 Micro Gas Chromatograph (Agilent, Santa Clara, CA). Sugars, alcohols and organic acids in culture supernatant fluids or in AFEX-CS acid hydrolysates were measured by HPLC (Waters, Milford, MA) at 30°C, as previously described (32) except that samples were filtered with 0.45 µm syringe filters (National Scientific, Rockwood, TN) prior to analysis. The number of electron equivalents available in each of the fermentation products was calculated by assuming their complete oxidation to CO_2 (mole of electrons available per mole of formate, 2; acetate, 8; lactate and ethanol, 12; and succinate, 14).

RESULTS

CBP of AFEX-CS coupled to fumarate reduction by *G. sulfurreducens*. Fifteen CBP strains grew anaerobically at 35°C with the AFEX-CS substrate in GS2 medium over the course of approximately two weeks (Table 3.1). Four actinobacterial strains had the highest ethanologenic yields (ca. 50% of the maximum theoretical yield) and robust growth (Table 3.1) and produced acetate, formate, lactate and succinate as fermentation byproducts (Table 3.2). Acetate accounted for 80.2% (± 1.8) of all of the electrons potentially available as electron donors for *G. sulfurreducens*, whereas the remaining electrons were distributed between formate (9.0 ± 0.7%), succinate (6.4 ± 2.0%) and lactate (4.4 ± 0.6%). Less than 10 μM of H_2 was detected in the culture headspace. *C. uda* 21399 was selected for further studies based on its robust anaerobic growth (47), co-fermentation of hexose and pentose sugars (14, 31, 36), and well-characterized cellulase and xylanase enzymes (34, 36, 51, 58) and physiology (47).

Table 3.1. Ethanol yields and growth rates for cellulolytic strains grown with 0.2% AFEX-pretreated corn stover [a].

Strain (designation)	Ethanol (% max) [b]	Growth Rate (d^{-1}) [c]
Cellulomonas gelida (ATCC 488)	55.0 (± 4.8)	0.29 (± 0.01)
Cellulosimicrobium cartae (ATCC 21681)	53.0 (± 1.6)	0.31 (± 0.02)
Cellulomonas biazotea (ATCC 486)	50.3 (± 3.3)	0.33 (± 0.02)
Cellulomonas uda (ATCC 21399)	48.6 (± 0.3)	0.32 (± 0.05)
Cellulosilyticum lentocellum (ATCC 27405)	43.0 (± 4.4)	0.35 (± 0.03)
Clostridium phytofermentans (ATCC 700394)	41.0 (± 6.4)	0.18 (± 0.02)
Cellulomonas fimi (ATCC 484)	39.5 (± 2.5)	0.15 (± 0.01)
Cellulomonas uda (ATCC 491)	37.0 (± 8.2)	0.07 (± 0.01)
Cellulomonas flavigena (ATCC 482)	36.4 (± 5.4)	0.18 (± 0.02)
Clostridium cellobioparum (ATCC 15832)	29.0 (± 8.0)	0.03 (± 0.01)
Clostridium cellulolyticum (ATCC 35319)	14.1 (± 7.6)	0.17 (± 0.01)
Clostridium hungatei B3B (ATCC 700213)	13.5 (± 1.0)	0.65 (± 0.05)
Clostridium cellulovorans (ATCC 35296)	12.3 (± 11.2)	0.25 (± 0.02)
Clostridium papyrosolvens C7 (ATCC 700395)	11.1 (± 7.1)	0.98 (± 0.07)
Clostridium papyrosolvens (NCIMB 11394)	ND [d]	0.02 (± 0.09)

[a] Shown are averages and, in parentheses, standard deviations of three replicates.

[b] Percent of maximum theoretical yield from glucose and xylose equivalents in acid-hydrolyzed AFEX-CS provided in the tubes. Based upon a maximum theoretical yield of 0.51 g ethanol per g sugars provided.

[c] Optical density at 660 nm of planktonic growth per day.

[d] ND, not detected.

Table 3.2. Yields of fermentation byproducts produced from 0.2% AFEX-corn stover by the top ethanologens [a].

Strain	Acetate (mM)	Formate (mM)	Lactate (mM)	Succinate (mM)
C. gelida	26.6 (± 0.9)	10.8 (± 0.2)	0.9 (± 0.1)	1.1 (± 0.1)
C. cartae	22.1 (± 2.4)	9.4 (± 0.9)	0.9 (± 0.1)	0.9 (±0.1)
C. biazotea	20.7 (± 2.4)	10.0 (± 1.2)	0.8 (± 0.3)	0.7 (± 0.1)
C. uda 21399	18.9 (± 3.6)	9.3 (± 0.3)	0.6 (± 0.1)	1.3 (± 0.1)

[a] Shown are averages and, in parentheses, standard deviations of three replicates.

The syntrophic growth of *C. uda* and *G. sulfurreducens* was investigated in batch cultures using DB medium (the standard MEC medium) with AFEX-CS as the sole carbon and energy source for *C. uda* and with fumarate serving as the terminal electron acceptor for *G. sulfurreducens* (Fig. 3.1A). The increases in optical density of the coculture and the *C. uda* monoculture both followed a polynomial biphasic distribution (R^2 = 0.991 and 0.975, respectively) as expected of cells that first grow exponentially and then enter stationary phase. Growth rates during the exponential phase of growth (approximately the first 4 days) were similar in the coculture (0.42 ± 0.03 d^{-1}) and the *C. uda* monoculture (0.48 ± 0.08 d^{-1}). However, growth yields were 2.4-fold higher in the coculture (0.50 ± 0.01, OD_{660}) than in the *C. uda* monoculture (0.21 ± 0.01, OD_{660}), as growth was stimulated when the two strains grew syntrophically. At the end of the coculture experiment, *G. sulfurreducens* accounted for 42% (± 7) of the cells in the coculture, suggesting that the growth of the two strains was syntrophically maintained at constant ratios (50:50) throughout the incubation period. No growth was observed in the *Geobacter* monocultures (Fig. 3.1A) or in monocultures of *G. sulfurreducens* in which fumarate had been replaced with acetate (data not shown). Thus, AFEX-CS was not used as either an electron donor or acceptor by *G. sulfurreducens*. Furthermore, doubling times (8.7 ± 0.5 h) and growth yields (0.77 ± 0.05, OD_{660}) in *G. sulfurreducens* monocultures with acetate and fumarate and supplemented with AFEX-CS were similar to cultures without the AFEX-CS (8.7 ± 0.3 h and 0.79 ± 0.04 OD_{660}, respectively), thereby ruling out any growth inhibition or stimulation by the AFEX-CS.

The maximum ethanol concentrations detected over the duration of the experiment were similar in the coculture (1.8 ± 0.1 mM) and the *C. uda* monocultures (1.6 ± 0.4 mM). No fermentation byproducts were detected in the coculture broth during the course of the experiment (Fig. 3.1B), nor was H_2 detected in the headspace of the coculture vessel. In contrast, acetate and formate accumulated in the *C. uda* monocultures (Fig. 3.1B) following the same biphasic polynomial distribution (R^2 = 0.966 and 0.952, respectively) as the optical density of the *C. uda* monoculture (Fig. 3.1A), as expected of a metabolic process coupled to cell growth. The removal of waste fermentation products by *G. sulfurreducens* in the coculture was coupled to the reduction of all of the fumarate to succinate with the transient accumulation of malate (Fig. 3.1C). In contrast, fumarate levels remained constant (ca. 40 mM) in the *C. uda* monocultures, and only fermentative succinate was produced (0.5 ± 0.1 mM). The removal of the organic acids by *G. sulfurreducens* also prevented the acidification of the coculture medium (Fig. 3.1D).

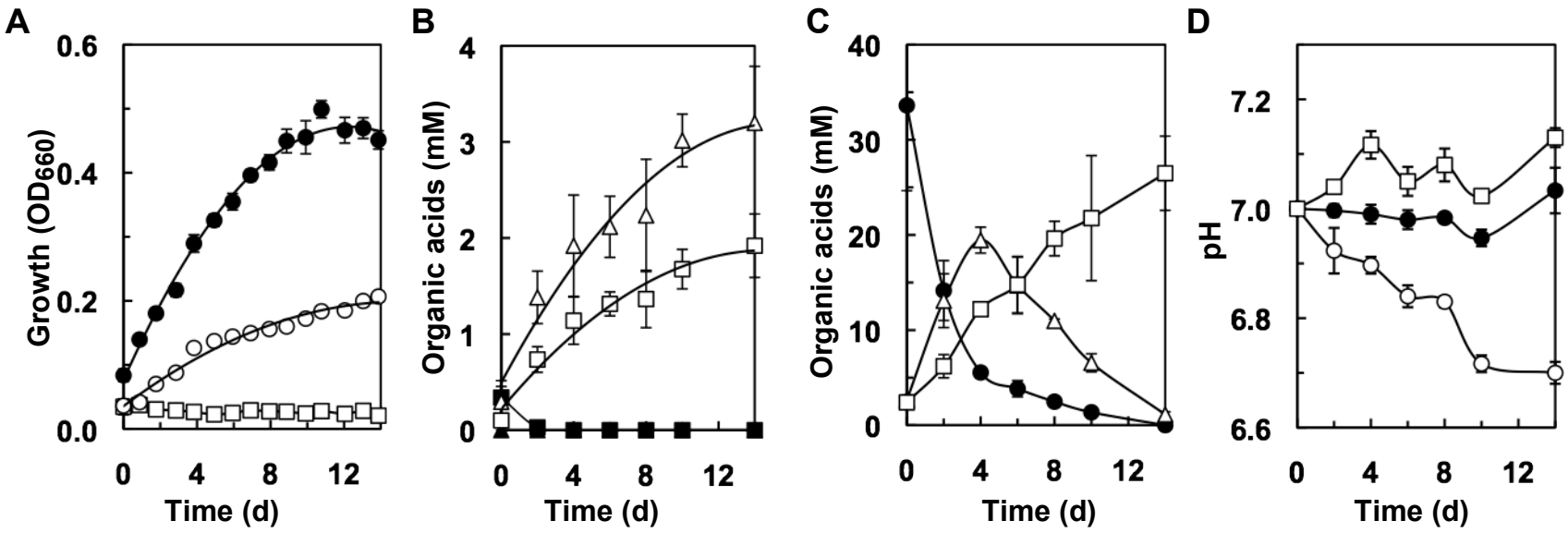

Fig. 3.1: Syntrophic growth of *G. sulfurreducens* and *C. uda* in batch cultures with AFEX-CS and fumarate at 30°C. (A) Growth (OD_{660}) of the coculture (solid circles) and *C. uda* (open circles) or *G. sulfurreducens* (open squares) monocultures. (B) AFEX-CS fermentation products in the coculture (solid symbols) and *C. uda* monoculture (open symbols). Only formate (triangles) and acetate (squares) were detected. (C) Reduction of fumarate (solid circles) to succinate (open squares) with the transient accumulation of malate (open triangles) in cocultures. (D) pH profile in the coculture (solid symbols) and *C. uda* (open circles) or *G. sulfurreducens* (open squares) monocultures.

CBP of AFEX-CS to ethanol in a MEC. We investigated the ability of the binary culture to couple the fermentation of AFEX-CS into ethanol and electricity in a MEC in reference to monoculture MEC controls. Current started soon after the two strains were inoculated simultaneously into anode chambers supplemented with AFEX-CS and increased exponentially (6.3 ± 0.2 mA h^{-1}) until reaching a maximum of 1.0 mA (± 0.1) (Fig. 3.2A). The current then decreased slowly to <0.1 mA over a period of four days, suggesting that growth had become limiting in one or both of the strains. Although some acetate (0.24 ± 0.03 mM in uninoculated controls, Fig. 3.2B) was provided in the AFEX-CS (1, 12), it was too low to support the growth of the anode biofilm of *G. sulfurreducens* and, as a result, no current was produced in MECs driven by *G. sulfurreducens* monocultures (Fig. 3.2A). Similarly, no current was produced in the *C. uda* monocultures (Fig. 3.2A).

Similar amounts of AFEX-CS were hydrolyzed in the *C. uda* monocultures (36 ± 8%) and in the coculture (42 ± 6%) and fermentation efficiencies (~ 99% for glucose and ~ 98% for xylose) were comparable in both. Furthermore, ethanol concentrations increased over the duration of the experiment and reached a similar plateau in both the *C. uda* monoculture (1.8 ± 0.5 mM) and the coculture (1.9 ± 0.6 mM). Acetate (2.2 ± 0.8 mM), formate (2.9 ± 1 mM), lactate (0.3 ± 0.1 mM) and succinate (0.6 ± 0.2 mM) accumulated in the *C. uda* monocultures but were removed in the coculture (Fig. 3.2B). Overall, 51% of the total electrons available through fermentation in the coculture were recovered as ethanol, 42% were diverted to current, and 7% remained as unutilized fermentation byproducts (Fig. 3.2B). Of the fermentation byproducts removed by *G. sulfurreducens,* approximately 60% were utilized for current production with the

remaining 40% being used to support the growth of the *G. sulfurreducens* anode biofilm. As a result, the net yield of moles of electrons recovered as current or fermentation products in the coculture MEC was lower than in the monoculture (Fig. 3.2B).

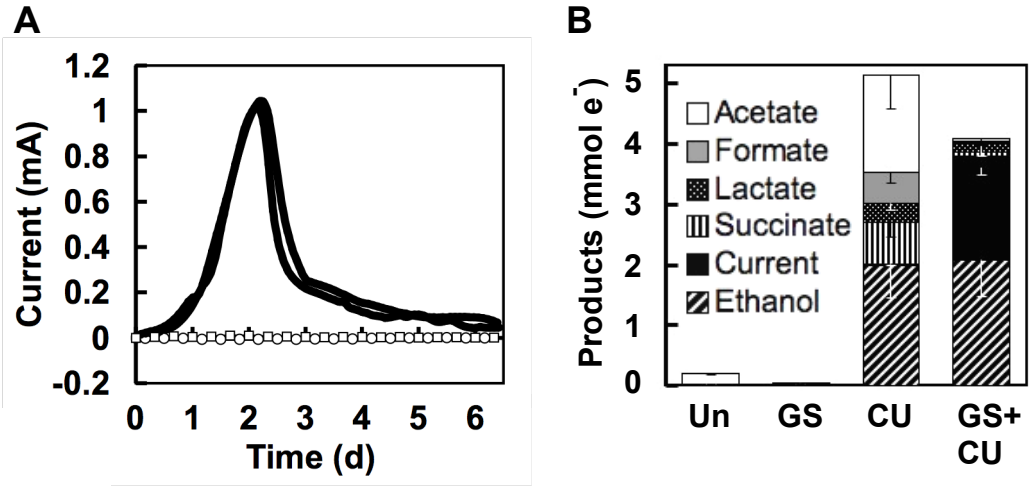

Fig. 3.2: Simultaneous inoculation of *G. sulfurreducens* and *C. uda* in MECs with AFEX-CS. (A) Current production by the coculture in two representative MECs (solid lines) and in controls with *G. sulfurreducens* (open circles) or *C. uda* (open squares) monocultures. (B) Yields of current and fermentation products (expressed in electron equivalents, mmol e^-) in the MECs described in (A). Shown are averages and standard deviations of three independent MECs for each. Un, uninoculated; GS, *G. sulfurreducens* monoculture; CU, *C. uda* monoculture; GS+CU, *G. sulfurreducens* and *C. uda* coculture.

The energy recovery from the fermentation of AFEX-CS to ethanol by the *C. uda* monocultures, which considered the energy outputs from the heat of combustion of ethanol and the energy inputs from the AFEX pretreatment of corn stover, was 32% (± 2) (Fig. 3.4). Despite the electrical input resulting from applying the MEC potential, energy recoveries from fermentation alone were similar (30 ± 9%) in the MEC-driven by the coculture. However, approximately 72% of the moles of H_2 that are theoretically possible from the measured current were also recovered as H_2 fuel in the headspace of the cathode chamber of the coculture MEC. When the energy output from the heat of combustion of the cathodic H_2 was included in the calculations, the energy recovery from the AFEX-CS in the MEC increased to 45% (± 10) (Fig. 3.4).

We also investigated the performance of the MEC platform when the microbial catalysts were sequentially inoculated, as previously reported for a binary culture of *C. cellulolyticum* and *G. sulfurreducens* (40). *G. sulfurreducens* anode biofilms produced some current from AFEX-CS in the MECs (Fig. 3.3A), due to the availability of AFEX-CS-derived acetate as an electron donor (0.17 ± 0.02 mmol e^-). However, substantially more current (2.0 ± 0.3 mmol e^-) was produced in the MECs inoculated with *C. uda* due to the syntrophic growth of the strains (Fig. 3.3A). Approximately, 28% (± 6) of the AFEX-CS was degraded in the coculture-driven MEC, which is lower than the hydrolysis efficiencies measured with the simultaneous strategy. Fermentation efficiencies (~ 99% for glucose and ~ 96% for xylose) were similar to those obtained in the simultaneous inoculation. Maximum ethanol yields (2.1 ± 0.6 mM) were also similar, yet approximately half of the succinate (0.3 ± 0.1 mM) produced in the *C. uda* monocultures accumulated

in the fermentation broth (Fig. 3.3B). Overall, the ethanol:current ratio (48:41% of all the electron equivalents available from fermentation) was similar as in the simultaneously inoculated platform (51:42%), but more electrons (11%) were lost to unutilized fermentation byproducts, mostly succinate (Fig. 3.3B). Succinate is not an electron donor for *G. sulfurreducens* but can be assimilated for carbon. As the anode biofilms were pre-grown with acetate, the carbon demands of the biofilms were low and less succinate was removed. Yet a higher percentage of the electrons in the fermentation products removed by *G. sulfurreducens* were converted into electrical current (69%) in the sequentially-inoculated MEC compared to the simultaneous inoculation strategy (60%), with the remaining (31%) being used for cell growth. As a result, the energy recovery as ethanol and H_2 in the MEC (49 ± 12%) was within the ranges calculated for the simultaneously inoculated MECs and was almost twice the energy recovery calculated for the fermentation to ethanol alone (29 ± 12%) (Fig. 3.4).

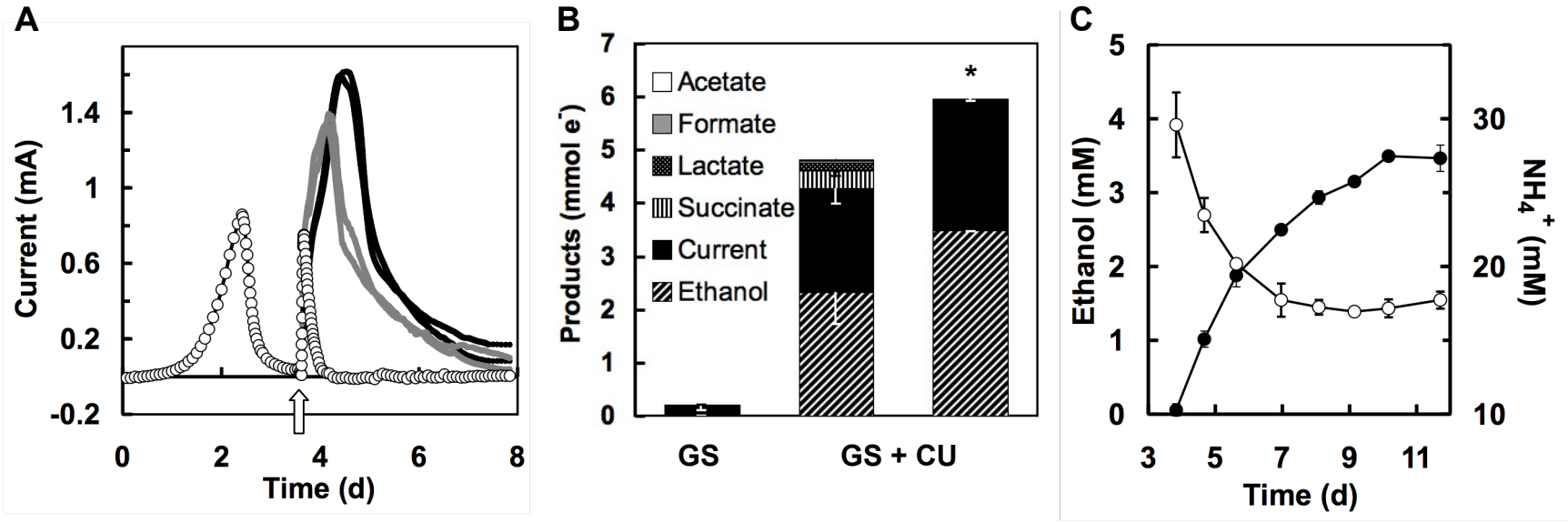

Fig. 3.3: Sequential inoculation of *G. sulfurreducens* and *C. uda* in MECs. (A) Current production by a *G. sulfurreducens* monoculture driven by an initial acetate supplementation and then by the residual acetate in AFEX-CS (open circles), which was added while exchanging the medium (arrow). Inoculating the MEC with *C. uda* during the media exchange increased and further sustained current production (gray solid lines, two representative experiments shown). Supplementing the AFEX-CS media with 35 mM NH_4Cl in the coculture increased electricity production further (black solid lines, two representative experiments shown). (B) Yields of current and fermentation products (expressed in electron equivalents, mmol e^-) measured in the anode chamber of MECs driven by the *G. sulfurreducens* monoculture (GS) and

the cocultures (GS+CU) without or with (star) NH_4Cl supplementation. (C) Ethanol production (solid symbols) from AFEX-CS and nitrogen assimilation (NH_4^+ equivalents, open symbols) in MECs supplemented with NH_4Cl.

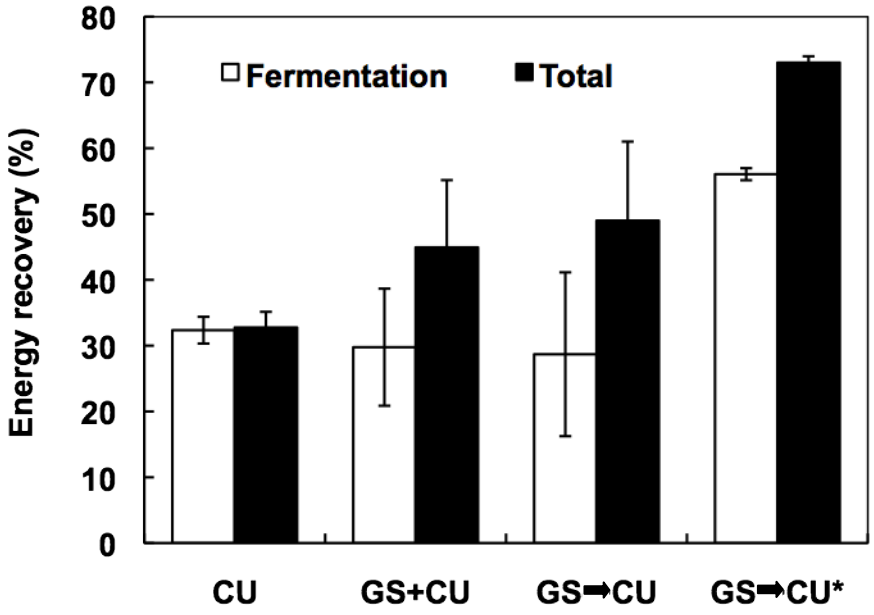

Fig. 3.4: Energy recoveries from AFEX-CS as ethanol (fermentation, open columns) or ethanol and cathodic H_2 (total, solid columns) in MECs driven by *C. uda* (CU) or by cocultures of *G. sulfurreducens* and *C. uda* inoculated simultaneously (GS+CU) or sequentially (GS→CU). The sequential coculture labeled with a star (*) was grown in medium supplemented with 35 mM NH_4Cl.

Stimulation of ethanol production in a MEC supplemented with nitrogen. Interestingly, the inoculation strategy did not affect the composition of the anode biofilms, which had confluent biofilms of mostly *G. sulfurreducens* cells (Fig. 3.5A and B), and the anode biofilms had, in both cases, more biomass than in the *G. sulfurreducens* monocultures (Fig. 3.5C). *C. uda* cells did not attach to the bare anode electrodes in the *C. uda* monocultures (Fig. 3.5D), and preferentially grew planktonically or as biofilms on the AFEX-CS solids (Fig. 3.5E). Acid hydrolysates of the AFEX-CS biofilms also contained glucose levels 1.25-fold higher than the glucan content provided in the initial amount of AFEX-CS. This is consistent with the acid hydrolysis of the curdlan (β-1,3 glucan) biofilm matrix of *C. uda*. As the curdlan matrix that enables *C. uda* cells to specifically attach to cellulosic substrates is induced when nitrogen is growth-limiting (59), we investigated if nitrogen availability limited the growth and metabolism of *C. uda* in the MEC driven by the coculture. For these experiments, we used a sequential inoculation strategy and pre-grew *G. sulfurreducens* anode biofilms with the standard low nitrogen medium and with acetate as electron donor. Once the current declined, the anode medium was replaced with AFEX-CS medium supplemented with 35 mM NH_4Cl (ca. 10-times the NH_4Cl concentration in the standard MEC medium, Fig. 3.6). After inoculating the anode chamber with *C. uda*, current increased to approximately 1.6 mA and then slowly decreased as all the fermentation byproducts were utilized (Fig. 3.3A). Hydrolysis efficiencies increased (46 ± 1%) to levels comparable to those measured in the simultaneously-inoculated MECs. Furthermore, ethanol yields were almost twice those measured in any of MEC platforms and all of the fermentation byproducts were converted into current (Fig. 3.3B). Ethanol

production and nitrogen assimilation occurred simultaneously and ethanol production reached a plateau once nitrogen assimilation stopped (Fig. 3.3C). The data thus support our original hypothesis that nitrogen availability limited the growth and metabolism of *C. uda* in the MECs. As a result, nitrogen supplementation alleviated the growth limitation of *C. uda* and promoted the hydrolysis of AFEX-CS and ethanologenesis. This resulted in two-fold increases in the energy recoveries from the fermentation of AFEX-CS to ethanol (56 ± 1%) (Fig. 3.4). Furthermore, by stimulating the electrical conversion of all the fermentation byproducts, nitrogen supplementation also minimized electron losses and resulted in high (73 ±1%) energy recoveries as ethanol and cathodic H_2 (Fig. 3.4).

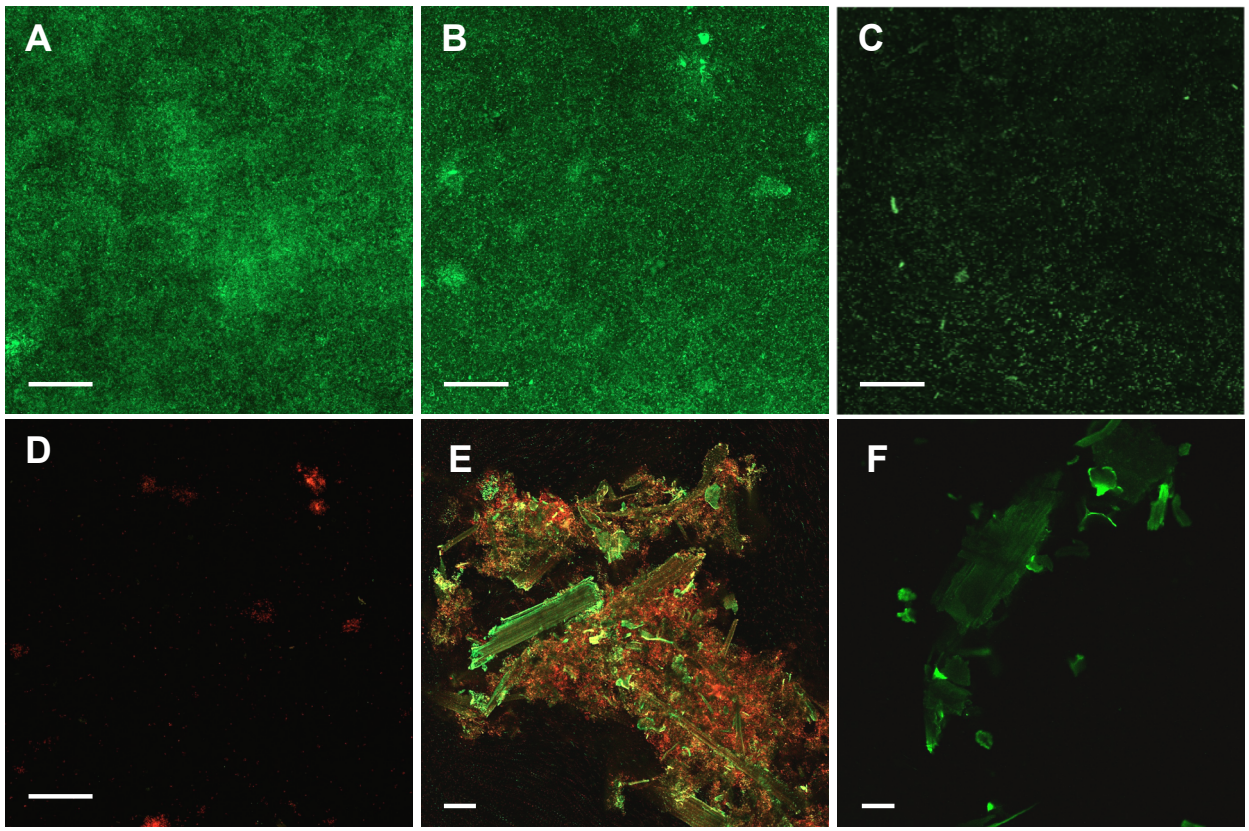

Fig. 3.5: CLSM micrograph projections of biofilms on the anode electrode (A-D) and AFEX-CS solids (E-F) in MECs of simultaneously (A) or sequentially (B) inoculated cocultures and of *G. sulfurreducens* (C) or *C. uda* (D and E) monocultures. The autofluorescence of the AFEX-CS solids from uninoculated MEC controls is shown in (F). *G. sulfurreducens* cells stained green with SYTO 9 and the Gram-positive cells of *C. uda* stained red with hexidium iodide. Bar, 50 µm.

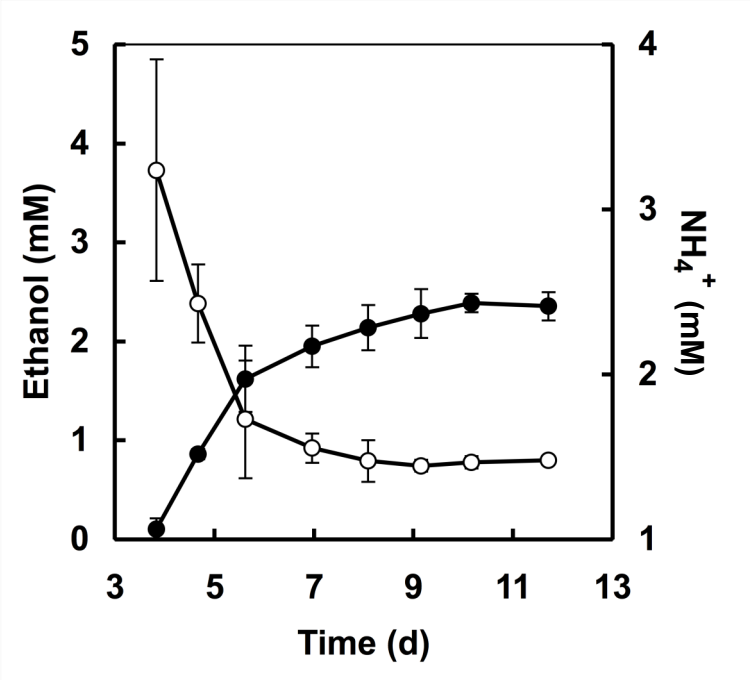

Fig. 3.6: Ethanol production (closed circles) coupled to nitrogen assimilation (NH_4^+ equivalents, open circles) in a MEC sequentially inoculated with *G. sulfurreducens* and *C. uda* using the standard MEC medium (DB medium).

DISCUSSION

The results show that the CBP of AFEX-CS to ethanol can be achieved with high energy recoveries in a MEC driven by a defined binary culture selected for its robust saccharification of AFEX-CS, ethanologenesis and electrochemical removal of waste fermentation products. The identification of a range of native CBP microorganisms from the Actinobacteria and Firmicutes groups with robust growth and high yields of ethanol with AFEX-CS is consistent with previous studies indicating that the AFEX pretreatment increases the digestibility of lignocellulose substrates (23, 42, 43) while minimizing the release of toxic byproducts (12). *C. uda*, in particular, had robust growth and produced high yields of ethanol with AFEX-CS. In addition, it produced fermentation byproducts (acetate, formate and lactate) that serve as electron donors for the exoelectrogen *G. sulfurreducens* (7, 9, 46). As a result, a MEC driven by the defined binary culture composed of *C. uda* and *G. sulfurreducens* converted AFEX-CS into ethanol while minimizing electron losses to waste fermentation products that limited the performance of previous MFC platforms (38, 40, 53). The removal of waste organic acids from the fermentation broth by *G. sulfurreducens* also prevented the acidification of the medium and the accumulation of feedback inhibitors. Acetate, in particular, is a noncompetitive inhibitor of cellobiose metabolism in *C. uda*, presumably because it interferes with cellobiose uptake (15). Hence, its removal by the exoelectrogen promotes the uptake of cellobiose by *C. uda* and also prevents cellobiose accumulation, which would otherwise feedback-inhibit cellulase synthesis (5).

Despite the electrical input in the MEC and the energy input required to pretreat the corn stover, total energy recoveries as ethanol and cathodic H_2 averaged 47% in

systems run with the standard (low nitrogen) medium that is routinely used to support the growth and electroactivity of the exoelectrogen *G. sulfurreducens* on the anode electrode (46). These recoveries are significantly higher than those reported in MFCs fed with raw (3.6%) or steam-pretreated (2%) corn stover, where only power is generated (54). Thus, ethanol production from AFEX-CS in a MEC, with the added value of converting current into H_2 at the cathode, is a competitive platform.

Ethanol yields were similar in MECs run with the standard medium when the strains were inoculated simultaneously (Fig. 3.2) or sequentially (Fig. 3.3). Each strategy has its own advantages. For example, more AFEX-CS was hydrolyzed in the simultaneous platform but fewer molar electron equivalents (ca. 86%) were recovered from the substrate that was hydrolyzed, as more of the fermentation byproducts were used as carbon sources and electron donors to sustain the growth of the anode biofilm. The simultaneous platform also simplifies MEC operation with the coinoculation of the strains, which reduces operational costs and the risk of contamination. On the other hand, a higher percentage of the electrons in the fermentation products were converted into electrical current (69%) in the sequentially-inoculated MEC and less were diverted to support cell growth. However, fermentation byproducts such as succinate were left unutilized, which could have had a feedback-inhibitory effect on sugar fermentation and hydrolysis efficiency (15).

The observation that *C. uda* biofilms formed on the AFEX-CS solids (Fig. 3.5) suggested that nitrogen availability in the MEC medium limited growth. This CBP bacterium secretes free cellulases to degrade lignocellulose substrates. However, cell-associated cellulases are expressed when nitrogen becomes growth-limiting and

function as cell adhesins for the specific colonization of cellulosic substrates (59). Although the biofilms continue to degrade the substrate, nitrogen limitation redirects fermentable sugars towards the synthesis of a curdlan biofilm matrix (59). Consistent with this, supplementing the MEC medium with excess nitrogen alleviated the growth limitation of *C. uda* and promoted the hydrolysis of AFEX-CS and ethanologenesis in the sequential platform. Nitrogen supplementation of the growth medium was also reportedly necessary to increase ethanol yields and AFEX-CS hydrolysis efficiencies by the CBP microorganism *C. phytofermentans*, which the authors attributed to the high energy demand derived from the secretion of hydrolytic enzymes (22). Overall, nitrogen supplementation in the MECs resulted in two-fold increases in energy recoveries from ethanologenesis alone (Fig. 3.4). It also promoted the removal and electrical conversion of all the fermentation byproducts and further increased the total energy recoveries as ethanol and cathodic H_2 to 73% (±1) (Fig. 3.4). Interestingly, nitrogen assimilation by *C. uda* stopped before all the available nitrogen was used (Fig. 3.3C), suggesting that other factors limited the growth of the CBP partner in the MECs over time. As ethanol production occurred simultaneously with nitrogen assimilation (Fig. 3.3C), further optimization of culturing parameters is likely to improve AFEX-CS hydrolysis and ethanol yields and the overall performance of the platform.

The MEC platform fed with AFEX-CS and described herein addresses the need to decouple bioenergy production from the food supply, to reduce processing costs through the use of lignocellulosic substrates, and to carry out a single-step hydrolysis and fermentation while minimizing the accumulation of low-value fermentation byproducts that can also function as feedback inhibitors (29). Relatively simple culturing

approaches such as nitrogen supplementation were sufficient to improve the growth of the CBP partner and the electrical conversion of waste fermentation products by the exoelectrogen in the MEC. Hence, further optimization of the culturing conditions shows promise to increase the activity of the microbial catalysts so as to improve the performance of the platform. This, and the possibility of genetically engineering and/or adaptively evolving the microbial catalysts for improved hydrolysis, saccharification, and electrical conversion, suggests that the processing of lignocellulose substrates in MECs can provide an economically and environmentally attractive CBP technology for ethanol and H_2.

REFERENCES

REFERENCES

1. **Aden, A., M. Ruth, K. Ibsen, J. Jechura, K. Neeves, J. Sheehan, B. Wallace, L. Montague, A. Slayton, and J. Lukas.** 2002. Lignocellulosic biomass to ethanol process design and economics utilizing co-current dilute acid prehydrolysis and enzymatic hydrolysis for corn stover Technical Report NREL/TP-510-32438. National Renewable Energy Laboratory.

2. **Alizadeh, H., F. Teymouri, T. I. Gilbert, and B. E. Dale.** 2005. Pretreatment of switchgrass by ammonia fiber explosion (AFEX). Appl. Biochem. Biotechnol. **121-124:**1133-41.

3. **Balan, V., L. da Costa Sousa, Chundawat, S. P. S. , D. Marshall, L. N. Sharma, C. K. Chambliss, and B. E. Dale.** 2009. Enzymatic digestibility and pretreatment degradation products of AFEX-treated hardwoods (*Populus nigra*). Biotechnol. Prog. **25:**365-375.

4. **Balat, M., H. Balat, and C. Öz.** 2008. Progress in bioethanol processing. Progr. En. Combust. Sc. **34:**551-573.

5. **Beguin, P., and H. Eisen.** 1977. Free and cellulose-bound cellulases in a *Cellulomonas* species. J. Gen. Microbiol. **101:**191-196.

6. **Bond, D. R., D. E. Holmes, L. M. Tender, and D. R. Lovley.** 2002. Electrode-reducing microorganisms that harvest energy from marine sediments. Science **295:**483-485.

7. **Bond, D. R., and D. R. Lovley.** 2003. Electricity production by *Geobacter sulfurreducens* attached to electrodes. Appl. Environ. Microbiol. **69:**1548-55.

8. **Borole, A. P., J. R. Mielenz, T. A. Vishnivetskaya, and C. Y. Hamilton.** 2009. Controlling accumulation of fermentation inhibitors in biorefinery recycle water using microbial fuel cells. Biotechnol. Biofuels. **2:**7.

9. **Call, D. F., and B. E. Logan.** 2011. Lactate oxidation coupled to iron or electrode reduction by *Geobacter sulfurreducens* PCA. Appl. Environ. Microbiol. **77:**8791-4.

10. **Cavedon, K., S. B. Leschine, and E. Canale-Parola.** 1990. Cellulase system of a free-living, mesophilic *clostridium* (strain C7). J. Bacteriol. **172:**4222-30.

11. **Cheng, S., and B. E. Logan.** 2007. Sustainable and efficient biohydrogen production via electrohydrogenesis. Proc. Nat. Acad. Sci. USA **104:**18871-18873.

12. **Chundawat, S. P., R. Vismeh, L. N. Sharma, J. F. Humpula, L. da Costa Sousa, C. K. Chambliss, A. D. Jones, V. Balan, and B. E. Dale.** 2010. Multifaceted characterization of cell wall decomposition products formed during ammonia fiber expansion (AFEX) and dilute acid based pretreatments. Bioresour. Technol. **101:**8429-38.

13. **Dale, B. E., C. K. Leong, T. K. Pham, V. M. Esquivel, I. Rios, and V. M. Latimer.** 1996. Hydrolysis of lignocellulosics at low enzyme levels: application of the AFEX process. Biores. Technol. **56:**111-116.

14. **Dermoun, Z., and J. P. Belaich.** 1985. Microcalorimetric study of cellulose degradation by *Cellulomonas uda* ATCC 21399. Biotechnol. Bioeng. **27:**1005-11.

15. **Dermoun, Z., C. Gaudin, and J. P. Belaich.** 1988. Effects of end-product inhibition of *Cellulomonas uda* anaerobic growth on cellobiose chemostat culture. J. Bacteriol. **170:**2827-31.

16. **Finneran, K. T., and D. R. Lovley.** 2001. Anaerobic degradation of methyl tert-butyl ether (MTBE) and tert-butyl alcohol (TBA). Environ. Sci. Technol. **35:**1785-90.

17. **Galbe, M., and G. Zacchi.** 2007. Pretreatment of lignocellulosic materials for efficient bioethanol production. Adv. Biochem. Eng. Biotechnol. **108:**41-65.

18. **Gao, D., S. P. Chundawat, C. Krishnan, V. Balan, and B. E. Dale.** 2010. Mixture optimization of six core glycosyl hydrolases for maximizing saccharification of ammonia fiber expansion (AFEX) pretreated corn stover. Bioresour. Technol. **101:**2770-81.

19. **Geelhoed, J. S., H. V. Hamelers, and A. J. Stams.** 2010. Electricity-mediated biological hydrogen production. Curr. Opin. Microbiol. **13:**307-15.

20. **Heaton, E. A., R. B. Flavell, P. N. Mascia, S. R. Thomas, F. G. Dohleman, and S. P. Long.** 2008. Herbaceous energy crop development: recent progress and future prospects. Curr. Opin. Biotechnol. **19:**202-9.

21. **Hendriks, A. T. W. M., and G. Zeeman.** 2009. Pretreatments to enhance the digestibility of lignocellulosic biomass. Bioresour. Technol. **100:**10-18.

22. **Jin, M., V. Balan, C. Gunawan, and B. E. Dale.** 2011. Consolidated bioprocessing (CBP) performance of *Clostridium phytofermentans* on AFEX-treated corn stover for ethanol production. Biotechnol. Bioeng. **108:**1290-7.

23. **Lau, M. W., and B. E. Dale.** 2009. Cellulosic ethanol production from AFEX-treated corn stover using *Saccharomyces cerevisiae* 424A(LNH-ST). Proc. Natl. Acad. Sci. USA **106:**1368-73.

24. **Lau, M. W., B. E. Dale, and V. Balan.** 2008. Ethanolic fermentation of hydrolysates from ammonia fiber expansion (AFEX) treated corn stover and distillers grain without detoxification and external nutrient supplementation. Biotechnol. Bioeng. Symp. **99:**529-39.

25. **Leschine, S. B.** 1995. Cellulose degradation in anaerobic environments. Annu. Rev. Microbiol. **49:**399-426.

26. **Logan, B. E.** 2008. Microbial fuel cells. Wiley-Interscience, Hoboken, N.J.

27. **Lu, Y., R. Warner, M. Sedlak, N. Ho, and N. S. Mosier.** 2009. Comparison of glucose/xylose cofermentation of poplar hydrolysates processed by different pretreatment technologies. Biotechnol. Prog. **25:**349-356.

28. **Lynd, L. R.** 1996. Overview and evaluation of fuel ethanol from cellulosic biomass: Technology, economics, the environment, and policy. Annu. Rev. Energy Env. **21:**403–465.

29. **Lynd, L. R., M. S. Laser, D. Bransby, B. E. Dale, B. Davidson, R. Hamilton, M. Himmel, M. Keller, J. D. McMillan, J. Sheehan, and C. E. Wyman.** 2008. How biotech can transform biofuels. Nat. Biotechnol. **26:**169-172.

30. **Lynd, L. R., P. J. Weimer, W. H. van Zyl, and I. S. Pretorius.** 2002. Microbial cellulose utilization: fundamentals and biotechnology. Microbiol. Mol. Biol. Rev. **66:**506-77.

31. **Marschoun, S., P. Rapp, and F. Wagner.** 1987. Metabolism of hexoses and pentoses by *Cellulomonas uda* under aerobic conditions and during fermentation. Can. J. Microbiol. **33:**1024-1031.

32. **McKinlay, J. B., J. G. Zeikus, and C. Vieille.** 2005. Insights into *Actinobacillus succinogenes* fermentative metabolism in a chemically defined growth medium. Appl. Environ. Microbiol. **71:**6651-6.

33. **Moniruzzaman, M., B. E. Dale, R. B. Hespell, and R. J. Bothast.** 1997. Enzymatic hydrolysis of high moisture corn fiber pretreated by AFEX and recovery and recycle of the enzyme complex. Appl. Biochem. Biotechnol. **67:**113-126.

34. **Nakamura, K., and K. Kitamura.** 1988. Cellulases of *Cellulomonas uda*. Methods Enzymol. **160:**211-216.

35. **Perlack, R., L. L. Wright, A. F. Turhollow, R. L. Graham, B. J. Stokes, and D. C. Erbach.** 2005. Biomass as feedstock for bioenergy and bioproducts industry: The technical feasibility of a billion-ton annual supply, DOE/GO-102995-2135, ORNL/TM-2005/66. U.S. Department of Energy and U.S. Department of Agriculture.

36. **Rapp, P., and F. Wagner.** 1986. Production and properties of xylan-degrading enzymes from *Cellulomonas uda*. Appl. Environ. Microbiol. **51:**746-752.

37. **Reguera, G., K. P. Nevin, J. S. Nicoll, S. F. Covalla, T. L. Woodard, and D. R. Lovley.** 2006. Biofilm and nanowire production lead to increased current in microbial fuel cells. Appl. Environ. Microbiol. **72:**7345-7348.

38. **Ren, Z., L. M. Steinberg, and J. M. Regan.** 2008. Electricity production and microbial biofilm characterization in cellulose-fed microbial fuel cells. Water Sci. Technol. **58:**617-622.

39. **Ren, Z., T. E. Ward, B. E. Logan, and J. M. Regan.** 2007. Characterization of the cellulolytic and hydrogen-producing activities of six mesophilic *Clostridium* species. J. Appl. Microbiol. **103:**2258-66.

40. **Ren, Z., T. E. Ward, and J. M. Regan.** 2007. Electricity production from cellulose in a microbial fuel cell using a defined binary culture. Environ. Sci. Technol. **41:**4781-6.

41. **Rezaei, F., D. Xing, R. Wagner, J. M. Regan, T. L. Richard, and B. E. Logan.** 2009. Simultaneous cellulose degradation and electricity production by *Enterobacter cloacae* in a microbial fuel cell. Appl. Environ. Microbiol. **75:**3673-8.

42. **Shao, Q., S. P. Chundawat, C. Krishnan, B. Bals, C. Sousa Lda, K. D. Thelen, B. E. Dale, and V. Balan.** 2010. Enzymatic digestibility and ethanol fermentability of AFEX-treated starch-rich lignocellulosics such as corn silage and whole corn plant. Biotechnol. Biofuels **3:**12.

43. **Shao, X., M. Jin, A. Guseva, C. Liu, V. Balan, D. Hogsett, B. E. Dale, and L. Lynd.** 2011. Conversion for Avicel and AFEX pretreated corn stover by *Clostridium thermocellum* and simultaneous saccharification and fermentation: insights into microbial conversion of pretreated cellulosic biomass. Bioresour. Technol. **102:**8040-5.

44. **Shapouri, H., J. A. Duffield, and M. Wang.** 2003. The energy balance of corn ethanol revisited. Transactions of the ASAE **46:**959-968.

45. **Sluiter, A., B. Hames, R. Ruiz, C. Scarlata, J. Sluiter, D. Templeton, and D. Crocker.** 2008. Determination of structural carbohydrates and lignin in biomass: Laboratory analytical procedure (LAP). National Renewable Energy Laboratory.

46. **Speers, A. M., and G. Reguera.** 2012. Electron donors supporting growth and electroactivity of *Geobacter sulfurreducens* anode biofilms. Appl. Environ. Microbiol. **78:**437-44.

47. **Stackebrandt, E., P. Schumann, and H. Prauser.** 2006. The family *Cellulomonadaceae*, p. 983-1001. *In* M. Dworkin (ed.), Prokaryotes, 3rd ed, vol. 3. Springer, Singapore.

48. **Sun, Y., and J. Cheng.** 2002. Hydrolysis of lignocellulosic materials for ethanol production: a review. Bioresour. Technol. **83:**1-11.

49. **Teymouri, F., L. Laureano-Perez, H. Alizadeh, and B. E. Dale.** 2005. Optimization of the ammonia fiber explosion (AFEX) treatment parameters for enzymatic hydrolysis of corn stover. Bioresour. Technol. **96:**2014-8.

50. **US Department of Energy.** 2006. Breaking the biological barriers to cellulosic ethanol: A joint research agenda. Report from the December 2005 Workshop, DOE/SC-0095. U.S. Department of Energy Office of Science (www.genomicscience.energy.gov/biofuels/).

51. **Van Hoorebeke, A., J. Stout, J. Kyndt, M. De Groeve, I. Dix, T. Desmet, W. Soetaert, J. Van Beeumen, and S. N. Savvides.** 2010. Crystallization and X-ray diffraction studies of cellobiose phosphorylase from *Cellulomonas uda*. Acta Crystallogr. F **66:**346-351.

52. **van Zyl, W. H., L. R. Lynd, R. den Haan, and J. E. McBride.** 2007. Consolidated bioprocessing for bioethanol production using *Saccharomyces cerevisiae*. Adv. Biochem. Eng. Biotechnol. **108:**205-35.

53. **Wang, A. J., D. Sun, G. L. Cao, H. Y. Wang, N. Q. Ren, W. M. Wu, and B. E. Logan.** 2011. Integrated hydrogen production process from cellulose by combining dark fermentation, microbial fuel cells, and a microbial electrolysis cell. Bioresour. Technol. **102:**4137-4143.

54. **Wang, X., Y. J. Feng, H. M. Wang, Y. P. Qu, Y. L. Yu, N. Q. Ren, N. Li, E. Wang, H. Lee, and B. E. Logan.** 2009. Bioaugmentation for electricity generation from corn stover biomass using microbial fuel cells. Environ. Sci. Technol. **43:**6088-6093.

55. **Wolin, M. J.** 1982. Hydrogen transfer in microbial communities. *In* A. T. Bull and J. H. Slater (ed.), Microbial interactions and communities, vol. 1. Academic Press, London.

56. **Wyman, C. E., B. E. Dale, R. T. Elander, M. Holtzapple, M. R. Ladisch, and Y. Y. Lee.** 2005. Coordinated development of leading biomass pretreatment technologies. Bioresour. Technol. **96:**1959-1966.

57. **Yang, B., and C. E. Wyman.** 2008. Pretreatment: the key to unlocking low-cost cellulosic ethanol. Biofuels Bioprod. Bioref. **2:**26-40.

58. **Yoon, M. H., and W. Y. Choi.** 2007. Characterization and action patterns of two beta-1,4-glucanases purified from *Cellulomonas uda* CS1-1. J. Microbiol. Biotechnol. **17:**1291-1299.

59. **Young, J. M., S. B. Leschine, and G. Reguera.** 27 September 2011. Reversible control of biofilm formation by *Cellulomonas* spp. in response to nitrogen availability. Environ. Microbiol. **14**: 594-604.

Chapter 4.
Fermentation of glycerol into ethanol and simultaneous hydrogen production in bioelectrochemical systems.

The material presented in this chapter was generated through equal collaboration with Jenna M. Young. All experiments were a joint effort except for adaptive evolution experiments with *Clostridium cellobioparum,* which were performed by J.M.Y., and adaptive evolutions experiments with *Geobacter sulfurreducens* and MFC experiments*,* which were performed by A.M.S.

ABSTRACT

Biodiesel is a liquid transportation fuel alternative to petrodiesel produced from plant, algae or animal oils. The major waste product from biodiesel production is wastewater containing glycerol and residual methanol or ethanol, which requires significant capital investment for its cleanup and disposal. *Clostridium cellobioparum* was identified from a screening of known fermentative strains for its ability to ferment glycerol into ethanol with high conversion efficiencies, as well as producing fermentative byproducts (formate, hydrogen, acetate and lactate) which could be utilized by the electrogen, *Geobacter sulfurreducens*, for electricity production in bioelectrochemical systems (BESs). Adaptive evolution was used to generate strains of the syntrophic partners, which could grow with industrially-relevant concentrations of glycerol (10% w/v). When the evolved strains were cocultured in batch culture and in BESs, glycerol fermentation was coupled syntrophically with the reduction of fumarate or electrodes. The growth of the coculture in microbial electrolysis cells (MECs) resulted in the production of cathodic H_2, and growth in microbial fuel cells (MFCs) resulted in current production. Improvements in glycerol consumption as well as metabolic shifts from ethanol to 1,3-propanediol fermentation were seen in both BES platforms compared with *C. cellobioparum* monocultures. Optimization of the platform in MECs by increasing buffering to stabilize the pH and removal of fermentative H_2 and CO_2 resulted in glycerol consumption of ca. 50 g/L, making this an attractive platform for the treatment of glycerol-containing waste water.

INTRODUCTION

Renewable fuel alternatives such as biodiesel are being developed to reduce dependence on dwindling petroleum resources and to keep up with the increasing energy demands of both established and burgeoning economies. Approximately 60% of the oil used globally each year is consumed by the transportation sector, and the global energy demands are expected to continue increasing by 1.8% per year, while petroleum reserves are predicted to be exhausted in the next century (1). Biodiesel is a transportation fuel alternative that can be used alone or in combination with petroleum-derived diesel fuel. Biodiesel has several beneficial characteristics compared with conventional diesel including a lower toxicity and higher biodegradability (47), a high cetane rating (45-70; (51)) which reflects a lower ignition point following fuel injection (1), a higher flash point enabling it to be classified as a non-hazardous fuel (51), a higher lubricity which reduces long-term engine wear (12, 25), and lower emissions of sulfates, carbon monoxide, particulates, hydrocarbons, and aromatic compounds (47). Additionally, burning biodiesel contributes only small amounts of net atmospheric CO_2 due to the closed loop of the CO_2 cycle (35). There are however, some challenges to biodiesel usage, including a heat of combustion that is 6.6% lower than conventional diesel, poor performance in cold temperatures, higher emissions of nitrogen oxides (NO_x), and faster fuel degradation by both oxidation and microbial contamination (51). If biodiesel blends above 20% are used, engine modifications are required to facilitate fuel injections due to the 10-15 times higher viscosity of the biodiesel (1), as well as to prevent corrosion (51).

Biodiesel can be produced from a wide variety of sources including edible and non-edible plant oils, animal fats, and oils derived from microbes (1). The feedstock represents at least 75% of the cost of biodiesel production and high feedstock costs are one of the greatest challenges to the economic sustainability of biodiesel (32). Oil derived from microalgae is expected to be the next generation feedstock for biodiesel production. Microalgae are especially efficient at converting solar energy to biomass (57), and have the highest potential oil yields per land area (58,700-136,900 L ha^{-1} $year^{-1}$) of any feedstock (1). They are also an attractive option because they can grow with low nutrient input and in saline or harsh conditions, and they do not compete with food crops for land (57). The greatest challenge to successful cultivation of microalgae is to reduce the energy inputs required to sustain rapid cell growth and high oil yields while scaling the technology into commercial bioreactors (41). If these challenges are overcome, microalgal oils are likely to be the feedstock with the greatest potential to supply the global biodiesel supply chain (1).

Triacylglycerol feedstocks are most commonly converted to biodiesel (alkyl esters) by transesterification (Fig. 4.1) with a short-chain alcohol and an alkaline catalyst such as NaOH (2). Methanol is the most widely used alcohol for transesterification, because it can be derived inexpensively during fossil fuel production (6). The use of ethanol, however, would allow biodiesel production to be increasingly divorced from fossil fuel inputs (6). Biodiesel composed of fatty acid methyl esters (FAMEs) produced from transesterification with methanol has been more widely characterized than biodiesel composed of fatty acid ethyl esters (FAEEs) produced by ethanolysis. Recent studies, however, indicate that both alkyl esters have similar

viscosity, heat of combustion, cetane rating, and oxidative stability, while FAEEs have a higher flash point and better cold flow properties than FAMEs (6).

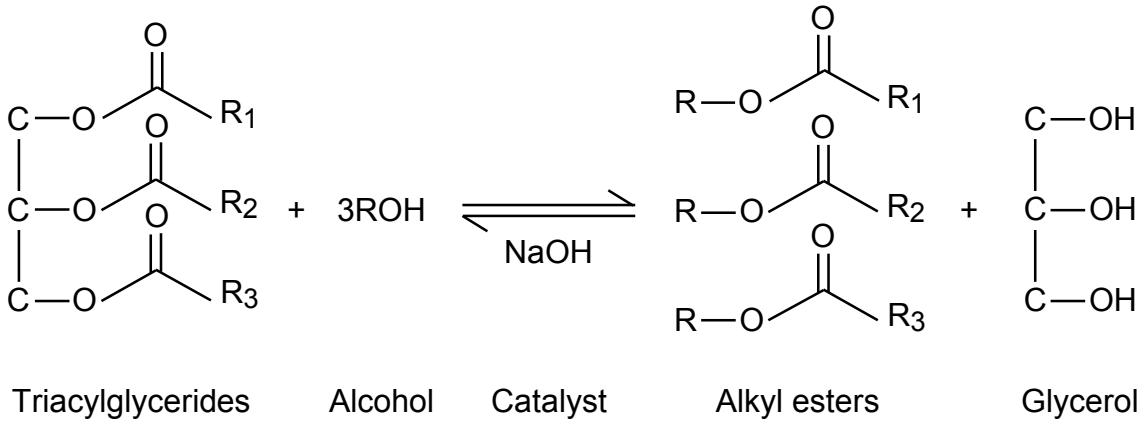

Fig. 4.1: Transesterification reaction of triacylglycerides and alcohol to produce either fatty acid methyl esters (R, CH_3) or fatty acid ethyl esters (R, CH_3CH_2). Adapted from (6).

The transesterification reaction generates 10 lb of glycerol for every 100 lb of biodiesel generated (62), and the glycerol must be thoroughly removed from the biodiesel in order for the biodiesel to meet international standards of fuel quality (1). Due to differences in density, the glycerol can be separated by settling or centrifugation. Complete separation has been shown to be easier for FAMEs than FAEEs (6), and water at pH 4.5 is often added to the crude biodiesel to improve the phase separation and remove additional contaminants such as residual catalyst and alcohol, unreacted mono-, di-, and triglycerides, and soaps (19). The biodiesel is separated from the water via centrifugation followed by vacuum drying until the final moisture content is below

0.050% (v/v) (19). The resulting waste stream contains ca. 10% glycerol and ca. 5% alcohol, which requires treatment prior to disposal. Hydrochloric acid is added to convert the soaps to free fatty acids, which are removed by centrifugation and disposed of as sewage. The waste stream is then neutralized and the residual alcohol is recovered by distillation for reuse in the transesterification reaction (19). Traditionally, the crude glycerol is partially purified to 80% (w/v) by distillation and sold to commercial refineries for further treatment. However, the ca. 22-fold increase in global biodiesel production between 2000 and 2010 (56) has resulted in the saturation of the glycerol markets and decreases in the price of glycerol from US $0.20-0.25 per pound in 2004 to US $0.06-$0.011 per pound in 2012 (36, 62). Because the price of biodiesel is highly responsive to the price of crude glycerol, the decrease in crude glycerol price has resulted in lowered profitability of the biodiesel industry, particularly for small to medium scale producers (19, 62).

Glycerol plays an existing role in the food, cosmetic and pharmaceutical industries (38), however purifying the crude glycerol from biodiesel waste streams for use in these industries is prohibitively expensive (19, 62). Recent research has therefore focused on finding uses for crude glycerol, which serves both to remove glycerol from the waste stream as well as to provide added value to the biodiesel refineries. The reduced nature of glycerol compared to other sugars means that it is an attractive substrate for microbial conversion into value added products such as ethanol or 1,3-propanediol (Fig. 4.2; (44, 62)). Several organisms have been identified that can ferment glycerol including *Escherichia coli* and several species of *Klebsiella, Bacillus, Clostridium, Lactobacillus, Enterobacter, Propionibacteria* and *Citrobacter* (3, 4, 13, 20,

22, 34, 37, 39, 43, 54). However, many of these bacteria are also classified as opportunistic pathogens, which greatly limits their practical applications. *Enterobacter aerogenes* (43) and *Bacillus subtilis* (37) have been shown to couple the degradation of low concentrations of glycerol (1% and 0.1%, respectively) with current production in microbial electrolysis cells (MECs), however coulombic efficiencies were low. In the case of *E. aerogenes,* current production from crude glycerol was enabled by the addition of a mediator, thionine, which would increase the cost of MEC operation and also make scaling up to a large-scale, flow-through system difficult. In experiments with *B. subtilis*, current production required purified glycerol and fermentation products were not quantified. In another MEC platform, *Shewanella oneidensis* was genetically engineered by knocking out the native phosphate acetyltransferase gene, heterologously expressing four *E. coli* genes for glycerol consumption and two ethanol production genes from *Zymomonas mobilis* to convert glycerol to ethanol (16). The fermentation proceeded with stoichiometric conversion of glycerol to ethanol and acetate in the presence of a poised electrode, which was required to consume the excess reducing power of the fermentation. However, low (ca. 0.5% w/v) concentrations of pure glycerol were used in this study and antibiotic supplementation was required to maintain the expression vectors (16). Similarly, an adaptively-evolved strain of *G. sulfurreducens* carrying a single point mutation in a transcriptional regulator was able to convert glycerol into electricity in a microbial fuel cell (MFC), however, the concentrations of glycerol processed by the exoelectrogen were even lower (0.05% w/v) (28). BECs driven by naturally-established microbial communities have been reported to partially recover energy from glycerol-containing wastewaters. However, power

densities were still low and the efficiency of glycerol removal was never assessed (10). Many of the glycerol-fermenting species are able to consume the excess reducing equivalents by reducing glycerol to 1,3-propanediol (Fig. 4.2), which is a valuable precursor to a new formulation of polyester, poly(propylene terephthalate), as well as biodegradable plastics (18, 44). *Clostridium acetobutylicum* for example, while unable to ferment glycerol naturally, was engineered to produce 1,3-propanediol through the introduction of genes from *Clostridium butyricum*, the resulting strain was able to consume ca. 6% (w/v) glycerol and produce primarily 1,3-propanediol with a molar yield of 0.64, and lactate, acetate, formate, butyrate and H_2 produced as waste products (18).

The waste products that are made during glycerol fermentations for ethanol and propanediol (Fig. 4.2) can act as feedback inhibitors and/or acidify the pH of the fermentation broth, thus inhibiting cell growth. As a result, extensive genetic engineering is often required to reroute the native metabolisms. For example, the efficient conversion of glycerol into ethanol by *E. coli* required nine gene knockout mutations to reduce the cell's central metabolism from over 15,000 possible pathways to a total of 28 glycerol-utilizing pathways and adaptive evolution was still needed to divert the metabolic flux towards ethanol production (54). Some of the waste products are coproduced to maintain the cell's redox balance and therefore cannot be eliminated by genetic engineering and must be otherwise removed to prevent inhibition of cell growth and fermentation. H_2, for example, is produced by *Clostridia cellobioparum* concomitantly during ethanol fermentation (Fig. 4.2) and has been found to be a potent inhibitor of growth (9). Chung (1976) investigated the effect of cocultivation of *C.*

cellobioparum with *Methanobacterium ruminantium* and found that as *M. ruminantium* removed the H_2 produced during glucose fermentation the culture reached a higher optical density and more H_2 was produced (9).

A similar approach is described in this chapter in which *C. cellobioparum*, which was identified from our lab culture collection as a robust glycerol-fermenting bacteria, is cocultured with *G. sulfurreducens* in two different bioelectrochemical systems (BESs). *G. sulfurreducens* converted the waste fermentation byproducts into cathodic H_2 in a microbial electrolysis cell (MEC) and into electricity in a microbial fuel cell (MFC), allowing the energy in the waste products to be recovered and stimulating the glycerol consumption and fermentation of *C. cellobioparum.*

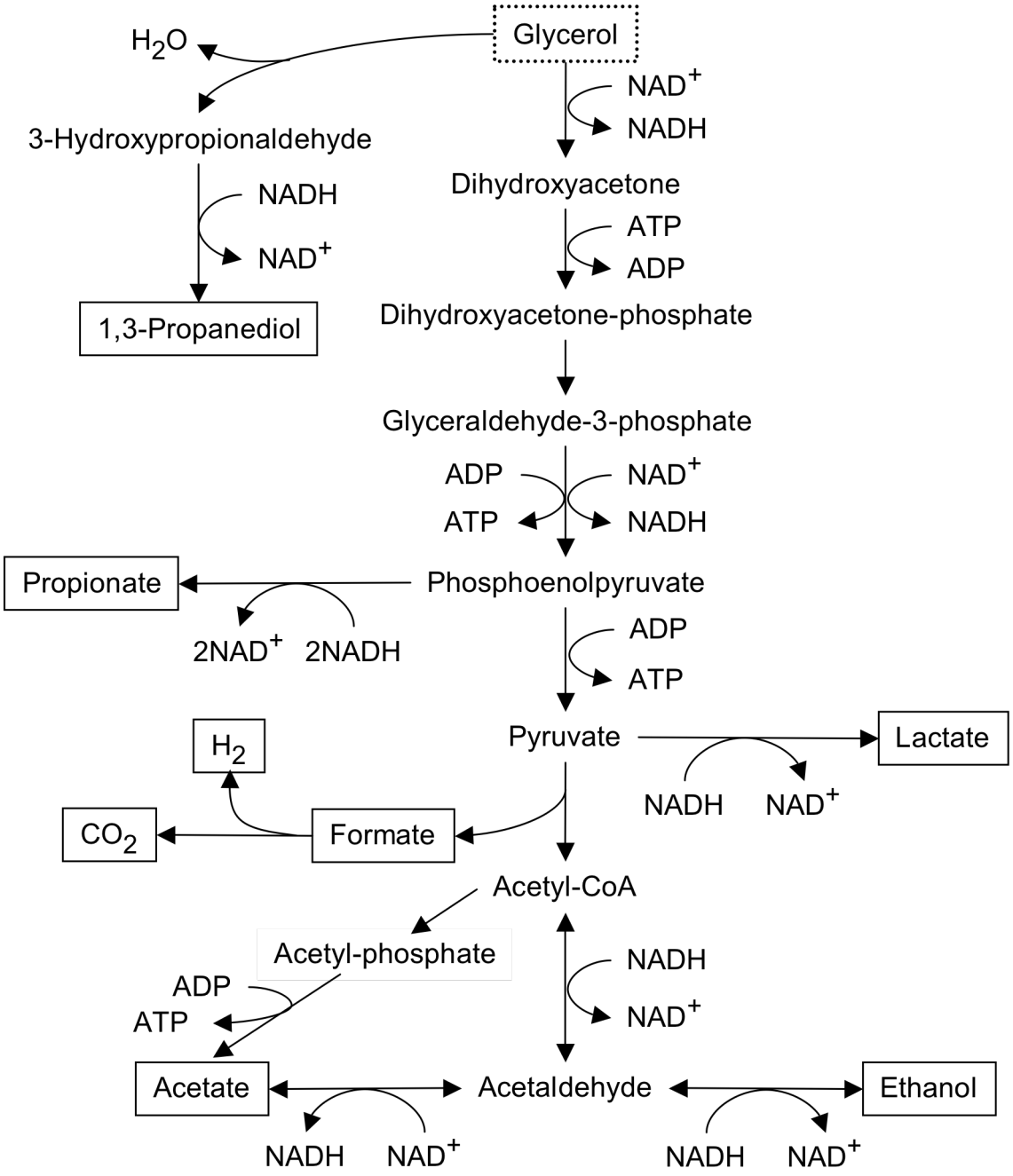

Fig. 4.2: The fermentative metabolism of glycerol into ethanol and 1,3-propanediol and the associated fermentative byproducts. Adapted from (3, 30, 42, 62).

MATERIALS AND METHODS

Bacterial strains and culture conditions. *Geobacter sulfurreducens* PCA was routinely cultured at 30°C in anaerobic minimal medium (DB medium; (50)) with 20 mM acetate and 40 mM fumarate (DB-AF). Ethanologenic, cellulolytic strains from our culture collection (Table 4.1) were routinely grown at 35°C in anaerobic GS2 medium (7) supplemented with 0.2% cellobiose (GS2-CB) or glycerol (GS2-glycerol). When indicated, 3-(N-morpholino)propanesulfonic acid (MOPS) was omitted from the medium (GS3).

Screening of fermentative strains for glycerol consumption. Ethanologenic strains from our culture collection (Table 4.1) were screened for their ability to ferment glycerol into ethanol at 35°C in anaerobic GS2 medium supplemented with approximately 0.31% (w/v) glycerol. Cultures were grown anaerobically in GS2-CB before inoculating to an initial optical density at 660 nm (OD_{660}) of 0.04 into triplicate tubes with 10 ml GS2-glycerol medium. Growth was monitored spectrophotometrically (OD_{600}) every 12 h.

Batch cultures of *C. cellobioparum* and *G. sulfurreducens*. Late-exponential phase cultures of *G. sulfurreducens* and *C. cellobioparum* grown anaerobically at 30°C in DB-AF and GS2-CB medium, respectively, were inoculated to an initial OD_{660} of 0.02 in the same (coculture) or separate (monoculture) tubes containing 10 ml GS2 medium supplemented with 0.25% (w/v) glycerol and 40 mM fumarate. Control monocultures of *G. sulfurreducens* and *C. cellobioparum* were also prepared in GS2 medium without glycerol to account for any growth from the yeast extract present in the medium or from

nutrients carried over in the inoculum. Controls of *G. sulfurreducens* in DB-AF with and without 0.25% (w/v) glycerol were also included. All cultures were incubated at 30°C and growth (OD_{660}) was monitored every 6 h.

Alcohol tolerance of *C. cellobioparum* and *G. sulfurreducens.* Late-exponential phase cultures of wild-type *C. cellobioparum* and *G. sulfurreducens* grown anaerobically at 30°C in GS3-CB and DB-AF medium, respectively, were inoculated to an initial OD_{660} of 0.02 in the same (coculture) or separate (monoculture) tubes with 10 ml GS3 medium containing 40 mM fumarate in the presence of glycerol (concentrations ranging from 0 and 10% (w/v)) or ethanol (concentrations between 0 and 5% (v/v)). The cultures were incubated at 30°C and growth was monitored every 12 h.

Adaptive evolution of *C. cellobioparum.* A glycerol-tolerant strain of *C. cellobioparum* was evolved by continuous subculturing in GS3 medium supplemented with increasing concentrations of glycerol starting at 6.3% (w/v). The cells were transferred into fresh medium when the culture reached stationary phase. The glycerol concentrations were increased to 8.8% (w/v) glycerol and finally 10% (w/v) once the growth rate and lag time of the cultures had stabilized. After approximately 16 months, a culture was adapted that grew with 10% (w/v) glycerol and clonal representatives were isolated on solidified (1.4% agar) GS2-CB using roll tubes (21) and subcultured three times to ensure the purity of the clone. Five clones were tested for growth, glycerol consumption, and fermentation product yields in medium with 10% (w/v) glycerol. The best performing strain was designated $CcelA_{10G}$ and its glycerol tolerance was assessed as described above.

Adaptive evolution of *G. sulfurreducens*. An ethanol-tolerant strain of *G. sulfurreducens* was evolved by continuous subculturing in DB-AF medium supplemented with increasing concentrations of ethanol (between 1 and 5% v/v). The cells were transferred into fresh medium when the culture reached stationary phase. The strain was routinely transferred in the same concentration of ethanol at least seven times or until growth rates improved and stabilized, before increasing the ethanol concentration by 0.5% increments. Cultures adapted for growth at each ethanol concentration were routinely preserved at -80°C in anaerobic vials containing 10% dimethyl sulfoxide (DMSO). Once a culture was adapted that grew at 5% ethanol after several transfers, clonal individuals were recovered as isolated colonies on solidified NBAF medium (11) in an anaerobic glove bag (Coy Laboratory Products, Inc.). Ten colonies were subcultured three times to ensure purity and the one with the most robust growth in DB-AF medium with 5% ethanol was designated $GsulA_{5E}$ and was selected for further study. $GsulA_{5E}$ was tested for tolerance to increasing concentrations of glycerol and ethanol, as described above.

MECs. Dual-chambered, H-type MECs were set up as described previously (50) and incubated at 30°C. They were autoclaved before the addition of 90 ml DB medium to the anode and cathode chambers. The medium in the anode chamber was supplemented with 1 mM acetate. The reference electrode (3 M Ag/AgCl, Bioanalytical Systems Inc.) was sterilized in 70% ethanol for 1 min and rinsed with sterile water before being added to the anode chamber. Before inoculation, the anode electrode was poised at 0.24 V with a VSP potentiostat (BioLogic) and the chambers were sparged with filter-sterilized N_2:CO_2 (80:20) gas. Once the current stabilized, the anode chamber

was inoculated with 10 ml of a cell suspension of the wild-type (Gsul) or ethanol-tolerant ($GsulA_{5E}$) strain of *G. sulfurreducens* in DB medium. The cell suspension was prepared by harvesting cells from a 40% (v/v) volume of an early stationary-phase cultures grown at 30°C in DB-AF medium by centrifugation (6,000 x *g,* 6 min, 25°C) under anaerobic conditions and washing them once before resuspending them in 10 ml DB medium.

Once all the acetate was consumed in the anode chamber (i.e., when the current declined to baseline levels), the medium was replaced with GS3 medium containing 10% (w/v) glycerol, and the chamber was inoculated with *C. cellobioparum* (the wild-type Ccel or the adapted $CcelA_{10G}$ strain). The Ccel or $CcelA_{10G}$ cells were harvested anaerobically by centrifugation (6,000 x *g*, 6 min, 25°C) from a 40% (v/v) inoculum of late exponential-phase cultures grown at 30°C in GS3-glycerol, washed once, and resuspended in 10 ml GS3-glycerol medium. The anode chamber was sparged briefly with N_2 following inoculation to ensure anaerobiosis, but no additional sparging was used to prevent the evaporation of fermentative ethanol. By contrast, the cathode chamber was sparged continuously with N_2:CO_2 (80:20) to prevent the crossover of H_2 into the anode chamber. The percent of cathodic H_2 recovered in the MEC system was determined by discontinuing the sparging of the cathode chamber, sampling the headspace and analyzing the gas composition by GC, as described below. Alternatively, other types of medium were used in place of GS3-glycerol to test their effect on MEC performance. Where indicated, GS2-glycerol or GS3-glycerol supplemented with 200 mM phosphate buffer were used as medium in the MECs to improve the buffering capacity of the medium in the anode chamber. Alternatively,

anode chambers with GS2-glycerol medium were continuously sparged with N_2 to remove the fermentative H_2 and CO_2 and investigate the potential effect of feedback inhibition or medium acidification, respectively, on MEC performance.

Controls with $GsulA_{5E}$ monocultures to test the glycerol tolerance in the MECs were performed as described above by first growing $GsulA_{5E}$ anode biofilms with DB medium containing 1 mM acetate. After current production declined, the medium was switched to fresh DB medium containing 1 mM acetate with and without 10% (w/v) glycerol. The anode supernatant was analyzed by HPLC as described below and the efficiency of acetate conversion into current (coulombic efficiency, CE) was calculated as the coulombs recovered divided by the total coulombs in the substrate (eq. 1).

$$CE = \frac{\int_0^t I \, dt}{8F \, \Delta A} \qquad (1)$$

The integral of the current (I) over the duration of the experiment (t) is given in coulombs (A*s). The number 8 represents the number of moles of electrons in 1 mol of acetate, F is Faraday's constant, and ΔA is the decrease of acetate (moles) over the duration of the experiment.

Controls with $CcelA_{10G}$ monocultures were also grown in the MECs. $CcelA_{10G}$ cells were harvested as described above and inoculated into MECs containing 90 ml GS3 medium and 10% glycerol. Where indicated, the anode electrode was poised at 0.24 V vs. Ag/AgCl and current production was monitored.

MFCs. MFCs were set up with the dual, H-type chambers described above and separated with a Nafion membrane (Ion Power, Inc., New Castle, DE). The anolyte was 90 ml DB medium with 5 mM acetate, and 90 ml 50 mM ferricyanide was used as the catholyte. Graphite felt electrodes (2.294 m^2 surface area, Keego Technologies) were used as the anode and cathode and connected by a 470 Ω resistor. A Fluke 45 digital multimeter (Fluke Corporation, Everett, WA) was used to monitor the voltage drop across the resistor over the duration of the experiment, and current production was calculated as the measured voltage divided by the resistance. $GsulA_{5E}$ cells were grown and harvested as described above except that an 80% (rather than 40%) (v/v) inoculum was used. The anode was sparged with N_2:CO_2 (80:20). Approximately 70 h after inoculation, the medium in the anode chamber was replaced with GS2-10% glycerol and then the $CcelA_{10G}$ cell suspension, grown and prepared as described above, was added. The anode was sparged briefly with N_2 and then the sparging was discontinued to prevent the evaporation of fermentative ethanol. Power density curves were generated periodically using a variable resistor (0-3 KΩ). Once the resistance was changed, the system was allowed to equilibrate for 30 min and the voltage was recorded. Power production at each resistance was calculated as the square of the voltage divided by the external resistance.

Energy recovery. Energy recovery η (%) for the MECs was calculated by dividing the energy outputs by energy inputs (60), as described in the following equation:

$$\eta = \frac{W_E + W_{HA} + W_H}{(W_G)m_G + (W_A)m_A + W_P} \qquad (2)$$

The energy outputs in eq. 2 included the amount of energy recovered as ethanol (W_E), which was calculated as the heat of combustion of the ethanol produced (upper heating value 23.4 MJ/L; (46)), and the energy recovered as H_2 at the cathode (W_H in eq. 2) plus the energy recovered as fermentative H_2 in the anode (W_{HA}), which were determined using the heat of combustion of H_2 (upper heating value 285.83 kJ/mol; (8)). The recovery of cathodic H_2 from the system was calculated as the number of moles of H_2 measured in the headspace of the cathode chamber at the end of the experiment divided by the maximum theoretical coulombic H_2 recovery (r_{CE}), which was obtained from the amount of current (I) produced in the MEC as follows:

$$r_{CE} = \frac{\int_0^t I\, dt}{2F} \qquad (3)$$

Where F is Faraday's constant and 2 represents the number of moles of electrons per mol of H_2 (8).

The energy inputs in eq. 2 included the energy input from glycerol (W_G), which was determined by the heat of combustion of glycerol (17,961 J/g; (53)) multiplied by the mass of glycerol consumed over the duration of the experiment (m_G), and the energy input from acetate (W_A) which was determined by the heat of combustion of the

acetate (870.28 kJ/mol; (8)) multiplied by the moles of acetate (m_A) consumed over the duration of the experiment. The electricity input from the potentiostat to maintain the cell voltage (W_P in eq. 2) over the duration of the experiment (t) was calculated as:

$$W_P = \int_{t=0}^{t} I\ E\ dt \qquad (4)$$

Where I is the measured current and E is the cell voltage (26). The applied potential of the cathode was measured with respect to a reference electrode (3 M Ag/AgCl, Bioanalytical Systems Inc.) inserted in the cathode chamber. The cell voltage was calculated as the difference between the measured cathodic potential and the applied potential at the anode electrode.

The energy recovery for the MFCs was calculated similarly (eq. 5), by taking into account the energy outputs from ethanol and fermentative H_2 as described above, as well as the power produced from the fuel cell (W_F) which is a product of the voltage and current over the duration of the experiment as seen in eq. 4. The energy inputs were from the amount of glycerol and acetate consumed over the duration of the experiment, as described above.

$$\eta = \frac{W_E + W_{HA} + W_F}{(W_G)m_G + (W_A)m_A} \qquad (5)$$

The energy recovery from the *C. cellobioparum* fermentation was determined as seen in eq. 6 and took into account only the energy inputs from the glycerol consumed and the fermentative ethanol and H_2 produced.

$$\eta = \frac{W_E + W_{HA}}{(W_G)m_G} \qquad (6)$$

Confocal laser scanning microscopy (CLSM). Anode biofilms were examined by CLSM at the end of the MEC experiments as previously described (50), except that *G. sulfurreducens* and *C. cellobioparum* cells were differentially stained with the BacLight Gram Stain Kit (Invitrogen) by following the manufacturer's recommendations. The electrodes were imaged with an Olympus FluoView FV1000 inverted microscope (Olympus; Center Valley, PA) equipped with a PLAPON 120X oil immersion objective (Olympus; numerical aperture [NA], 1.42**).** The excitation wavelength was 488 nm for both dyes. The emission spectra were detected with a BA505-525 band pass filter (SYTO 9, green) and a BA650IF long pass filter (hexidium iodide, red). Image stacks were collected every 0.4 μm and image projections were generated using the FV10-ASW 3.0 software (Olympus).

Analytical techniques. At the end of each experiment, when the cultures had reached stationary phase, the composition of the fermentation broth and the headspace atmosphere were analyzed by High Pressure Liquid Chromatography (HPLC) and Gas Chromatography (GC), respectively. The gas composition was analyzed by GC using a Varian CP-4900 Micro Gas Chromatograph (Agilent, Santa Clara, CA). Alcohols and organic acids in culture supernatant fluids were measured by HPLC (Waters, Milford, MA) at 30°C, as previously described (31) except that samples were filtered with 0.45 μm syringe filters (National Scientific, Rockwood, TN) prior to analysis. Where indicated the pH was also measured with an Orion Aplus pH meter (Thermo Electron, Beverly, MA).

RESULTS

Identification of a glycerol-fermenting ethanologenic strain. Seven ethanologenic strains from our laboratory culture collection grew in rich medium containing approximately 0.31% (w/v) (or 34.2 mM) glycerol at 35°C. Only *C. cellobioparum* coupled growth to the fermentation of glycerol to ethanol (Table 4.1), growing to an OD_{660} of 0.37 ± 0.01 and consuming 84.5 (± 2.0)% of the glycerol provided, or the equivalent of 28.9 (± 0.7) mM. Ethanol (31.3 ± 1.2 mM) was the main product of fermentation followed by acetate (19.7 ± 0.8 mM), lactate (10.8 ± 0.5 mM) and H_2 (7.7 ± 0.2 mM). The amount of glycerol fermented corresponds well with the amount of ethanol produced (0.29:0.31 mmol). The maximum theoretical molar conversion of glycerol to ethanol is 1:1; therefore the apparent high (more than 100%) fermentation yields from glycerol suggest that substrates available in the rich medium and/or carried over in the inoculum were also used for fermentation. In fact, the GS2 medium without glycerol supported the growth of *C. cellobioparum* to yields of 0.21 ± 0.01 (OD_{660}) and produced ethanol (4.2 ± 0.9 mM), acetate (3.9 ± 1.7 mM), formate (1.9 ± 1.5 mM), lactate (1.1 ± 0.5 mM) and H_2 (2.7 ± 0.3 mM). Furthermore, although glycerol was not efficiently consumed by the other strains tested, they still grew in the GS2 medium (Table 4.1).

Table 4.1: Screening of fermentative strains for glycerol consumption. [a]

Strain (designation)	Glycerol consumed (mM)	Ethanol produced (mM)	Growth rate (d^{-1}) [b]
Cellulomonas uda (ATCC 21399)	0.9 (± 1.5)	6.0 (± 1.1)	1.5 (± 0.1)
Cellulomonas biazotea (ATCC 486)	1.8 (± 1.5)	4.8 (± 0.5)	1.0 (± 0.1)
Cellulosimicrobium cartae (ATCC 21681)	0.3 (± 0.3)	5.1 (± 0.3)	1.8 (± 0.1)
Cellulomonas gelida (ATCC 488)	0.4 (± 0.5)	2.7 (± 0.8)	1.7 (± 0.1)
Clostridium cellobioparum (ATCC 15832)	28.9 (± 0.7)	31.2 (± 2.7)	1.5 (± 0.1)
Cellulosilyticum lentocellum (ATCC 27405)	0.6 (± 0.9)	0.8 (± 0.4)	14.7 (± 1.4)
Clostridium papyrosolvens (NCIMB 11394)	0.7 (± 0.7)	2.1 (± 1.1)	5.3 (± 0.2)

[a] Shown are averages and, in parentheses, standard deviations of three replicate cultures provided with 34.2 mM glycerol.

[b] Determined by optical density at 660 nm of planktonic growth.

Syntrophic growth of *G. sulfurreducens* and *C. cellobioparum* in batch cultures with fumarate as the electron acceptor. The syntrophic growth of *C. cellobioparum* and *G. sulfurreducens* was investigated in batch cultures grown at 30°C in GS2-glycerol medium supplemented with fumarate to serve as the terminal electron acceptor for *G. sulfurreducens* (Fig. 4.3A). Monocultures of *C. cellobioparum* in medium with and without glycerol, and monocultures of *G. sulfurreducens* in medium with glycerol were included as controls (Fig. 4.3A). A small amount of growth (OD_{660}, 0.22) was also seen in *C. cellobioparum* monocultures without glycerol (Fig. 4.3A), suggesting that growth was being sustained by the yeast extract or carryover from the inoculum. Consistent with this, small amounts of fermentation products were also detected (Fig. 4.3B; ethanol, 1.1 ± 0.6 mM; lactate, 0.5 ± 0.01 mM; acetate, 3.6 ± 0.3 mM; formate, 1.2 ± 0.2 mM; H_2, 3.0 ± 0.6 mM; CO_2, 1.1 ± 0.2 mM). The basal GS2 medium with glycerol and fumarate was unable to support high growth yields for *G. sulfurreducens* (OD_{660}, 0.15) and no glycerol was consumed and no fermentation products were detected in the culture broth. *C. cellobioparum* monocultures were able to couple glycerol fermentation to growth and reached higher yields (OD_{660}, 0.47) (Fig 4.3A). The *C. cellobioparum* monoculture consumed 82.8 (± 2.3)% of the glycerol provided (the equivalent of 22.7 ± 0.6 mM) and produced ethanol (30.3 ± 1.2 mM), lactate (15.6 ± 0.9 mM), acetate (10.2 ± 0.8 mM), formate (2.4 ± 2.3 mM), H_2 (7.4 ± 0.4 mM) and CO_2 (3.1 ± 0.3 mM) (Fig 4.3B). In the coculture, 85.8 (±1.5)% of the glycerol was consumed (the equivalent of 23.5 ± 0.4 mM). Coculture supernatants contained ethanol (26.6 ± 2.6 mM) and lactate (14.5 ± 1.1 mM), while no acetate or formate were detected (Fig. 4.3B). H_2

concentrations in the headspace were decreased (1.4 ± 0.2 mM) and CO_2 production increased (4.3 ± 0.2 mM) in the coculture compared to the *C. cellobioparum* monoculture. The observed consumption of the preferred electron donors for *G. sulfurreducens* (acetate, formate and H_2) coupled with the stimulated growth yields (OD_{660}, 1.2; Fig. 4.3A), increased CO_2 production of the cocultures (Fig. 4.3B), and 1.3-fold increases in growth rate of the coculture (2.3 ± 0.1 d^{-1}) compared with the *C. cellobioparum* monoculture (1.7 ± 0.1 d^{-1}), indicate that the two strains were growing syntrophically. The growth of *G. sulfurreducens* was unaffected by the addition of 0.25% (w/v) glycerol as growth rates were similar in GS2 medium with acetate and fumarate in the presence (2.4 ± 0.1 d^{-1}) and absence (2.2 ± 0.1 d^{-1}) of glycerol (data not shown).

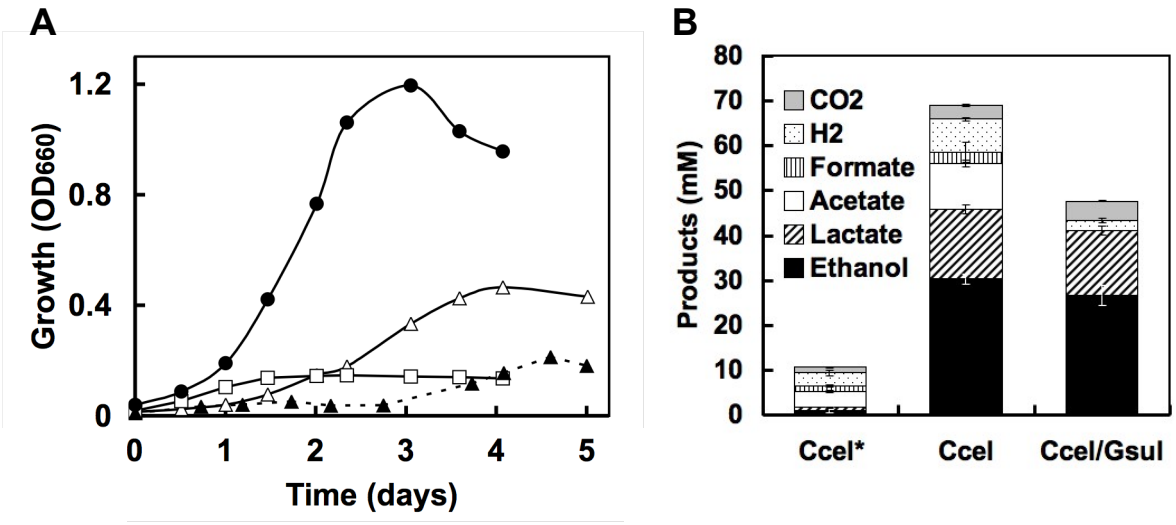

Fig. 4.3: Syntrophic growth of *G. sulfurreducens* and *C. cellobioparum* in batch cultures with glycerol and fumarate at 30°C. (A) Growth of the coculture (solid circles), and *C. cellobioparum* monocultures with glycerol (open triangles), *C. cellobioparum* monocultures without glycerol (solid triangles) and *G. sulfurreducens* monocultures (open squares). Growth was monitored as optical density at 660 nm (OD_{660}). (B) Glycerol fermentation products at the end of the experiment in *C. cellobioparum* monocultures with (Ccel) and without (Ccel*) glycerol and in the coculture (Ccel/Gsul).

Tolerance of wild-type strains to glycerol. The tolerance of the wild-type *C. cellobioparum* to increasing concentrations of glycerol was investigated in batch cultures at 30°C with glycerol concentrations ranging from 0-10% (w/v) (Fig 4.4A). The growth rates increased 1.4-fold as glycerol concentrations increased from 0.25% to 1% and more substrate was available for growth. Growth rates decreased to ca. 79% of the maximum for cultures grown in glycerol concentrations between 3 and 7%, presumably due to inhibition from the increased viscosity of the medium. No growth was observed at 10% glycerol concentrations. The tolerance of the wild-type *G. sulfurreducens* to increasing concentrations of glycerol was also investigated (Fig 4.4A). *G. sulfurreducens* was tolerant to glycerol concentrations up to 3% (w/v) with modest decreases in growth rate (81% of maximum). Growth was inhibited at 5% glycerol concentrations where growth rates decreased to 47% of the maximum. No growth was observed at 7% and 10% glycerol concentrations. The two strains were also cocultured with increasing concentrations of glycerol (Fig 4.4A). The highest growth rates were observed up to 3% glycerol loadings and then declined at 5% glycerol to 69% of the maximum growth rate. No growth was observed at 7 and 10% glycerol. These results suggest that the *G. sulfurreducens* strain is more sensitive to glycerol than *C. cellobioparum,* and that the growth of *G. sulfurreducens* was the bottleneck that drove the growth of the coculture.

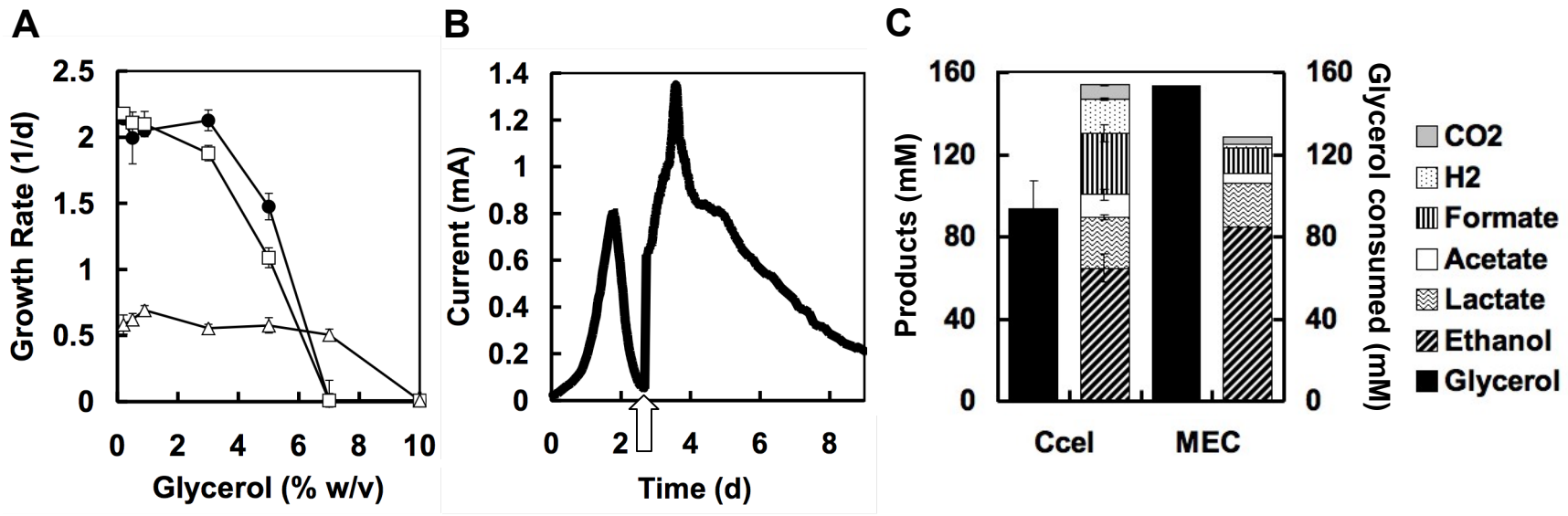

Fig. 4.4: (A) Tolerance of wild-type *C. cellobioparum* (open triangles), *G. sulfurreducens* (open squares) and the coculture (closed circles) to increasing concentrations of glycerol. Error bars show standard deviations from three replicate cultures. (B) Current production of a sequentially inoculated MEC. *G. sulfurreducens* was inoculated first and supplemented with 1 mM acetate, the anode medium was then exchanged (arrow) for GS3 medium supplemented with 3.8% (w/v) glycerol and inoculated with *C. cellobioparum.* (C) Glycerol consumption and fermentation products from the MEC shown in panel B compared with a *C. cellobioparum* monoculture (Ccel) in 90 ml GS3-3.8% glycerol medium. Error bars show standard error of two replicates.

Fermentation of glycerol to ethanol in a MEC. We investigated the ability of the coculture of *G. sulfurreducens* and *C. cellobioparum* to couple the fermentation of glycerol with current production in a MEC. A sequential inoculation strategy was followed in which *G. sulfurreducens* was first inoculated into the MEC and supplemented with 1 mM acetate to provide optimal conditions for biofilm formation (Fig. 4.4B). The current increased exponentially at a rate of 3.1 d^{-1} and peaked at 0.8 mA after 42 h, and then declined once the acetate was consumed. Once the current was < 0.1 mA, the anode medium was replaced with GS3 containing 3.8% (w/v) glycerol, a concentration chosen because it could support robust growth of the coculture (Fig. 4.4A), and the MEC anode was inoculated with *C. cellobioparum* (Fig. 4.4B). The current immediately resumed and peaked at 1.34 mA before declining to < 0.2 mA over a period of ca. 5 d, producing 3.4 mmol of electrons. For comparison, the same 40% (v/v) inoculum of *C. cellobioparum* used in the MEC was inoculated into 2 serum bottles containing 90 ml GS3-glycerol medium. HPLC analysis of the culture supernatant fluids at the end of the experiment showed a nearly stoichiometric conversion of glycerol (93.5 ± 13.5 mM) into ethanol (64.8 ± 6.7 mM), lactate (24.8 ± 1.1 mM) and acetate (10.9 ± 2.5 mM), with the concomitant production of formate (29.8 ± 4.0 mM), H_2 (16.5 ± 0.5 mM) and CO_2 (7.0 ± 0.2 mM) in the *C. cellobioparum* monoculture (Fig. 4.4C). Growth of the coculture in the MECs stimulated glycerol fermentation: 1.6-fold more glycerol was consumed (153.8 mM) and 1.3-fold more ethanol was produced (85.0 mM). The concentration of acetate (4.6 mM), formate (12.5 mM), and H_2 (1.79 mM) was lower than in the monoculture due to consumption by *G. sulfurreducens* as electron donors.

The concentration of lactate was only slightly lower (21.2 mM), indicating that less was consumed because it is not a preferred electron donor for *G. sulfurreducens* (Fig. 4.4C). The concentration of CO_2 (3.55 mM) was also lower in the MEC, which was unexpected because both *C. cellobioparum* and *G. sulfurreducens* produce CO_2 during their metabolism. This may suggest that some headspace gases escaped from the MEC during operation and the concentrations of H_2 and CO_2 are therefore underestimated.

Adaptive evolution of *C. cellobioparum*. Adaptive evolution was used to increase the tolerance of the *C. cellobioparum* strain to industrially-relevant glycerol loadings (10% w/v, Fig. 4.5). Wild-type *C. cellobioparum* was found to have growth limitations in glycerol concentrations between 3% and 7% (Fig. 4.4A). Consequently, adaptive evolution was initiated at glycerol loadings of 6.3%, where growth rates were diminished but growth was sustainable over many serial transfers. The strain was continually subcultured from stationary phase cells in order to take advantage of the error-prone DNA polymerase IV, which is expressed when the culture enters stationary phase and which lacks 5'-3' proofreading ability, thereby increasing the rate of mutation in the culture and selecting for strains with "growth advantage in stationary phase" (GASP) mutations (15). The strain was transferred in medium containing 6.3% glycerol for ca. 2 months. During this period, the time it took the culture to grow to stationary phase decreased from 16 to 7 d (Fig. 4.5A), lag times decreased from 120 to 24 h (Fig. 4.5B), and growth rates (Fig. 4.5C) and yields (Fig.4.5D) increased from 0.5 to 0.8 d^{-1} and 0.40 to 0.81 (OD_{660}), respectively. The strain was then increased to 8.8% glycerol concentrations. Initially, growth performance declined compared to 6.3%, but after ca. 1

month the parameters improved (Fig 4.5). The growth time to stationary phase remained at 7 days, the lag time decreased from 48 to 24 h, the growth rate increased 0.6 to 0.9 d^{-1}, and the yield increased from 0.62 to 0.64 (OD_{660}). The glycerol concentration was then increased to the industry target of 10% and a decrease in growth rate was observed (0.7 d^{-1}). The culture was maintained under these conditions for approximately 13 months, during which time the growth performance improved substantially (Fig. 4.5). At the end of the adaptive evolution experiment, the growth time to stationary phase was 4 days, the lag time was 12 h, growth rates were 1.3 d^{-1}, and growth yield was 0.93 (OD_{660}).

Following the adaptive evolution of *C. cellobioparum* for enhanced growth with glycerol, five single colonies were isolated in roll-tubes (21) and subcultured 3 times to ensure the purity of the strains as monoclonal populations. These clonal populations were tested for growth, glycerol consumption, and fermentation product yields on 10% (w/v) (or the equivalent of 1,086 mM) glycerol-containing medium. The best performing strain was designated $CcelA_{10G}$ and grew at a rate of 1.1 d^{-1}, consumed 3.5% of the glycerol provided (or the equivalent of 37.9 ± 1.8 mM) and produced 39.5 (± 0.9) mM ethanol, 21.2 (± 1.8) mM formate, 5.5 (± 0.3) mM H_2 and 5.9 (± 0.4) mM CO_2. Interestingly, unlike the wild-type strain (Fig. 4.3B), no lactate or acetate was produced, indicating that the adapted strain had become optimized for stoichiometric ethanol production with the concomitant formation of formate, H_2 and CO_2.

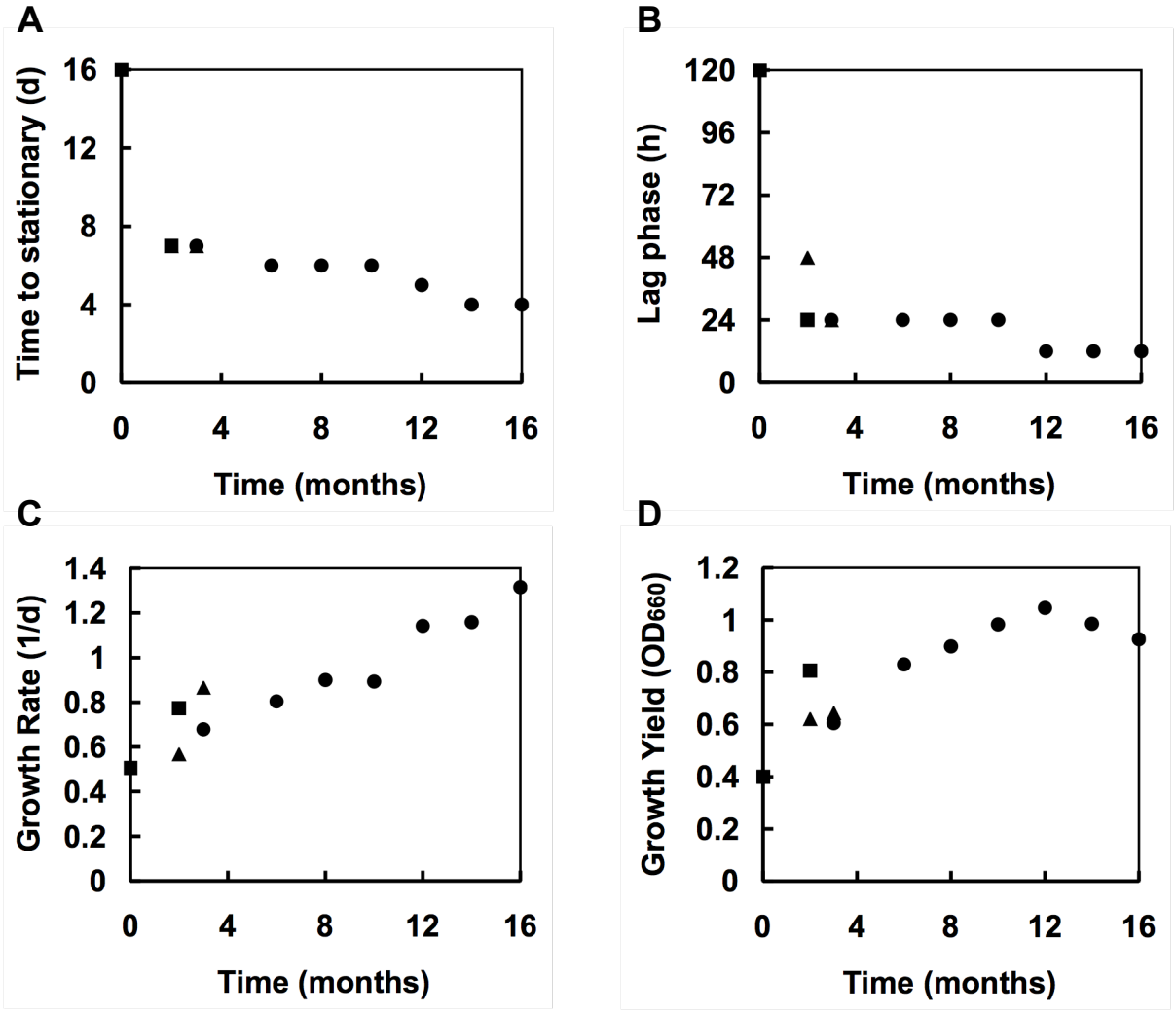

Fig. 4.5: Adaptive evolution of glycerol tolerance in *C. cellobioparum*. Points shown are representative transfers at approximately 2-month intervals of the adaptive evolution at 6.3% (w/v) glycerol (squares), 8.8% (w/v) glycerol (triangles) and 10% (w/v) glycerol (circles). (A) Time the cultures took to grow to stationary phase; (B) duration of the lag phase; growth rate (C) and growth yield (D) determined from OD_{660} of planktonic growth.

Adaptive evolution of *G. sulfurreducens*. An adaptive evolution strategy was also used to improve the tolerance of *G. sulfurreducens* to high concentrations of alcohol. As *G. sulfurreducens* would be exposed to high ethanol concentrations during coculture with *C. cellobioparum*, and because an ethanol-tolerant *G. sulfurreducens* strain would also be a valuable component of the consolidated bioprocessing platform described in Chapter 3, ethanol tolerance was the first goal of the adaptive evolution. The tolerance of the wild-type strain to ethanol was investigated with increasing concentrations of ethanol from 0 to 5% (v/v) (Fig. 4.6A). Growth rates decreased dramatically to 37% of the maximum as ethanol concentrations increased from 0 to 1%, and continued to decline steadily until reaching the inhibitory concentration of 5%, where no growth was observed. The adaptive evolution experiment was therefore started at 1% ethanol loading. The strain was continually transferred from cells in stationary phase cultures to take advantage of GASP mutations as described above for *C. cellobioparum.* After at least 7 transfers at a given concentration, the concentration of ethanol added to the culture was increased by 0.5%. After approximately 10 months, the strain was able to sustain growth in medium containing 5% ethanol at which point ten isolated colonies were obtained in an anaerobic chamber and subcultured three times to ensure that they came from a monoclonal population. The ten strains were then grown in the presence and absence of ethanol to identify the strain with the most robust growth. Interestingly, two growth phenotypes were observed for the strains; in three strains the cells grew planktonically and in the remaining seven strains they grew as microcolonies (Fig 4.4B). The strain with the highest growth rate in the presence (0.6 d^{-1}) and absence (4.7 d^{-1}) of ethanol ($GsulA_{5E}$) was among those that grew planktonically

and was chosen for further studies. HPLC analysis of the culture broth at the beginning and end of strain growth showed no decrease in ethanol concentration (data not shown), indicating that GsulA$_{5E}$ had not adapted to utilize ethanol as a carbon or electron donor, like the closely related species *Geobacter metallireducens.*

GsulA$_{5E}$ was tested for ethanol tolerance at varying concentrations (0-6%) as described above for the wild-type strain (Fig. 4.6A). Interestingly, the growth rate of the adapted strain in the absence of ethanol was increased 1.3-fold higher than the wild-type strain (Fig. 4.6A) although it achieved lower growth yields (0.62 ± 0.01, OD$_{660}$) than the wild-type (0.74 ± 0.02, OD$_{660}$). The growth rate at 2-3% ethanol concentrations was stimulated ca. 4-fold compared to wild-type and was 63 and 45% of the maximum, respectively (Fig. 4.6A). The growth yields at 2% ethanol were similar for GsulA$_{5E}$ (0.47 ± 0.02, OD$_{660}$) and wild-type (0.48 ± 0.02, OD$_{660}$), while yields at 3% were higher for GsulA$_{5E}$ (0.46 ± 0.01, OD$_{660}$) than wild-type (0.33 ± 0.02, OD$_{660}$). The adapted strain grew at 5% ethanol (0.38 ± 0.02, OD$_{660}$), and even grew slowly at 6% ethanol although yields were low (0.19 ± 0.04, OD$_{660}$), while the wild-type was unable to sustain growth at these concentrations.

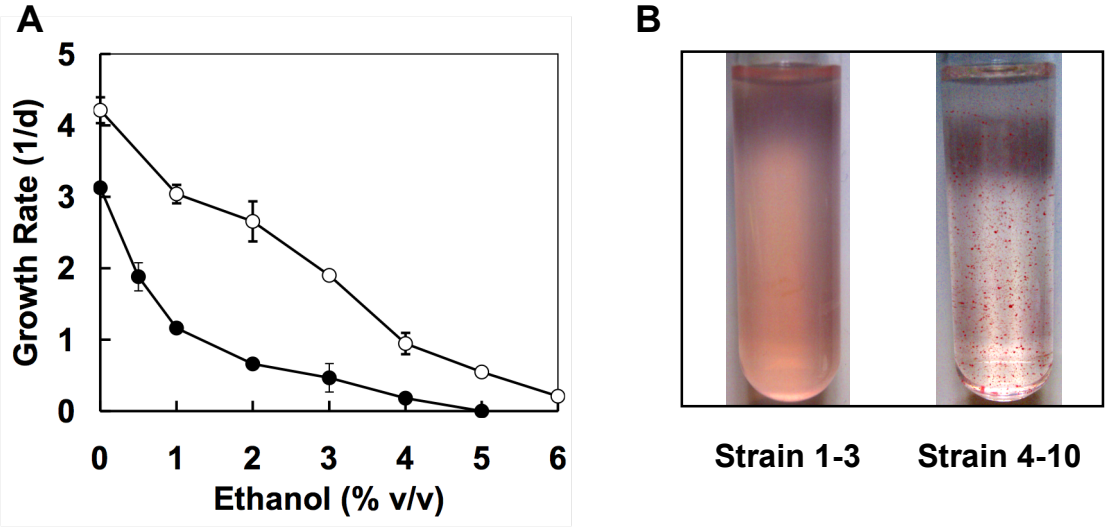

Fig. 4.6: (A) Tolerance of wild-type *G. sulfurreducens* (solid symbols) and the ethanol-adapted strain (GsulA$_{5E}$, open symbols) to increasing concentrations of ethanol. (B) Two phenotypes obtained from the adaptive evolution of *G. sulfurreducens* for ethanol tolerance. Three strains grew planktonically (left image) while seven grew as microcolonies (right image). The adapted strain that was chosen for further investigation (GsulA$_{5E}$) was among those that grew planktonically.

Glycerol tolerance of $GsulA_{5E}$ and $CcelA_{10G}$. It was hypothesized that the ethanol-adapted strain $GsulA_{5E}$ would display a nonspecific tolerance to other alcohols such as glycerol. The tolerance was tested as described previously for the wild-type strain at glycerol concentrations between 0 and 10% (w/v) (Fig. 4.4A). The growth rate for $GsulA_{5E}$ was similar to the wild-type at concentrations between 0 and 5% showing decreases in growth rate up to 61% of the maximum as glycerol concentrations increased. At glycerol concentrations greater than 7%, the wild-type strain was unable to grow whereas $GsulA_{5E}$ was able to sustain growth rates greater than 39% of the maximum (Fig. 4.7A). $CcelA_{10G}$ was also tested for glycerol tolerance. The growth rate of the adapted strain increased 2-fold as glycerol concentrations increased from 0.6% to 2.5%, and was constant at approximately 1.0 d^{-1} between glycerol concentrations of 2.5% and 10% (Fig. 4.7A). This represents a significant improvement compared to the wild-type strain, which was unable to sustain growth at 10% glycerol loadings (Fig. 4.4A).

The adapted strains $GsulA_{5E}$ and strains $CcelA_{10G}$ were also grown together at varying concentrations of glycerol to investigate the tolerance of the coculture to glycerol (Fig. 4.7A). The growth rates of both the wild-type coculture (Fig. 4.4A) and the adapted coculture increased 1.6-fold as concentrations of glycerol increased from approximately 0.5 to 3%. At 5% glycerol concentrations and greater, the adapted coculture out-performed the wild-type coculture with growth rates only decreased to 76% of the maximum at 10% glycerol. Interestingly, the growth rate of the adapted

coculture at 10% glycerol (1.5 ± 0.1 d^{-1}, Fig. 4.7A) was higher than either the $CcelA_{10G}$ or $GsulA_{5E}$ monocultures (1.1 ± 0.1 d^{-1} and 0.9 ± 0.1 d^{-1}, respectively), suggesting that the growth was stimulated by the synergistic action of the two strains. Consistent with this, the glycerol consumption (Fig. 4.7B) and ethanol production (Fig. 4.7C) were both stimulated approximately 1.4-fold in the coculture compared with $CcelA_{10G}$ monocultures when starting glycerol concentrations were high (i.e. greater than 5% w/v).

In addition to experiments in batch culture, the effect of 10% glycerol loadings on the $GsulA_{5E}$ anode biofilms in MECs was investigated (Fig. 4.8). The anode biofilms were first grown with medium containing 1 mM acetate. When the acetate was depleted and the current declined to less than 0.1 mA, the medium in the anode was replaced with fresh medium containing 1 mM acetate with or without 10% glycerol. The current immediately resumed in all the fuel cells regardless of the presence of glycerol. While the MECs without glycerol reached a higher current (1.46 ± 0.01 mA) than those with glycerol (1.12 ± 0.02 mA), the coulombic efficiency for acetate conversion to current was similar in the presence (92 ± 1%) or absence (88 ± 2%) of glycerol. No glycerol was consumed over the duration of the experiment. These results indicate that the electronic efficiency of $GsulA_{5E}$ anode biofilms is not inhibited by 10% glycerol loadings.

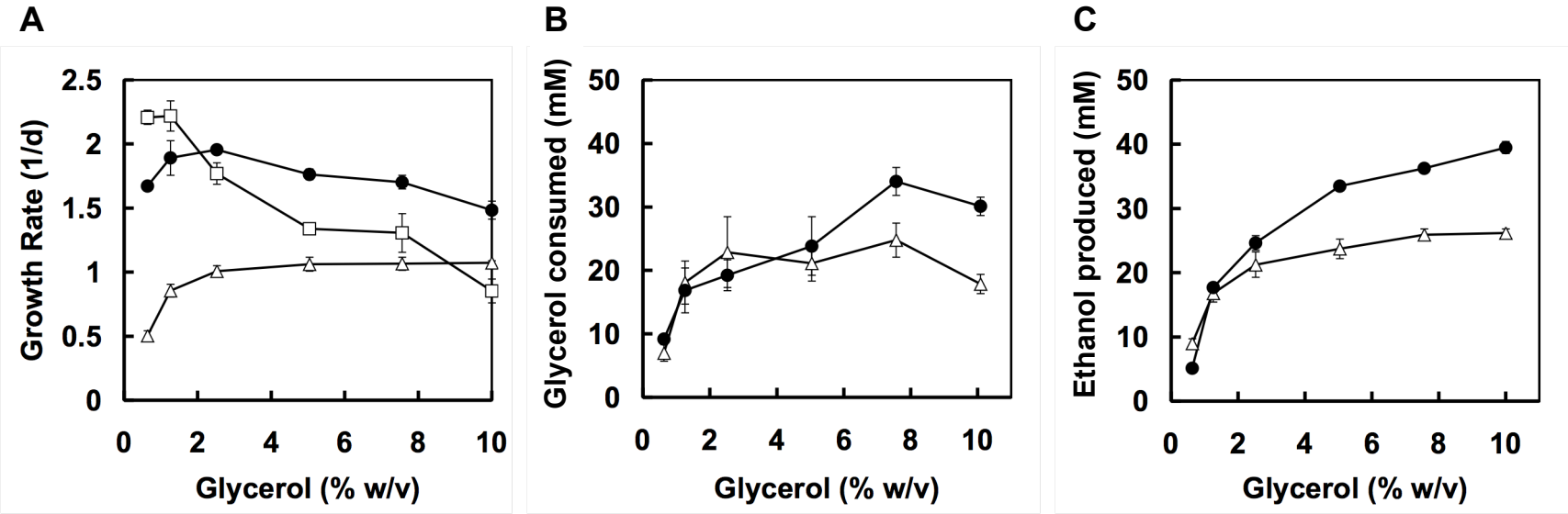

Fig. 4.7: (A) Growth rates of CcelA$_{10G}$ (open triangles), GsulA$_{5E}$ (open squares) and the coculture of the adapted strains (solid circles) when grown in increasing concentrations of glycerol. (B-C) The amount of glycerol consumed (B) and ethanol produced (C) in the CcelA$_{10G}$ monocultures (open triangles) and cocultures (solid circles) shown in (A). Error bars show standard deviations from three replicate cultures.

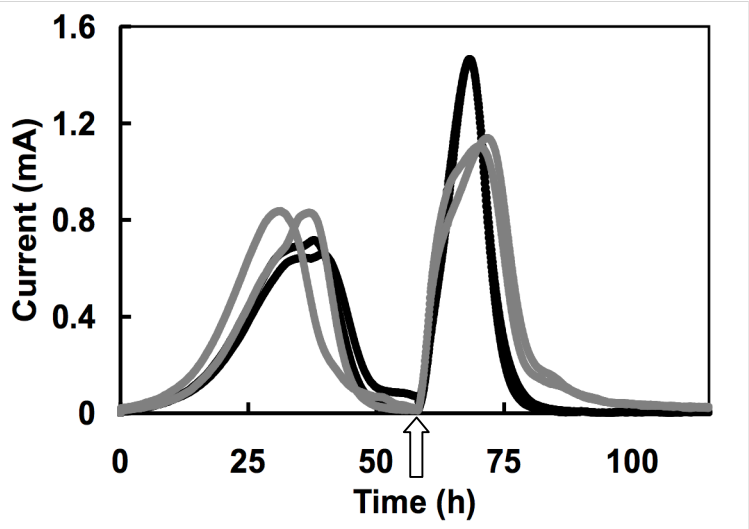

Fig. 4.8: Tolerance of $GsulA_{5E}$ anode biofilms to glycerol in a MEC. $GsulA_{5E}$ was initially grown with 1 mM acetate. When the acetate was consumed and the current declined, the medium was replaced (arrow) with medium containing 1 mM acetate (black lines, two replicate experiments shown) or 1 mM acetate and 10% (w/v) glycerol (gray lines, two replicate experiments shown).

MECs with 10% (w/v) glycerol loading. The adapted strains, $GsulA_{5E}$ and $CcelA_{10G}$, were shown to be tolerant to industrially relevant glycerol concentrations (10% w/v) and to syntrophically couple glycerol fermentation by $CcelA_{10G}$ with fumarate reduction by $GsulA_{5E}$ in batch cultures. We next investigated the ability of the coculture to couple the fermentation of 10% glycerol with current production in a MEC. As described previously, a sequential inoculation strategy was followed in which $GsulA_{5E}$

was first inoculated into the MEC and supplemented with 1 mM acetate to provide optimal conditions for biofilm formation (Fig. 4.9A). The current increased exponentially at a rate of 6.9 (± 1.0) d^{-1} and peaked at 1.1 (± 0.2) mA after approximately 30 h, and then declined once the acetate was consumed. When the current was < 0.1 mA, the anode medium was replaced with GS3 containing 10% (w/v) glycerol and the MEC anode was inoculated with $CcelA_{10G}$ (Fig. 4.9A). Following inoculation with $CcelA_{10G}$, the current immediately resumed and peaked at 1.4 (± 0.2) mA before declining to < 0.2 mA over a period of ca. 3 days, producing 2.0 (± 0.2) mmol e^- (Fig. 4.9B). For comparison, $CcelA_{10G}$ was grown as a monoculture in the MECs, however no current production was observed (Fig. 4.9A inset). At the end of the experiment, the anode electrode was removed from the MEC, stained with fluorescent dyes that differentially stain Gram positive (red) and Gram negative (green) cells, and imaged using confocal microscopy (Fig. 4.9C). Both red ($CcelA_{10G}$) and green ($GsulA_{5E}$) cells were visible on the anode electrode with the $GsulA_{5E}$ positioned closer to the electrode and $CcelA_{10G}$ forming a layer on top. While the anode culture broth was visibly turbid, a result of $CcelA_{10G}$ growth, the close proximity of the cells on the anode electrode may be facilitating interspecies metabolite transfer.

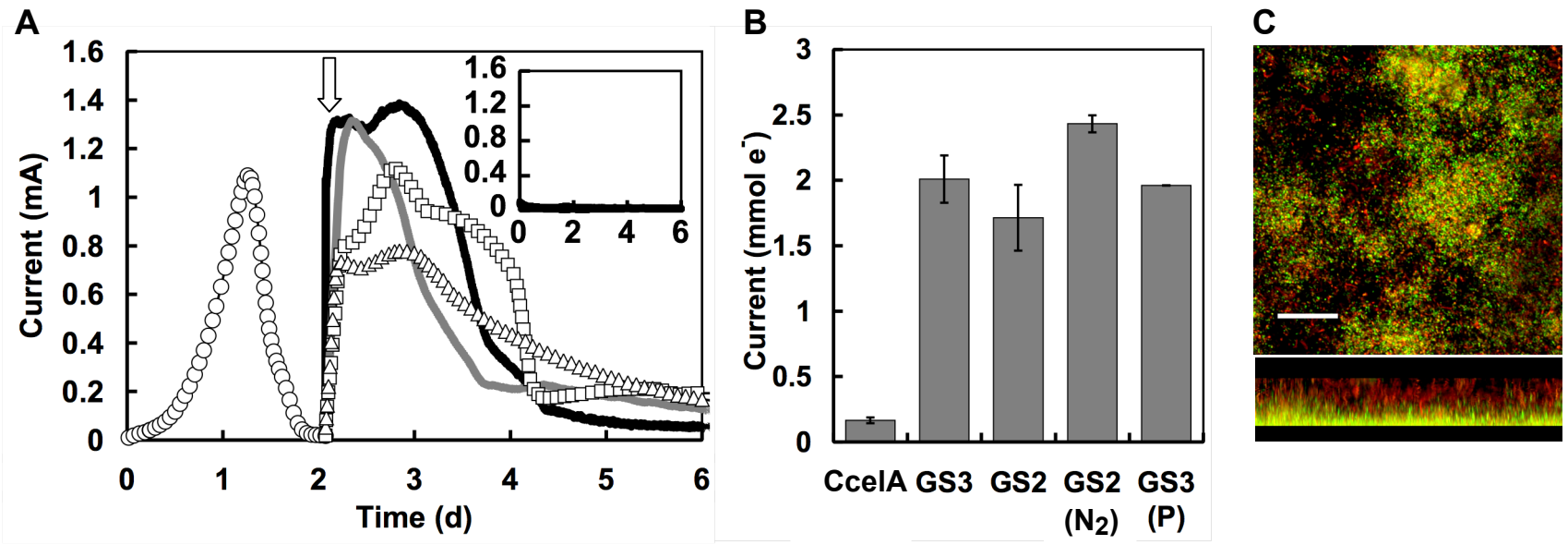

Fig. 4.9: Current production of sequentially inoculated MECs. (A) $GsulA_{5E}$ was inoculated first and supplemented with 1 mM acetate (open circles), the medium was then exchanged (arrow) for GS3 (black line), GS2 (grey line), GS3 with 200 mM phosphate buffer (open triangles), or GS2 medium that was then sparged with N_2 over the duration of the experiment (open squares). All MECs were supplemented with 10% (w/v) glycerol and inoculated with $CcelA_{10G}$. Controls of $CcelA_{10G}$ monocultures are also shown (inset, two representatives shown); the *x* axis is time in days; the *y* axis is current in mA. (B) Current production expressed in mmol electron equivalents (e^-) following the inoculation of $CcelA_{10G}$ into the MEC and the addition of 10% (w/v) glycerol. $CcelA_{10G}$ monocultures, Ccel; MECs sparged continuously, N_2; MECs with

200 mM phosphate buffer, P. (C) The anode biofilm shown in panel A (black line) was stained with the BacLight Gram Stain Kit (green, Gram negative, *G. sulfurreducens*; red, Gram positive, *C. cellobioparum*) and imaged with CLSM. Top view and corresponding projection in the *x* axis (bottom) is shown; scale bar, 10 µm.

At the end of the MEC experiment when the current had declined below 0.1 mA, the composition of the anode supernatant was analyzed by HPLC and compared to $CcelA_{10G}$ negative controls grown in GS2-10% glycerol medium in the MECs in the presence and absence of a poised anode electrode (Fig. 4.10B). Although less than 0.2 mmol e^- were produced from $CcelA_{10G}$ grown with a poised electrode (Fig 4.9B), growth in the presence of the poised anode increased glycerol consumption 1.9-fold from 72.3 (± 18.8) mM to 140.5 (± 53.8) mM (Fig. 4.10A). Consequently, ethanol production also increased by 2.2-fold from 46.2 (± 10.1) mM to 101.8 (± 43.9) mM. This improved performance corresponds with an increase in pH from 5.3 (± 0.4) to 5.7 (± 0.4) (Fig. 4.10A), although the cause of the pH increase is uncertain. Both $CcelA_{10G}$ cultures grown in the MECs produced acetate and lactate which was unexpected as previous experiments with $CcelA_{10G}$ grown in batch culture in 10 ml pressure tubes following the adapted evolution resulted in only ethanol, formate, H_2 and CO_2 produced.

The glycerol consumption was similar in the MEC with the $CcelA_{10G}$ monoculture with a poised electrode and the MEC pregrown with $GsulA_{5E}$ (151.6 ± 10.4 mM; Fig.

4.10A). Interestingly, the ethanol production decreased in the coculture (29.0 ± 2.8 mM) due to some of the carbon being shunted to the formation of 1,3-propanediol (22.7 ± 4.4 mM) and propionate (7.7 ± 1.0 mM), which were not produced in any of the $CcelA_{10G}$ monocultures (Fig. 4.10B). The production of ethanol, acetate and lactate began immediately after inoculation of $CcelA_{10G}$ into the anode chamber with $GsulA_{5E}$, while the production of propionate and 1,3-propanediol were first detected in the culture broth approximately 5 d after inoculation and at the same time as the ethanol production was reaching a plateau. This suggests that there was metabolic switch that diverted fluxes away from the production of ethanol and toward 1,3-propanediol and propionate (Fig. 4.2). The energy recoveries for the $CcelA_{10G}$ monocultures were high (poised anode, 62.4 ± 2.3%; unpoised anode, 57.6 ± 3.2%) because approximately 68% of the glycerol was converted to ethanol. The energy recoveries in the MEC, calculated assuming cathodic H_2 recovery efficiencies of 72% as described previously (49), were lower (16 ± 2%) because only ca. 19% of the glycerol consumed was recovered at ethanol. The energy recovered from the fermentation alone made up 15% (3.44 ± 0.22 KJ) of the energy recovered while cathodic H_2 production from the MEC contributed only 1% (0.27 ± 0.03 kJ).

The current production ceased in the MEC although acetate, lactate, formate and H_2 remained in the anode chamber at the end of the experiment (Fig. 4.10B), indicating that something was limiting the performance of the *G. sulfurreducens* anode biofilm. We measured the pH at the end of the experiment and found that the MEC anode broth was

pH 5.1 (± 0.1), which was substantially lower than the CcelA$_{10G}$ monoculture (pH, 5.7 ± 0.4). Because the thermodynamics of energy conversions at the anode are sensitive to pH changes (26, 37), we hypothesized that this had caused the drop in current production despite the abundance of electron donors available for *G. sulfurreducens*. Consequently, we repeated the MEC experiments and used MOPS-buffered GS2 medium with 10% glycerol to replace the medium in the anode chamber at the time of CcelA$_{10G}$ inoculation (Fig. 4.9). As before, the current increased immediately upon inoculation of the CcelA$_{10G}$, peaking at 1.3 (± 0.1) mA before decreasing over a period of ca. 3 d to <0.2 mA. The pH of the anode broth at the end of the experiment (5.1 ± 0.2) was similar to the GS3 medium despite the additional buffering. This was possibly due to the increased accumulation of CO_2 in the anode chamber (26.0 ± 3.4 mM) compared with the GS3 MECs (8.0 ± 0.4 mM), which, when dissolved into the medium, results in the production of carbonic acid. Likely as a consequence of the low pH, the predicted increase in current production was not observed (Fig. 4.9B). There was, however, a 1.3-fold increase in the amount of glycerol consumed (193.5 ± 7.1 mM), and a 2.2-fold increase in total fermentation products detected at the end of the experiment (Fig. 4.10). The percent of the glycerol consumed that was recovered as ethanol increased to ca. 30%; the energy recoveries also increased accordingly to 27% (± 2). As seen previously, the energy recoveries were primarily due to the fermentation (26%) with only a small contribution from the MEC (1%).

Because we suspected that the CO_2 accumulation in the anode headspace resulted in the acidification of the medium, we repeated the MEC experiment with GS2

medium as described above, and following the inoculation of $CcelA_{10G}$, the anode and cathode medium were sparged continuously with N_2 gas (Fig. 4.7). As before, the current immediately resumed upon inoculation of $CcelA_{10G}$, reaching ca. 0.8 mA, however it took an additional day for the current to reach a maximum of 1.1 (± 0.1) mA. This difference is likely due to the fact that hydrogen was removed from the anode vessel by sparging, and that it took some time for the $CcelA_{10G}$ to start fermenting glycerol into products that could be used as electron donors by $GsulA_{5E}$. The current declined to ca. 0.2 mA over a period of 3.7 d and was maintained at ca. 0.2 mA for approximately 6 d. It was this sustained low level of current production that resulted in higher electron recoveries (2.4 ± 0.1 mmol e^-) (Fig. 4.9B) than were observed in either of the other MEC experiments. Removing the H_2 by sparging the anode did not decrease the current production, which indicates that *G. sulfurreducens* was preferentially using the organic acids as electron donors. However, lactate (5.8 ± 0.2 mM) and acetate (28.2 ± 5.9 mM) still remained in the anode supernatant at the end of the experiment and were not converted into current. As expected, removing CO_2 resulted in increased pH (6.0 ± 0.2, Fig. 4.10A) compared with MOPS-buffered medium alone (5.1 ± 0.2). The glycerol consumed by $CcelA_{10G}$ increased 2.4-fold compared with the unsparged GS2 MEC, and ca. 43% of the glycerol that was provided was removed (Fig. 4.10A). This increase is likely due to the removal of H_2 as a feedback inhibitor of the fermentation (9). Correspondingly, 1.7-fold more fermentation products

were detected at the end of the experiment, however this number does not include the H_2 and CO_2 that were produced, which were removed by sparging. Interestingly, formate was not detected at the end of the experiment. As H_2 and CO_2 are in equilibrium with formate through the action of formate dehydrogenase, their removal probably drove the reaction in the direction of H_2 and CO_2 production. Some formate may also have been removed by *G. sulfurreducens.* Approximately 40% of the glycerol consumed was recovered as ethanol (Fig. 4.10) or the equivalent of 187.8 (± 48.5) mM, although it is worth noting that this may be an underestimate of ethanol production because some ethanol may have evaporated during the sparging. Energy recoveries also increased compared with the GS2 medium without sparging to 34% (± 8), and 33.6% was a result of the fermentation while 0.4% was from cathodic H_2 production in the MEC.

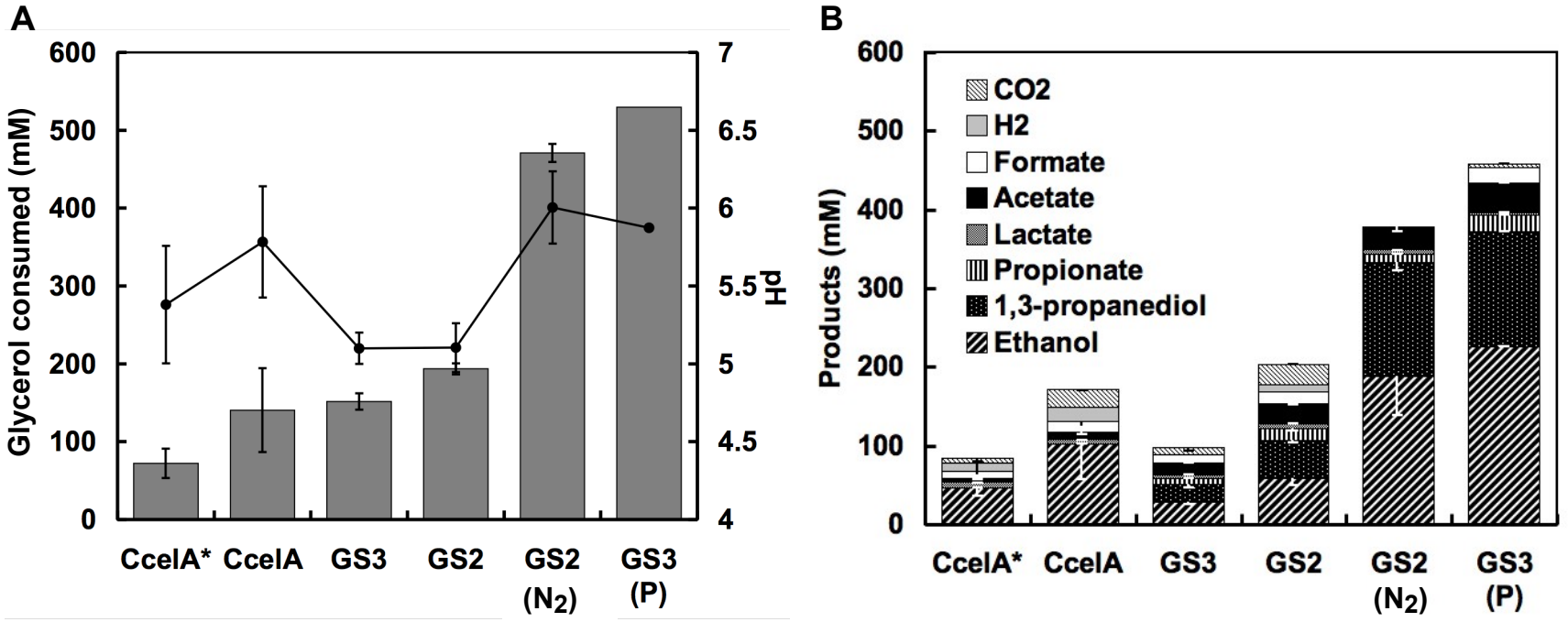

Fig. 4.10: Glycerol consumed (bars in panel A), fermentation products produced (B) and final pH (line in panel A) measured at the end of the experiment in each of the MECs shown in Fig. 4.9A (N_2, MECs sparged continuously; P, MECs with 200 mM phosphate buffer). Monocultures of $CcelA_{10G}$ grown in GS3 medium with 10% glycerol in MECs with (CcelA) and without (CcelA*) a poised anode electrode are shown for comparison.

MOPS buffer is a useful laboratory chemical that because of its price does not lend itself well to widespread industrial applications. We therefore tested the effectiveness of 200 mM phosphate buffered GS3 medium in the MECs (Fig. 4.9A). As seen previously, the current immediately resumed following the replacement of the medium and inoculation of $CcelA_{10G}$, however the maximum current production (ca. 0.77 mA) was only 60% of that seen in the MECs with standard GS3 medium (Fig 4.9A), suggesting that the phosphate buffer was detrimental to the *G. sulfurreducens* anode biofilm. Consistent with this, large amounts of electron donors (lactate, 2.2 mM; acetate, 37.8 mM; formate, 19.8 mM) remained in the supernatant after the current production stopped. Despite this difference, the total current production (ca. 2 mmol e^-) was similar to that of GS3 medium without the phosphate buffer (Fig. 4.9B). The pH of the anode medium at the end of the experiment (5.9) was similar to MEC that was run with continuous sparging (Fig. 4.10A), demonstrating that the phosphate buffer was effective at counteracting the fermentative CO_2 production. Glycerol consumption was stimulated 3.5-fold compared to standard GS3 medium, and approximately 50% of the glycerol that was provided in the medium was consumed (Fig. 4.10A). 43% of the glycerol consumed was converted to ethanol and correspondingly the energy recovery increased to ca. 36%. Consistent with the poor conversion efficiency of the electron donors into current, only 0.2% of the energy recovery was due to the MEC.

Coupling glycerol fermentation to power production in a microbial fuel cell. We investigated the ability of a $GsulA_{5E}$ and $CcelA_{10G}$ coculture to sustain power production in a MFC. The MFC design was the same as the H-type configuration used

in the MECs except that ferricyanide was used at the catholyte. High-surface area graphite felt electrodes were used so the initial acetate concentration was increased to 5 mM and the anode was inoculated with twice as many $GsulA_{5E}$ cells. Before inoculation with $GsulA_{5E}$, the open circuit voltage (OCV) was 180 mV; following inoculation, the current increased from 0.2 mA to 0.48 mA over a period of 2 d (Fig. 4.11A), at this time the OCV was 718 mV. After 3 d, the medium in the anode was exchanged with GS2-glycerol medium and inoculated with $CcelA_{10G}$ (Fig. 4.11A). When $CcelA_{10G}$ was inoculated the current immediately increased to 0.8 mA, where it remained for approximately 14 h until steadily decreasing to ca. 0.01 mA over a period of 5.5 d. The total current produced following the inoculation of $CcelA_{10G}$ was 1.5 mmol e^-, which was lower than any of the MEC experiments (Fig. 4.9B). Current production in controls without $CcelA_{10G}$ increased to 0.52 mA following the exchange of the anode medium, decreased to 0.34 mA after 14 h where it plateaued for ca. 2 d before decreasing to ca. 0.01 mA over a period of 3 d. The total current produced in the control was 1.3 mmol e^-, indicating that $GsulA_{5E}$ was able to sustain power production from the components of the rich medium alone, although the maximum current production was lower than in the MFC inoculated with $CcelA_{10G}$. Control monocultures with $CcelA_{10G}$ alone were also inoculated into an MFC with GS3-glycerol medium (Fig. 4.11A inset). The current production started at 0.3 mA and decreased steadily to 0.06 mA over a period of 8 d. A total of 0.97 mmol e^- were produced over this period, which was more

than the amount of current produced in a similarly inoculated MEC (Fig. 4.9B; 0.17 mmol e^-).

The internal resistance of the MEC before and after $CcelA_{10G}$ inoculation was determined by performing a power density curve from 0-3 KΩ (Fig 4.11B). The power production is greatest when the external applied resistance is the same as the internal resistance. The power density for $GsulA_{5E}$ alone peaked at 51 μWm^{-2} at 1.1 KΩ, and the power density for the coculture was 115 μWm^{-2} at 0.3 KΩ, suggesting that the internal resistance decreased upon addition of GS2-glycerol medium and inoculation with $CcelA_{10G}$. Controls without $CcelA_{10G}$ reached a maximum power density at 54 μWm^{-2} and 1.3 KΩ, indicating that the decrease in resistance seen in the coculture was a result of $CcelA_{10G}$ inoculation and not due to the change in medium. Controls with $CcelA_{10G}$ monocultures had a maximum power density of 4 μWm^{-2} at 01.1 KΩ (Fig. 4.11B).

Analysis of the composition of the anode supernatant revealed that $CcelA_{10G}$ monocultures consumed 7.7% of the glycerol provided (the equivalent of 83.7 mM), converting 24% to ethanol (20.3 mM). The production of lactate (0.4 mM), acetate (3.7 mM), formate (6.8 mM), H_2 (0.01 mM) and CO_2 (0.6 mM) were also observed (Fig. 4.11C). In the coculture, glycerol consumption increased to 13% of the glycerol that was provided (the equivalent of 136.6 mM, Fig. 4.11C). Approximately 20% of the glycerol consumed was recovered as ethanol (27.3 mM) with the remaining carbon being

diverted to the production of 1,3-propanediol (30.2 mM), propionate (10.3 mM), lactate (13.8 mM), acetate (9.4 mM), formate (11.8 mM), H_2 (0.01 mM) and CO_2 (8.8 mM). Just as in the MECs (Fig. 4.10A), the pH measured at the end of the experiment was low for both the $CcelA_{10G}$ monoculture and the coculture (4.9 and 5.0, respectively). This may have contributed to the *G. sulfurreducens* electron donors remaining unconsumed in the culture broth (Fig. 4.11C). The ca. 2,000-fold increased surface area of the anode electrodes did not improve the conversion efficiency of the electron donors compared with the MECs. The energy recovery from the $CcelA_{10G}$ monoculture was 21%, while the energy recovery from the coculture MFC was lower (17.1%) due to some of the carbon being diverted to the production of 1,3-propanediol and propionate. The energy recovered from the fuel cell (0.2% or 0.06 J) was very small compared to the energy recovered from the fermentation alone (16.9% or 3.44 KJ).

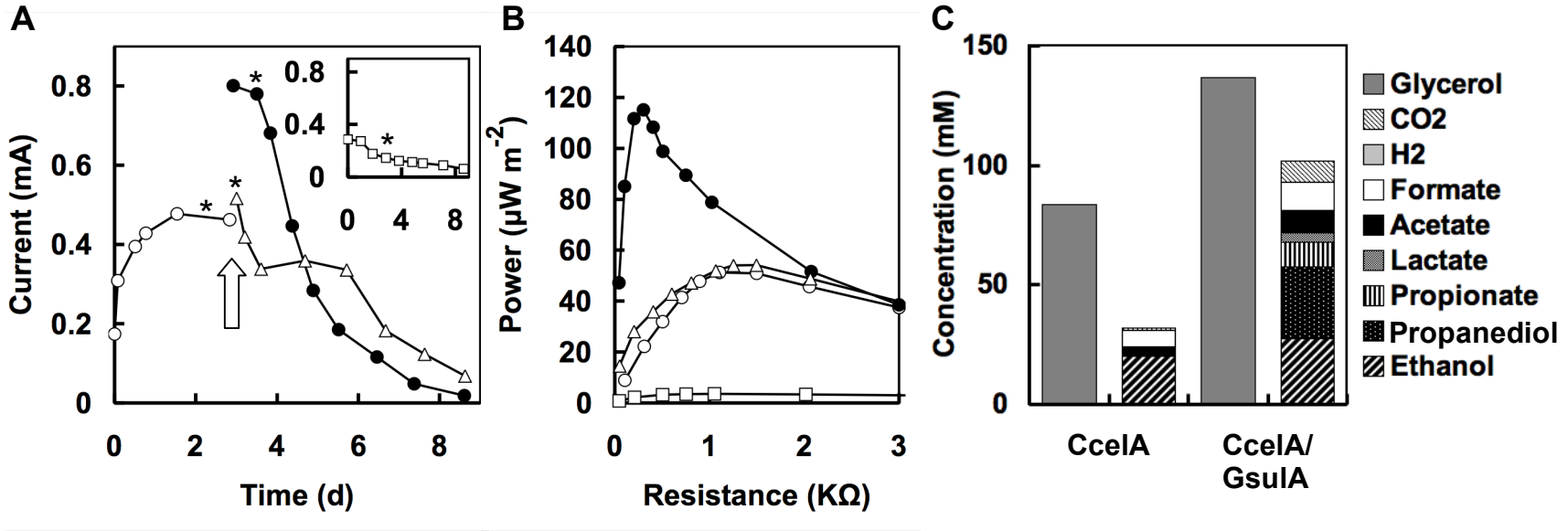

Fig. 4.11: (A) Current production over time in a MFC by a monoculture of $GsulA_{5E}$ grown with 5 mM acetate (open symbols), the anode medium was replaced with GS3-10% glycerol medium (arrow), and inoculated with $CcelA_{10G}$ (closed circles) or left uninoculated (open triangles). Current production over time for a $CcelA_{10G}$ monoculture is also shown (inset); the *x* axis is time in days; the *y* axis is current in mA. (B) Power density curves performed when indicated in panel A (*) for the $CcelA_{10G}$ monoculture (open squares), $GsulA_{5E}$ monoculture (open circles), following the change of anode medium (open triangles) and the inoculation of $CcelA_{10G}$ (closed circles). (C) The glycerol consumed and fermentation products detected at the end of the experiment in the $CcelA_{10G}$ monoculture (CcelA) and the coculture (CcelA/GsulA).

DISCUSSION

Finding alternative uses for the crude glycerol produced as a major byproduct of the biodiesel industry without purification is an important consideration for improving the economic viability of the industry. Fermentation of crude glycerol into ethanol would have the added benefit of supplying the biodiesel refinery with a maximum of one third of the ethanol feedstock required for the transesterification reaction, thereby reducing costs of the chemical inputs (presently 12% of the cost of biodiesel production; (1)), and making the production of biodiesel increasingly independent of fossil fuel inputs. Several organisms have been found to consume crude glycerol wastewater and produce ethanol, 1,3-propanediol and/or H_2 as added value products (34, 43).

In this chapter we identified *C. cellobioparum* as a robust ethanologenic strain capable of fermenting refined glycerol. *C. cellobioparum* is placed phylogenetically in Cluster III of the family Clostridiaceae (61) which was reclassified to the family Ruminococcaceae (29). To our knowledge, no other member of this cluster has been reported to ferment glycerol; in fact, *Clostridium papyrosolvens,* a closely related species, was tested during this study and did not couple the fermentation of glycerol to growth (Table 4.1). The wild-type *C. cellobioparum* sustained low growth rates in concentrations of glycerol up to 7% (w/v) (Fig. 4.4A). Glycerol at high concentration changes the viscosity and osmotic pressure of the medium, and because the cell membrane is highly permeable to glycerol, intracellular glycerol concentrations will affect the viscosity of the cytoplasm and therefore enzyme activities (58). Because the concentration of crude glycerol in biodiesel wastewater are generally at least 10% (w/v), strain improvements via adaptive evolution were required to achieve growth under these

conditions (Fig. 4.5). The growth rates of this adapted strain ($CcelA_{10G}$) were greatly improved compared to the wild-type strain at glycerol concentrations above 2% (w/v) (Fig. 4.7A) and robust growth was observed at 10% (w/v) glycerol. Both the wild-type and adapted strains only fermented a fraction of the glycerol that was provided (ca. 20% and 6% respectively), and both produced fermentative byproducts including lactate, acetate, formate, H_2, and CO_2. These byproducts, especially H_2 (9), are potential inhibitors of fermentation and growth due to feedback inhibition of reversible enzymatic processes and organic acid and CO_2 production lead to the acidification of the culture medium. The cocultivation of *C. cellobioparum* with *G. sulfurreducens* is therefore an attractive option because *G. sulfurreducens* can consume many of these products, converting them to electrical current in BESs. Interspecies metabolite transfer with *G. sulfurreducens* was shown to be possible both with fumarate and an electrode as the electron acceptor for *Geobacter* (Fig. 4.3 and 4.4), however, *G. sulfurreducens* growth was also inhibited at high concentrations of glycerol and ethanol. Adaptive evolution was employed to produce a strain of *G. sulfurreducens* ($GsulA_{5E}$) that was tolerant to ethanol at industrially relevant concentrations of 5% (v/v). This tolerance to ethanol also conferred upon $GsulA_{5E}$ the ability to grow in 10% (w/v) glycerol concentrations, suggesting a non-specific alcohol tolerance. Ethanol toxicity is attributed to increases in cell membrane fluidity, and the disruption of phospholipids, nutrient and ion transport through the cell membrane, and ATPases resulting in a decreased intracellular pH and collapse of the H^+ gradient across the membrane (24). As a result, adaptations which

confer solvent tolerance are complex, requiring multiple genetic changes, which affect general cellular stress response mechanisms as well as changes in membrane fatty acid, phospholipids and protein composition (24, 45, 63). As we hypothesized, coculturing the adapted strains in batch cultures with fumarate increased the amount of glycerol consumed and ethanol produced (Fig. 4.7B and C). Genome sequencing is underway for both the wild-type and adapted strains from both species so that the genetic basis for glycerol and ethanol tolerance can be investigated. An important future direction of this research will be to test the growth of both organisms in crude glycerol wastewater from the biodiesel industry to identify any additional contaminants that may inhibit growth and which will require additional strain improvements.

Previous experiments with *Clostridium propionicum* showed that this strain was capable of current production in a MFC (21.78 mW/m^2) with cysteine and resazurin as mediators of electron transfer (64). The ability of $CcelA_{10G}$ to produce current was tested by growing the strain in the absence of *G. sulfurreducens* in a MEC with and without a poised anode electrode and in a MFC with a 470 Ω external resistance. The effect of the poised anode electrode MEC was to increase glycerol fermentation and ethanol production (Fig. 4.10B) although very little current production was observed (Fig. 4.9). Conversely, the growth of $CcelA_{10G}$ in the MFC resulted in similar amounts of glycerol consumption as the unpoised anode, produced a measurable amount of current although maximum power densities were low (4 $\mu W/m^2$), and converted only a small percentage of the glycerol consumed into ethanol (Fig. 4.11). The GS2 and GS3 medium used in this study contain 2 g/L cysteine so it is possible that $CcelA_{10G}$ was

able use it as a mediator for current production, and that current production in the MFC was detectable due to the higher surface area of the anode electrode compared with the MEC. Replacing the anode electrode of the MEC with the high-surface-area graphite felt electrodes and changing the poised anode potential may serve to amplify the current production to detectable levels. The low ethanol recoveries in the MFC could be explained by the excess reducing equivalents derived from glycerol oxidation to pyruvate (Fig. 4.2) being used for current production through a respiratory metabolic pathway rather than for ethanol production through a fermentative pathway. Other *Clostridia* species including an isolate from a mediator-less microbial fuel cell that was similar to *Clostridium butyricum* was shown to be capable of Fe(III) and electrode reduction (40). The ability of CcelA$_{10G}$ to sustain continuous current production in continuous flow MFCs or over repeated batch cycles should be investigated. Additionally, electrochemical characterization with CcelA$_{10G}$ grown in BESs without cysteine or with alternative electron mediators may help to clarify the nature of the interaction of CcelA$_{10G}$ with the anode electrode.

The growth of GsulA$_{5E}$ and CcelA$_{10G}$ in coculture in BESs with high glycerol concentrations was also studied. Cocultivating the strains in MECs with GS3 medium did not serve to greatly increase the glycerol consumption compared with CcelA$_{10G}$ monoculture controls in the presence of poised anode electrodes (Fig. 4.10A), although beneficial effects were seen in the MFC on glycerol consumption and power production of the coculture compared to the monoculture (Fig. 4.11). However, the synergistic interaction of the two strains in the BESs resulted in a shift in the glycerol metabolism of

$CcelA_{10G}$ away from ethanol and toward propionate and 1,3-propanediol (Fig. 4.10B). This effect was not seen in any of the $CcelA_{10G}$ monocultures or in batch cocultures of $GsulA_{5E}$ and $CcelA_{10G}$ with fumarate as an electron acceptor. Propionate is a chemical used in antifungal agents, herbicides, solvents and perfumes (30) and 1,3-propanediol is used as a precursor to renewable plastics (18, 44). Because 1,3-propanediol has great potential to improve the economics of the biodiesel industry and its production has been widely studied (3, 17, 30, 34). The nature of this metabolic shift is not yet understood and would benefit from further investigation through the use of enzyme activity assays and the quantification of intracellular $NADH/NAD^+$ pools as described previously (18). The discovery that the native *C. cellobioparum* has the metabolic pathways to produce 1,3-propanediol opens up exciting new avenues for research and strain development. Genetic engineering of the strain could be used to target the metabolic pathway for either ethanol production or 1,3-propanediol production by knocking out the enzymes required for competing pathways. For example, eliminating the pathways to lactate, acetate, propionate and 1,3-propanediol production could result in increases in ethanol yields (48, 55), up to the maximum theoretical yields of 1 mol of ethanol per mol of glycerol. Alternatively, the highest theoretical yield for 1,3-propanediol (0.72 mol per mol glycerol) is achieved when acetate is coproduced for ATP synthesis (30). This could be achieved by eliminating the pathways for ethanol, lactate, formate and propionate production. Although a genetic system has not yet been developed for *C. cellobioparum*, the closely related species *Clostridium cellulolyticum* and *Clostridium thermocellum* have proved to be genetically tractable and many new

genetic tools for the group are available (5, 23, 52, 55). Sequencing and annotation of the genome for *C. cellobioparum* will be instrumental in understanding and manipulating the metabolic networks.

In either scenario of metabolic engineering, fermentative waste products are produced (formate and H_2 during ethanol fermentation, or acetate during 1,3-propanediol fermentation) which could be used by *G. sulfurreducens* for electricity production in BESs. Although the BESs in our study did not greatly contribute to the overall energy recoveries, the optimization of BES operation and medium conditions through increased buffering and removal of H_2 and CO_2 was shown to have a marked effect on glycerol consumption of $CcelA_{10G}$ (Fig. 4.10A, Fig. 4.11B). The high energy recoveries through ethanol fermentation are useful values if the ethanol will be burned for electricity production, however in the biodiesel biorefinery model the ethanol will be treated as a value added chemical rather than as an energy source. The fermentative and cathodic H_2 production on the other hand can be considered as an energy source for the refinery. The energy costs required to operate the refinery make up approximately 2% of the cost of biodiesel production (1), and replacing this energy input with renewable alternatives is another route to making biodiesel production independent of fossil fuels. H_2 is an attractive energy source if produced and consumed locally because it can be stored for use when other methods of energy production are low, for example at night when photovoltaic panels are not operating. Removing the H_2 from the anode chamber did not decrease the efficiency of the current production, indicating that

G. sulfurreducens sustained most of the current production from oxidation of organic acids. Moreover, consumption of H_2 at the anode in a MEC is redundant as it is simply produced again at the cathode, and over-potentials at the cathode will result in electron losses and decreased conversion efficiency. The fermentative CO_2 could also be collected as an added value product and used during the cultivation of microalgae for oil feedstocks, as high CO_2 concentrations are required in order to maximize growth and oil production (41, 59).

In order for H_2 production or current production to be viable energy sources, the BES design must be improved and scaled up. The two-chamber design used in this study is widely regarded as the first generation BES (33), useful for laboratory operations but not scaleable due to the presence of an expensive Nafion membrane (US $1,616 per m^2), low electrode surface area, batch operation and small size. Improvements in BES design include membrane-less reactors, decreasing the distance between the anode and cathode electrode, increasing the electrode surface area, improving the conductive properties of the anode and cathode electrodes, and using oxygen as the catholyte (27, 33). Optimizations such as these have resulted in power production as high as 1,010 W/m^3 (14). The results presented here also point to other areas for optimization including a responsive buffering system to prevent the damaging effect of low pH on the anode biofilm and the removal and collection of H_2 and CO_2 from the anode chamber. Another interesting result of the synergistic interaction of the two organisms was observed in the MFCs where the internal resistance decreased

when CcelA$_{10G}$ was added. This decrease could not be explained by the change in medium or by the operation of CcelA$_{10G}$ monocultures which both had similar internal resistances to the MFCs operated with GsulA$_{5E}$ alone (Fig. 4.11B). The internal resistance has an inverse effect on the power production generated from a MFC, so its minimization is key to the optimization of fuel cell design (26).

These experiments demonstrate that glycerol fermentation can be coupled to current production in either MECs or MFCs at high glycerol loadings (10%) by a coculture of alcohol tolerant *G. sulfurreducens* and *C. cellobioparum*. Glycerol removal was high (ca. 50 g/L) making this platform attractive for the treatment of crude glycerol waste streams of the biodiesel industry. Several avenues for improvement have been highlighted including further genetic engineering or adaptive evolution of the partner organisms, improvements to the BES designs, and investigation of the platform performance with crude glycerol derived from the biodiesel industry.

REFERENCES

REFERENCES

1. **Atabani, A. E., A. S. Silitonga, I. A. Badruddin, T. M. I. Mahlia, H. H. Masjuki, and S. Mekhilef.** 2012. A comprehensive review on biodiesel as an alternative energy resource and its characteristics. Renew. Sust. Energ. Rev. **16:**2070-2093.

2. **Basha, S. A., and K. R. Gopal.** 2012. A review of the effects of catalyst and additive on biodiesel production, performance, combustion and emission characteristics. Renew. Sust. Energ. Rev. **16:**711-717.

3. **Biebl, H., K. Menzel, A. P. Zeng, and W. D. Deckwer.** 1999. Microbial production of 1,3-propanediol. Appl. Microbiol. Biotechnol. **52:**289-97.

4. **Biebl, H., and C. Sproer.** 2002. Taxonomy of the glycerol fermenting clostridia and description of *Clostridium diolis* sp. nov. Syst. Appl. Microbiol. **25:**491-7.

5. **Blouzard, J. C., O. Valette, C. Tardif, and P. de Philip.** 2010. Random mutagenesis of *Clostridium cellulolyticum* by using a Tn1545 derivative. Appl. Environ. Microbiol. **76:**4546-9.

6. **Brunschwig, C., W. Moussavou, and J. Blin.** 2012. Use of bioethanol for biodiesel production. Prog. Energ. Combust. **38:**283-301.

7. **Cavedon, K., S. B. Leschine, and E. Canale-Parola.** 1990. Cellulase system of a free-living, mesophilic *clostridium* (strain C7). J. Bacteriol. **172:**4222-30.

8. **Cheng, S., and B. E. Logan.** 2007. Sustainable and efficient biohydrogen production via electrohydrogenesis. Proc. Nat. Acad. Sci. USA **104:**18871-18873.

9. **Chung, K. T.** 1976. Inhibitory effects of H_2 on growth of *Clostridium cellobioparum*. Appl. Environ. Microbiol. **31:**342-8.

10. **Clauwaert, P., D. van der Ha, and W. Verstraete.** 2008. Energy recovery from energy rich vegetable products with microbial fuel cells. Biotechnol. Lett. **30:**1947-1951.

11. **Coppi, M. V., C. Leang, S. J. Sandler, and D. R. Lovley.** 2001. Development of a genetic system for *Geobacter sulfurreducens*. Appl. Environ. Microbiol. **67:**3180-7.

12. **Demirbas, A.** 2008. New liquid biofuels from vegetable oils via catalytic pyrolysis. Energy Educ. Sci. Tech. **21:**1-59.

13. **Dharmadi, Y., A. Murarka, and R. Gonzalez.** 2006. Anaerobic fermentation of glycerol by *Escherichia coli*: a new platform for metabolic engineering. Biotechnol. Bioeng. **94:**821-9.

14. **Fan, Y. Z., H. Q. Hu, and H. Liu.** 2007. Enhanced coulombic efficiency and power density of air-cathode microbial fuel cells with an improved cell configuration. J. Power Sources **171:**348-354.

15. **Finkel, S. E.** 2006. Long-term survival during stationary phase: evolution and the GASP phenotype. Nat. Rev. Microbiol. **4:**113-20.

16. **Flynn, J. M., D. E. Ross, K. A. Hunt, D. R. Bond, and J. A. Gralnick.** 2010. Enabling unbalanced fermentations by using engineered electrode-interfaced bacteria. MBio. **1**: e00190-10.

17. **Gonzalez-Pajuelo, M., J. C. Andrade, and I. Vasconcelos.** 2004. Production of 1,3-propanediol by *Clostridium butyricum* VPI 3266 using a synthetic medium and raw glycerol. J. Ind. Microbiol. Biotechnol. **31:**442-6.

18. **Gonzalez-Pajuelo, M., I. Meynial-Salles, F. Mendes, P. Soucaille, and I. Vasconcelos.** 2006. Microbial conversion of glycerol to 1,3-propanediol: physiological comparison of a natural producer, *Clostridium butyricum* VPI 3266, and an engineered strain, *Clostridium acetobutylicum* DG1(pSPD5). Appl. Environ. Microbiol. **72:**96-101.

19. **Haas, M. J., A. J. McAloon, W. C. Yee, and T. A. Foglia.** 2006. A process model to estimate biodiesel production costs. Bioresour. Technol. **97:**671-678.

20. **Himmi, E. H., A. Bories, A. Boussaid, and L. Hassani.** 2000. Propionic acid fermentation of glycerol and glucose by *Propionibacterium acidipropionici* and *Propionibacterium freudenreichii* ssp. *shermanii*. Appl. Microbiol. Biotechnol. **53:**435-40.

21. **Hungate, R. E., and J. Macy.** 1973. The roll-tube method for cultivation of strict anaerobes. Bull. Ecol. Res. Comm. **17:**123-125.

22. **Ito, T., Y. Nakashimada, K. Senba, T. Matsui, and N. Nishio.** 2005. Hydrogen and ethanol production from glycerol-containing wastes discharged after biodiesel manufacturing process. J. Biosci. Bioeng. **100:**260-5.

23. **Jennert, K. C., C. Tardif, D. I. Young, and M. Young.** 2000. Gene transfer to *Clostridium cellulolyticum* ATCC 35319. Microbiology **146:**3071-80.

24. **Jia, K., Y. Zhang, and Y. Li.** 2010. Systematic engineering of microorganisms to improve alcohol tolerance. Eng. Life Sci. **10:**422–429.

25. **Lapuerta, M., O. Armas, and J. Rodriguez-Fernandez.** 2008. Effect of biodiesel fuels on diesel engine emissions. Prog. Energ. Combust. **34:**198-223.

26. **Logan, B. E.** 2008. Microbial fuel cells. Wiley-Interscience, Hoboken, N.J.

27. **Logan, B. E.** 2010. Scaling up microbial fuel cells and other bioelectrochemical systems. Appl. Microbiol. Biotechnol. **85:**1665-1671.

28. **Lovley, D. R., Z. M. Summers, S. A. Haveman, and M. Izallalen.** 2011. *Geobacter* strains that use alternate organic compounds, methods of making, and methods of use thereof. U.S.A. University of Massachusetts (Boston, MA, US) 20110151544.

29. **Ludwig, W., K.-H. Schleifer, and W. B. Whitman.** 2009. Revised road map to the phylum Firmicutes, p. 1-13. *In* P. Vos, G. M. Garrity, D. Jones, N. R. Krieg, W. Ludwig, F. A. Rainey, K.-H. Schleifer, and W. B. Whitman (ed.), Bergey's Manual of Systematic Bacteriology. Springer New York.

30. **Maervoet, V. E. T., M. D. Mey, J. Beauprez, S. D. Maeseneire, and W. K. Soetaert.** 2011. Enhancing the microbial conversion of glycerol to 1,3-propanediol using metabolic engineering. Org. Process. Res. Dev. **15:**189-202.

31. **McKinlay, J. B., J. G. Zeikus, and C. Vieille.** 2005. Insights into *Actinobacillus succinogenes* fermentative metabolism in a chemically defined growth medium. Appl. Environ. Microbiol. **71:**6651-6.

32. **Meng, X., J. M. Yang, X. Xu, L. Zhang, Q. J. Nie, and M. Xian.** 2009. Biodiesel production from oleaginous microorganisms. Renewable Energy **34:**1-5.

33. **Minteer, S. D., P. Atanassov, H. R. Luckarift, and G. R. Johnson.** 2012. New materials for biological fuel cells. Materials Today **15:**166-173.

34. **Moon, C., J. H. Ahn, S. W. Kim, B. I. Sang, and Y. Um.** 2010. Effect of biodiesel-derived raw glycerol on 1,3-propanediol production by different microorganisms. Appl. Biochem. Biotechnol. **161:**502-10.

35. **Ng, J. H., H. K. Ng, and S. Gan.** 2010. Recent trends in policies, socioeconomy and future directions of the biodiesel industry. Clean Technol. Envir. **12:**213-238.

36. **Nicol, R. W., K. Marchand, and W. D. Lubitz.** 2012. Bioconversion of crude glycerol by fungi. Appl. Microbiol. Biotechnol. **93:**1865-1875.

37. **Nimje, V. R., C. Y. Chen, C. C. Chen, H. R. Chen, M. J. Tseng, J. S. Jean, and Y. F. Chang.** 2011. Glycerol degradation in single-chamber microbial fuel cells. Bioresour. Technol. **102:**2629-34.

38. **Nitayavardhana, S., and S. K. Khanal.** 2012. Biofuel residues/wastes: Ban or boon? Crit. Rev. Env. Sci. Tec. **42:**1-43.

39. **Oh, B. R., J. W. Seo, S. Y. Heo, W. K. Hong, L. H. Luo, M. H. Joe, D. H. Park, and C. H. Kim.** 2011. Efficient production of ethanol from crude glycerol by a *Klebsiella pneumoniae* mutant strain. Bioresour. Technol. **102:**3918-22.

40. **Park, H. S., B. H. Kim, H. S. Kim, H. J. Kim, G. T. Kim, M. Kim, I. S. Chang, Y. K. Park, and H. I. Chang.** 2001. A novel electrochemically active and Fe(III)-reducing bacterium phylogenetically related to *Clostridium butyricum* isolated from a microbial fuel cell. Anaerobe **7:**297-306.

41. **Petkov, G., A. Ivanova, I. Iliev, and I. Vaseva.** 2012. A critical look at the microalgae biodiesel. Eur. J. Lipid Sci. Tech. **114:**103-111.

42. **Saint-Amans, S., L. Girbal, J. Andrade, K. Ahrens, and P. Soucaille.** 2001. Regulation of carbon and electron flow in *Clostridium butyricum* VPI 3266 grown on glucose-glycerol mixtures. J. Bacteriol. **183:**1748-54.

43. **Sakai, S., and T. Yagishita.** 2007. Microbial production of hydrogen and ethanol from glycerol-containing wastes discharged from a biodiesel fuel production plant in a bioelectrochemical reactor with thionine. Biotechnol. Bioeng. **98:**340-348.

44. **Saxena, R. K., P. Anand, S. Saran, and J. Isar.** 2009. Microbial production of 1,3-propanediol: Recent developments and emerging opportunities. Biotechnol. Adv. **27:**895-913.

45. **Shao, X., B. Raman, M. Zhu, J. R. Mielenz, S. D. Brown, A. M. Guss, and L. R. Lynd.** 2011. Mutant selection and phenotypic and genetic characterization of ethanol-tolerant strains of *Clostridium thermocellum*. Appl. Microbiol. Biotechnol. **92:**641-52.

46. **Shapouri, H., J. A. Duffield, and M. Wang.** 2003. The energy balance of corn ethanol revisited. Trans. ASAE **46:**959-968.

47. **Sharma, Y. C., B. Singh, and S. N. Upadhyay.** 2008. Advancements in development and characterization of biodiesel: A review. Fuel **87:**2355-2373.

48. **Shaw, A. J., K. K. Podkaminer, S. G. Desai, J. S. Bardsley, S. R. Rogers, P. G. Thorne, D. A. Hogsett, and L. R. Lynd.** 2008. Metabolic engineering of a thermophilic bacterium to produce ethanol at high yield. Proc. Natl. Acad. Sci. USA **105:**13769-13774.

49. **Speers, A. M., and G. Reguera.** 2012. Consolidated bioprocessing of AFEX-pretreated corn stover to ethanol and hydrogen in a microbial electrolysis cell. Environ. Sci. Technol. **46**:7875–7881.

50. **Speers, A. M., and G. Reguera.** 2012. Electron donors supporting growth and electroactivity of *Geobacter sulfurreducens* anode biofilms. Appl. Environ. Microbiol. **78:**437-44.

51. **Szulczyk, K. R., and B. A. McCarl.** 2010. Market penetration of biodiesel. Renew. Sust. Energ. Rev. **14:**2426-2433.

52. **Tardif, C., H. Maamar, M. Balfin, and J. P. Belaich.** 2001. Electrotransformation studies in *Clostridium cellulolyticum*. J. Ind. Microbiol. Biotechnol. **27:**271-4.

53. **Thompson, J. C., and B. B. He.** 2006. Characterization of crude glycerol from biodiesel production from multiple feedstocks. Appl. Eng. Agric. **22:**261-265.

54. **Trinh, C. T., and F. Srienc.** 2009. Metabolic engineering of *Escherichia coli* for efficient conversion of glycerol to ethanol. Appl. Environ. Microbiol. **75:**6696-705.

55. **Tripathi, S. A., D. G. Olson, D. A. Argyros, B. B. Miller, T. F. Barrett, D. M. Murphy, J. D. McCool, A. K. Warner, V. B. Rajgarhia, L. R. Lynd, D. A. Hogsett, and N. C. Caiazza.** 2010. Development of pyrF-based genetic system for targeted gene deletion in *Clostridium thermocellum* and creation of a pta mutant. Appl. Environ. Microbiol. **76:**6591-6599.

56. **U.S Energy Information Administration.** 2012. Total biofuels production (thousand barrels per day). Available from: http://www.eia.gov/cfapps/ipdbproject/iedindex3.cfm?tid=79&pid=81&aid=1&cid=&syid=2000&eyid=2010&unit=TBPD.

57. **Verma, N. M., S. Mehrotra, A. Shukla, and B. N. Mishra.** 2010. Prospective of biodiesel production utilizing microalgae as the cell factories: A comprehensive discussion. Afr. J. Biotechnol. **9:**1402-1411.

58. **Walter, R. P., J. G. Morris, and D. B. Kell.** 1987. The roles of osmotic stress and water activity in the inhibition of the growth, glycolysis and glucose phosphotransferase system of *Clostridium pasteurianum*. J. Gen. Microbiol. **133:**259-66.

59. **Wang, X., Y. Feng, J. Liu, H. Lee, C. Li, N. Li, and N. Ren.** 2010. Sequestration of CO_2 discharged from anode by algal cathode in microbial carbon capture cells (MCCs). Biosens. Bioelectron. **25:**2639-43.

60. **Wang, X., Y. J. Feng, H. M. Wang, Y. P. Qu, Y. L. Yu, N. Q. Ren, N. Li, E. Wang, H. Lee, and B. E. Logan.** 2009. Bioaugmentation for electricity generation from corn stover biomass using microbial fuel cells. Environ. Sci. Technol. **43:**6088-6093.

61. **Wiegel, J., R. Ranner, and F. A. Rainey.** 2006. An introduction to the family Clostridiaceae, p. 654-678. *In* M. Dworkin (ed.), The Prokaryotes, 3rd ed, vol. 4.

62. **Yazdani, S. S., and R. Gonzalez.** 2007. Anaerobic fermentation of glycerol: a path to economic viability for the biofuels industry. Curr. Opin. Biotechnol. **18:**213-9.

63. **Yomano, L. P., S. W. York, and L. O. Ingram.** 1998. Isolation and characterization of ethanol-tolerant mutants of *Escherichia coli* KO11 for fuel ethanol production. J. Ind. Microbiol. Biotechnol. **20:**132-8.

64. **Zhu, L., H. Chen, L. Huang, J. Cai, and Z. Xu.** 2011. Electrochemical analysis of *Clostridium propionicum* and its acrylic acid production in microbial fuel cells. Eng. Life Sci. **11:**238–244.

Chapter 5.
Conclusions and future directions.

CONCLUSIONS

The research presented in this dissertation sought to expand the range of applications of BESs by identifying customizable consortia of bacteria that could cooperate to degrade sustainable substrates (e.g. corn stover and glycerol), producing value-added chemicals such as ethanol and 1,3-propanediol, in addition to H_2 and electricity in MECs and MFCs, respectively. Consortia of bacteria routinely perform better than monocultures in BESs (9). However, inocula from sediments or wastewater, for example, contain mixed species and often result in electroactive communities that are highly variable in species composition and diversity, and even include members which do not contribute to the electrochemical performance of the system (2). This often leads to variability in performance for BESs operated under identical conditions, thereby complicating experimental reproduction, predictability and manipulation. By contrast, defined consortia enable independent studies of the metabolism of each organism as well as in the coculture. Furthermore, the consortium partners can be studied at the genomic and transcriptional level and metabolic traits of interest can be customized through genetic engineering or adaptive evolution.

FUTURE DIRECTIONS

The study of *G. sulfurreducens* metabolism in Chapter 2 led to a better understanding of the range of electron donors that *G. sulfurreducens* can use for growth as an anode biofilm and current production. The ability of this exoelectrogen to use lactate as an electron donor in a BES was simultaneously reported by us (14) and one other group (4). Our work also demonstrated that lactate is a poor carbon source for *G. sulfurreducens* anode biofilms unless a preferred source of carbon such as acetate is provided. This information is important because lactate is commonly used as an electron donor and carbon source to enrich for anode biofilms; however, our studies provide the tools to design enrichment protocols that could maximize the enrichment of *Geobacter* spp. and the growth of robust electroactive biofilms. Contrary to previous reports (3), we found that formate could be used by *G. sulfurreducens* as both a carbon and electron source, although its assimilation was improved in the presence of acetate. These results together suggest that *G. sulffureducens* may grow best when provided with a combination of substrates, making it an ideal partner organism for coculturing with fermentative bacteria that produce a mixture of these fermentative products. The research presented here focused only on combinations of two electron donors at a time with acetate being one of the substrates. More research therefore is needed to investigate the combination of the three electron donors (lactate, acetate and formate) needed for optimal *Geobacter* biofilm growth and current production in a MEC. This will also suggest avenues for strain improvements in the fermentative partner organism to tailor the fermentative product yields to the optimal needs of the *G. sulfurreducens.* Additionally, the experiments presented here were run over a short duration with either

one or two batch cycles. Future experiments should examine the ability of the different electron donors to sustain the activity of the *G. sulfurreducens* biofilms for prolonged periods of time.

Research on the electron donors of *G. sulfurreducens* was performed in MECs with a relatively high set anode potential (0.24 V vs. Ag/AgCl). The higher the difference between the redox potential of the substrate and the anode potential, the more energy can theoretically be gained by the bacteria; however, maximizing the MEC voltage requires keeping the anode potential as low as possible (11). This tradeoff between optimal bacterial metabolism and optimal MEC voltage should be further investigated in the context of these different electron donors, as each has a different redox potential. It is possible that altering the potential of the anode electrode can improve the utilization of each substrate as an electron donor, and this effect should be studied when each substrate is provided alone and in combination. The effect of these electron donors on *G. sulfurreducens* electricity production needs to be tested in a MFC, where the potential of the anode electrode is determined by the relative percentages of reducing equivalents ($NADH/NAD^+$ or other redox molecules) in the cell rather than a potentiostat, as in an MEC (10).

In Chapter 3, I described a MEC platform in which ethanol and H_2 could be simultaneously produced from corn stover, an agricultural waste product. *C. uda* was identified from among a variety of cellulolytic organisms to be a good partner organism for *G. sulfurreducens* due to its high ethanol yields and the composition of other fermentative products. In addition to acetate, formate and lactate, some low levels of succinate were produced, which were partially used by the *G. sulfurreducens* biofilm.

More research is therefore warranted to investigate the metabolism of succinate in *G. sulfurreducens* and the effect of its assimilation on the growth and electroactivity of the anode biofilms, following a similar approach to that described in Chapter 2.

Corn stover is an attractive feedstock for ethanol production due to its wide availability. However, it is unable to provide enough biomass to supply the future targets for cellulosic ethanol production. The AFEX-pretreatment process has also been optimized for other biomass feedstocks, including dedicated bioenergy crops such as switchgrass (1) and woody biomass such as Black Locust (6). Thus, it would be interesting to investigate the suitability of *C. uda* for consolidated bioprocessing of these feedstocks to ethanol. Further improvement of AFEX-CS hydrolysis by *C. uda* also warrants investigation. Approaches include developing improved strains that process high solid loadings with improved efficiencies. Current research in the Reguera lab suggests that improvements in ethanol titers can be obtained through optimization of culturing parameters such as temperature, agitation, substrate loadings, and the addition of yeast extract (Jenna M. Young, personal communication). Additional improvements may also be gained through genetic engineering or adaptive evolution. Adaptive evolution has been successfully used to develop a strain of *C. uda* with improved ethanol tolerance and fermentative metabolism and ongoing genome sequencing will provide the tools for further improvement via genetic engineering (Jenna M. Young, personal communication). The adaptively-evolved strain of *C. uda* provides an ideal genetic background to develop genetically engineered strains that express more and improved biomass-degrading enzymes and have higher ethanol titers through the elimination of competing metabolic pathways such as acetate and lactate (13).

Additional improvements in the energy recovery of the platform could be garnered through improvements in MEC operation. I used a relatively high anode potential, thus increasing the energy inputs to the system and reducing energy recoveries. However, varying the applied voltage of the system and monitoring the current response could provide information about the internal resistance of the system and the overpotentials present at both electrodes. This information could, in turn, be used to determine the minimum applied voltage needed for H_2 evolution at the cathode as well as the optimal voltage required for maximum H_2 recovery (10). In previous experiments the minimum voltage needed for H_2 production was 0.23 V and the optimal for H_2 production was 0.5 V (5), suggesting that we could decrease our applied voltage without seeing a drop in performance. The use of a catalyst at the cathode my also greatly improve the H_2 production and decrease the voltage input needed (8).

In Chapter 4, I described a platform for treatment of glycerol-rich wastewaters from the biodiesel industry coupled with the production of ethanol and H_2 in a MEC. The ethanol produced could theoretically be used in the biodiesel production process as one of the chemical reactants for the transesterification reaction with the triglyceride feedstocks, providing further economic benefit to the biodiesel producers. Glycerol consumption by *C. cellobioparum* was significantly improved by adaptively evolving the strain for increased glycerol tolerance and through optimization of the culturing conditions in the MEC. *G. sulfurreducens* was also adaptively evolved for increased alcohol tolerance (ethanol and glycerol) which allowed for the removal of the

fermentative byproducts produced by *C. cellobioparum* when they were cocultured at 10% (w/v) glycerol loadings. As described above for *C. uda*, the genomes of the adapted and wild-type strains of *C. cellobioparum* are being sequenced, and this information could be used to genetically manipulate this organism for improved ethanol production from glycerol. Comparison of sequenced genomes of the wild-type and adapted strains will also provide insight into the genetic basis of alcohol and glycerol tolerance of the organisms.

Interestingly, coculturing *C. cellobioparum* and *G. sulfurreducens* in MECs and MFCs, resulted in the production of 1,3-propanediol in addition to ethanol. As 1,3-propanediol was not considered an energy output of the system, energy recoveries were diminished. However, 1,3-propanediol is a valuable precursor for renewable plastics (7, 12), and is therefore of great interest for further study due to the possibility of genetically engineering *C. cellobioparum* for the production of 1,3-propanediol exclusively. The nature of the interaction between the *G. sulfurreducens* and *C. cellobioparum* strains that led to the production of 1,3-propanediol is presently unknown but it appears to only be produced by the coculture of the alcohol-adapted strain in the BECs, and not when grown in batch coculture. The basis for this effect could be determined by transcriptome sequencing of the *C. cellobioparum* strain when grown in monocultures compared to growth in BECs with *G. sulfurreducens.*

Ultimately, the value of this platform for the biodiesel industry will be in the treatment of real biodiesel waste streams containing crude glycerol and impurities such as residual alcohol, soaps, salts, and free fatty acids. The ability of *C. cellobioparum* and *G. sulfurreducens* to tolerate these conditions and maintain high rates of ethanol

and current production, respectively, must be evaluated. The potential economic value of the platform for the biodiesel industry should also be evaluated through a life cycle analysis. Avenues for cost decreases should also be investigated. For example, the rich media used in this study is not economically scalable. Some promising results from our lab show that *C. cellobioparum* can be adaptively evolved to grow in minimal media with small amounts of yeast extract supplementation (0.05%) and 10% glycerol loadings (Jenna M. Young, personal communication). These strains should be investigated further and tested in the BESs.

Results from Chapter 4 also indicated that *G. sulfurreducens* biofilms in the anode electrode could not keep up with the vast product formation of *C. cellobioparum*. This was likely due to the accumulation of products that lowered the pH, making current production no longer thermodynamically favorable, but also due to limitations in the MEC system itself such as low electrode surface area and high internal resistances. Scaling up the MECs and MFCs will be required for any additional platform improvements and will provide vital information for economic and life cycle analyses. Preliminary results comparing both platforms suggest that the MECs were more energy efficient despite the additional voltage input from a potentiostat. However, determining which platform would be optimal for implementation as part of the biodiesel production process is a topic for future investigation following scaled-up BES experiments.

REFERENCES

REFERENCES

1. **Bals, B., C. Rogers, M. J. Jin, V. Balan, and B. Dale.** 2010. Evaluation of ammonia fibre expansion (AFEX) pretreatment for enzymatic hydrolysis of switchgrass harvested in different seasons and locations. Biotechnol. Biofuels **3:**1-11.

2. **Borole, A. P., G. Reguera, B. Ringeisen, Z.-W. Wang, Y. Feng, and B. H. Kim.** 2011. Electroactive biofilms: Current status and future research needs. Energy Environ. Sci. **4**:4813-4834

3. **Caccavo, F., Jr., D. J. Lonergan, D. R. Lovley, M. Davis, J. F. Stolz, and M. J. McInerney.** 1994. *Geobacter sulfurreducens* sp. nov., a hydrogen- and acetate-oxidizing dissimilatory metal-reducing microorganism. Appl. Environ. Microbiol. **60:**3752-9.

4. **Call, D. F., and B. E. Logan.** 2011. Lactate oxidation coupled to iron or electrode reduction by *Geobacter sulfurreducens* PCA. Appl. Environ. Microbiol. **77:**8791-8794.

5. **Ditzig, J., H. Liu, and B. E. Logan.** 2007. Production of hydrogen from domestic wastewater using a bioelectrochemically assisted microbial reactor (BEAMR). Int. J. Hydrogen Energy **32:**2296-2304.

6. **Garlock, R. J., Y. S. Wong, V. Balan, and B. E. Dale.** 2012. AFEX pretreatment and enzymatic conversion of Black Locust (*Robinia pseudoacacia* L.) to soluble sugars. Bioenergy Res. **5:**306-318.

7. **Gonzalez-Pajuelo, M., I. Meynial-Salles, F. Mendes, P. Soucaille, and I. Vasconcelos.** 2006. Microbial conversion of glycerol to 1,3-propanediol: physiological comparison of a natural producer, *Clostridium butyricum* VPI 3266, and an engineered strain, *Clostridium acetobutylicum* DG1(pSPD5). Appl. Environ. Microbiol. **72:**96-101.

8. **Liu, H., S. Grot, and B. E. Logan.** 2005. Electrochemically assisted microbial production of hydrogen from acetate. Environ. Sci. Technol. **39:**4317-4320.

9. **Logan, B. E.** 2009. Exoelectrogenic bacteria that power microbial fuel cells. Nat. Rev. Microbiol. **7:**375-381.

10. **Logan, B. E.** 2008. Microbial fuel cells. Wiley-Interscience, Hoboken, N.J.

11. **Logan, B. E., B. Hamelers, R. Rozendal, U. Schroder, J. Keller, S. Freguia, P. Aelterman, W. Verstraete, and K. Rabaey.** 2006. Microbial fuel cells: methodology and technology. Environ. Sci. Technol. **40:**5181-92.

12. **Saxena, R. K., P. Anand, S. Saran, and J. Isar.** 2009. Microbial production of 1,3-propanediol: Recent developments and emerging opportunities. Biotechnol. Adv. **27:**895-913.

13. **Shaw, A. J., K. K. Podkaminer, S. G. Desai, J. S. Bardsley, S. R. Rogers, P. G. Thorne, D. A. Hogsett, and L. R. Lynd.** 2008. Metabolic engineering of a thermophilic bacterium to produce ethanol at high yield. Proc. Natl. Acad. Sci. USA **105:**13769-13774.

14. **Speers, A. M., and G. Reguera.** 2012. Electron donors supporting growth and electroactivity of *Geobacter sulfurreducens* anode biofilms. Appl. Environ. Microbiol. **78:**437-44.

APPENDIX

Appendix A.
Syntrophic growth of *Anabaena variabilis* and *Geobacter sulfurreducens* in light-driven microbial electrolysis cells.

The material presented in this appendix was generated in collaboration with Kwi S. Kim.

Introduction

The direct photobiological production of H_2 has the potential to provide an environmentally sustainable, renewable energy source that does not contribute to greenhouse gas emissions (6). It has been estimated that if 10% solar energy conversion efficiency is achieved, enough H_2 could be produced in an area of approximately 70x70 miles to power the entire U.S. fleet of cars and light trucks (18). There are, however, challenges associated with the use of H_2 as a transportation fuel including a low volumetric energy density, and the need to manufacture storage tanks that are impermeable to H_2 (6, 7). Additionally, conversion of H_2 into electricity in traditional H_2 fuel cells is not possible unless the H_2 is purified from the O_2 that is co-produced during photosynthesis. The direct conversion of photosynthetic H_2 into electricity in microbial fuel cells (MFCs) by *Geobacter sulfurreducens*, which can use H_2 as an electron donor with approximately 95% efficiency (2), is an attractive alternative because it eliminates the need for H_2 storage, and the anode biofilm can protect the electrode from interactions with O_2 (15).

Filamentous cyanobacteria in the genus *Anabaena* produce H_2 during oxygenic photosynthesis as a byproduct of nitrogen fixation (23). The nitrogenase enzymes are sensitive to O_2 and, for this reason, they are expressed in differentiated, non-vegetative cell compartments, or heterocysts, maintained under microoxic conditions (24). Heterocysts are amenable to genetic manipulation and thus show promise for large-

scale H_2 generation (23). For example, deletion of the uptake hydrogenase operon (*hupSL*) expressed in the heterocysts of *Anabaena variabilis* ATCC 29413 (mutant strain AVM13), resulted in a 3-fold increase in H_2 production compared to the wild-type strain (8). Many species of Cyanobacteria also produce bidirectional *hox* hydrogenases, which are expressed in vegetative cells and may contribute to H_2 evolution (23). Due to the reversibility of this reaction, it is possible that removing the H_2 as it is produced through cocultivation with *G. sulfurreducens* will prevent feedback inhibition and increase the rates of H_2 evolution.

A microbial electrolysis cell (MEC) platform was used for initial investigations into interspecies H_2 transfer between *A. variabilis* AVM13 and *G. sulfurreducens.* A potentiostat was used to set a potential that permitted the formation of *G. sulfurreducens* biofilms on the anode electrode to minimize electron losses to O_2 at the electrode surface. We demonstrated the coupling of H_2 formation and current production in cocultures of *A. variabilis* and *G. sulfurreducens* under anaerobic conditions both in nitrogen-supplemented and nitrogen-limited conditions. Current production by *G. sulfurreducens* ceased under conditions that permitted oxygenic photosynthesis by *A. variabilis*, consistent with the diversion of electrons towards O_2 rather than the electrode by *G. sulfurreducens* as a detoxification mechanism (11). We therefore screened a library of transposon-insertion mutants of *G. sulfurreducens* to identify mutants able to grow in the presence of O_2 yet unable to use it as an electron

acceptor under microaerobic conditions. These mutants show promise for harnessing electrical currents from H_2 produced during oxygenic photosynthesis and for powering MFCs in oxygenic environments.

Materials and Methods

Bacterial strains and culture conditions. Wild-type (WT) *G. sulfurreducens* PCA was routinely cultured at 30°C in anaerobic DB medium (20) with 20 mM acetate and 40 mM fumarate (DB-AF). When indicated, fresh water medium ((3); FW) supplemented with 15 mM acetate and 40 mM fumarate was used (FW-AF). All media were sparged with N_2:CO_2 (80:20), sealed with butyl rubber stoppers, and autoclaved prior to use. *Anabaena variabilis* AVM13 (8) was grown photoautotrophically on solid Allen and Arnon medium ((1); AA) containing nitrate and 1% agar (ATCC 1142; AA+N). Liquid cultures were grown in an 8-fold dilution of AA medium with nitrate ((21); AA/8+N) with shaking at 135 rpm. All cultures were incubated at 30°C and illuminated with fluorescent lights. When indicated, nitrate was eliminated from the media to promote N_2 fixation (AA/8). Alternatively, *A. variabilis* AVM13 was grown under anaerobic conditions in AA/8 medium with 5 mM fructose as a carbon source and 10 μM dichlorophenyldimethylurea (DCMU) to inhibit oxygen evolution from photosystem II (22).

MECs. Dual-chambered, H-type MECs were set up as described previously (20), incubated at 30°C and illuminated with fluorescent lights. 90 ml of DB medium was added to the anode and cathode chambers. The medium in the anode was supplemented with 1 or 3 mM acetate as indicated. The reference electrode was sterilized in 70% ethanol for 1 min before rinsing with sterile water. The anode electrode was poised to 0.24 V with a VSP potentiostat (BioLogic) and the MEC chambers were sparged with filter-sterilized N_2:CO_2 (80:20) gas until the current stabilized. *G.*

sulfurreducens cells were grown in DB-AF medium and harvested as described previously (19) before inoculation into the anode chamber of the MEC. The *G. sulfurreducens* grew as an anode biofilm and produced current until the acetate was depleted. In *G. sulfurreducens* monoculture experiments, filter-sterilized air was periodically injected into the anode chamber. In coculture experiments, the medium in the anode chamber was replaced with fresh DB medium, when acetate was depleted and the current declined. When indicated, 5 mM fructose and 10 μM DCMU were added, and/or the nitrogen source (NH_4Cl) was omitted from the medium. In MECs operated under aerobic conditions the medium was buffered with 25 mM 4-(2-hydroxyethyl)-1-piperazineethanesulfonic acid (HEPES) at pH 7. *A. variabilis* AVM13 was grown to mid-exponential phase in AA/8 with or without nitrate as indicated, and 100 ml of culture was harvested by centrifugation, washed once and resuspended in 10 ml DB medium. The resuspended *A. variabilis* cells were inoculated into the anode chamber of the MEC following the medium exchange, and sparging of the MEC was discontinued to prevent the removal of H_2. *A. variabilis* AVM13 monoculture controls were also inoculated in the same volume of DB medium in tandem with the MECs and incubated under the same conditions (30°C, with stirring and illumination).

The amount of H_2 and O_2 produced by the *A. variabilis* was determined by analysis of the headspace atmosphere of the monocultures and MECs by gas chromatography (GC) using a Varian CP-4900 Micro Gas Chromatograph (Agilent, Santa Clara, CA). The efficiency of the H_2 conversion into current by *G. sulfurreducens*

(coulombic efficiency, CE) was calculated as the coulombs recovered as current divided by the total coulombs available from H_2 (eq. 1).

$$CE = \frac{\int_0^t I\, dt}{2F\, H_2} \qquad (1)$$

The integral of the current (*I*) over the duration of the experiment (*t*) is given in coulombs (A*s). The number 2 represents the number of moles of electrons in 1 mol of H_2, *F* is Faraday's constant, and H_2 represents the moles of H_2 produced by *A. variabilis* AVM13 monocultures over the duration of the experiment as measured by GC.

Confocal laser scanning microscopy (CLSM). At the end of the MEC experiments, the anode electrode biofilms were stained with the BacLight viability kit (Invitrogen, Carlsbad, CA) following the manufacturer's instructions and imaged by CLSM, as previously described (20), using an Olympus FluoView FV1000 inverted microscope equipped with a UPLFLN 10X objective (Olympus, NA 0.30).

Transposon mutagenesis of *G. sulfurreducens* and selection of mutants. WT *G. sulfurreducens* cultures were grown to mid-log phase in NB medium supplemented with 15 mM acetate, 40 mM fumarate, 1 mM cysteine, and 0.1% yeast extract ((5); NBAFCYE). The cells were harvested by centrifugation and washed twice with ice-cold, anaerobic electroporation buffer to make them electrocompetent as previously described (5). Using an Eppendorf 2510 Electroporator operated at 1.47 kV, the *G. sulfurreducens* electrocompetent cells were electroporated with the linear EZ-Tn5 Transposome Complex (Epicentre Biotechnologies) following the manufacturer's

recommendations. The cells were recovered for ~18 h in 10 ml NBAFYE medium at 30°C. Following recovery, 0.2 ml of culture was inoculated into 10 soft-agar tubes pre-warmed to 55°C and containing 10 ml NBAFCYE medium, 0.3% noble agar, 0.1% resazurin, and 50 µg/ml kanamycin (KM^{50}). The tubes were inverted several times to disperse the cells into the agar and were incubated for 72 h at 30°C. The headspace of the tubes was then replaced with filter-sterilized air and the tubes were incubated an additional 48 h at 30°C until colonies were visible. Using a needle and syringe, 11 colonies were aspirated from the oxygenated region of the soft-agar (determined by color change of the resazurin from clear to pink) and transferred into anaerobic FW-AF medium containing KM^{50}. The oxygen tolerant (oxt) strains derived from these colonies were designated oxt1-11.

Identification of transposon-insertion sites via rescue cloning. The site of transposon insertion in the oxt mutants was determined via rescue cloning, as described previously (10). Briefly, genomic DNA was purified using the MasterPure DNA Purification Kit (Epicentre Biotechnologies) according to the manufacturer's specifications. 1 µg genomic DNA was digested overnight with HindIII restriction enzyme (New England Biolabs) and self-ligated using T4 Ligase (Invitrogen), and the resulting plasmids were transformed into chemically-competent *pir+ Escherichia coli.* The transformants were plated on LB agar supplemented with KM^{50}. Colonies were picked and grown in liquid LB with KM^{50} before isolating the plasmid DNA using the Plasmid Mini Kit (Quiagen). Sequencing of the Tn5 flanking regions was carried out using the provided Tn5 reverse sequencing primer (R6KAN-2-RP-1: 5'

CTACCCTGTGGAACACCTACATCT 3') at the Genomics Core of the Research Technology Support Facility (Michigan State University). The sequence of the region flanking the Tn5 insertion was identified using the Basic Local Alignment Search Tool (BLAST) available at http://www.ncbi.nlm.nih.gov/BLAST/Blast.cgi.

Growth with Fe(III) oxides. The WT and oxt strains were grown in FW media containing approximately 125 mM amorphic Fe(III) oxides prepared as described previously (12) and supplemented with 1 mM nitrilotriacetic acid (NTA). Growth was monitored by measuring the HCl-extractable Fe(II) resulting from the reduction of Fe(III) as previously described (13).

Survival in atmospheric oxygen. The ability of the WT and oxt (1-11) strains to tolerate O_2 exposure was determined as previously described (11). Late-exponential phase cultures of WT and oxt strains were grown in NBAFYE media buffered with 20 mM 3-(N-morpholino)propanesulfonic acid (MOPS) at pH 7.0. The strains were inoculated to an initial optical density of 600 nm (OD_{600}) of 0.04 into 50-ml serum bottles containing 25 ml aerobic NBAFYE-MOPS and incubated at 35°C. After 36 h, the cells were diluted to an OD_{600} of 0.02 into triplicate pressure tubes containing 10 ml anaerobic NBAFYE-MOPS medium. The tubes were incubated at 35°C and growth was monitored (OD_{600}) every ca. 6 h. For comparison, anaerobic cultures of the WT and oxt strains (unchallenged with O_2) were grown in anaerobic NBAFYE-MOPS medium at 35°C and growth was monitored as described above.

Growth with O_2 as the sole electron acceptor. The ability of the WT and oxt strains to grow with O_2 as the sole electron acceptor was determined as previously described (11) with the following modifications. The WT and oxt strains were inoculated to an initial OD_{600} of 0.02 into triplicate anaerobic pressure tubes containing 10 ml modified NBAFYE-MOPS. For these experiments, cysteine was omitted from the medium and fumarate was provided in limiting concentrations (20 mM). The tubes were incubated at 35°C and growth (OD_{600}) was monitored until the culture reached stationary phase and fumarate was depleted. Filter-sterilized air (8.5 mL) was added to the headspace of the tubes to provide an O_2 concentration of ca. 10% (v/v), and growth was monitored for an additional ca. 36 h.

Results and Discussion

Anaerobic MECs with WT *G. sulfurreducens* and *A. variabilis* AVM13. I investigated the ability of the binary culture to perform interspecies H_2 transfer to sustain current production in a MEC (Fig. A.1). The experiments were performed under anaerobic conditions and DCMU and fructose were added to prevent O_2 evolution by *A. variabilis* and to act as an alternate carbon source for *A. variabilis,* respectively. The growth of *G. sulfurreducens* was not affected by the presence of DCMU when grown in batch culture in FW-AF medium, and fructose was not used as an electron donor (data not shown). Because H_2 production by *A. variabilis* is coupled to N_2 fixation, MEC experiments were carried out both in the presence of 0.2 g/L NH_4Cl (Fig. A.1A) and in the absence of NH_4Cl (Fig. A.1B), the latter being conditions that require the cells to fix nitrogen in order to support their growth. As *G. sulfurreducens* can also fix N_2, we first monitored current production by *G. sulfurreducens* with 1 mM acetate provided as the electron donor in the medium with the presence or absence of NH_4Cl supplementation. While the NH_4Cl-supplemented MECs reached a maximum current of 0.7 mA (Fig. A.1A), current production was greatly diminished under N_2-fixing conditions, reaching a maximum at 0.1 mA (Fig. A.1B). This growth disadvantage is likely due to the energy intensive nature of nitrogen fixation, which requires 16 molecules of ATP for every 1 molecule of N_2 assimilated (23). Regardless of the availability of exogenous nitrogen in the media, the addition of *A. variabilis* to the MECs once acetate was depleted and

current declined resulted in sustained current production for at least 6 d (Fig. A.1A and B), consistent with the syntrophic growth of *G. sulfurreducens* and *A. variabilis* via interspecies H_2 transfer. The maximum current produced by the coculture (ca. 0.12 mA) was similar in both MECs and was significantly less than the current sustained from acetate as an electron donor. No O_2 was detected in the headspace of the MECs over the duration of the experiments, indicating that the DCMU was effectively preventing photosynthesis, despite the illumination of the MECs with fluorescent lighting.

Monoculture controls of *A. variabilis* were inoculated in media with and without nitrogen supplementation to provide a reference for the amount of H_2 produced by *Anabaena* under both conditions. The nitrogen-fixing monocultures produced 2.5-fold more H_2 (4.7 ± 0.3 mM) than the monocultures provided with NH_4Cl (1.9 ± 0.1 mM), suggesting that the nitrogenase enzymes were contributing significantly to H_2 evolution. However, H_2 was also produced when NH_4Cl was available, consistent with the contribution of alternative hydrogenases, such as the bidirectional *hox* hydrogenases present in the vegetative cells (23), to H_2 production by *A. variabilis.*

The electron recovery of the MECs (coulombic efficiency, CE) was calculated by dividing the total electrons transferred to the MEC circuit by *G. sulfurreducens* by the electrons available in the H_2 produced by the *A. variabilis* monoculture controls. The CE of the N_2-fixing MEC (Fig. A.1B) was 97%, and less than 0.03 mM H_2 was detected in the headspace of the MEC over the duration of the experiment. Thus, most of the H_2

produced by *Anabaena* was recovered as current. The CE of the MEC supplemented with NH_4Cl was 394%, and less than 0.02 mM H_2 was detected in the headspace of the anode chamber over the duration of the experiment. The high electron recovery in the coculture-driven MECs compared to the monoculture controls is consistent with a 4-fold stimulation in H_2 production by *A. variabilis* during syntrophoic growth with *G. sulfurreducens*. These results support the hypothesis that H_2 accumulation in *Anabaena* monocultures feedback inhibits the bidirectional hydrogenases. As H_2 is efficiently removed by *G. sulfurreducens* in the coculture MECs, feedback inhibition is alleviated or prevented and more H_2 is produced by *Anabaena.* Hence, the improved performance observed in the NH_4Cl-supplemented MECs likely reflects the ability of *G. sulfurreducens* to efficiently consume H_2 and prevent feedback inhibition, thus stimulating the production of H_2 by *A. variabilis* during N_2 fixation via interspecies H_2 transfer.

Over the duration of the experiment, the anode supernatant became increasingly clear, and the *Anabaena* cells coated the *Geobacter* biofilms that formed on the anode electrode (Fig. A.1C). The confocal images of biofilm cells stained with the BacLight viability dyes enabled the visualization of *Geobacter* cells with the green SYTO9 dye, whereas the propidium iodide (red) preferentially stained the *Anabaena* cells. While the *Geobacter* biofilms grew in contact with the anode electrode, the *Anabaena* cells formed an outer layer on the anode biofilm maintaining a close association between two

organisms. This intimate association favors interspecies H_2 transfer and may have contributed to the high electron recoveries observed in the coculture MECs.

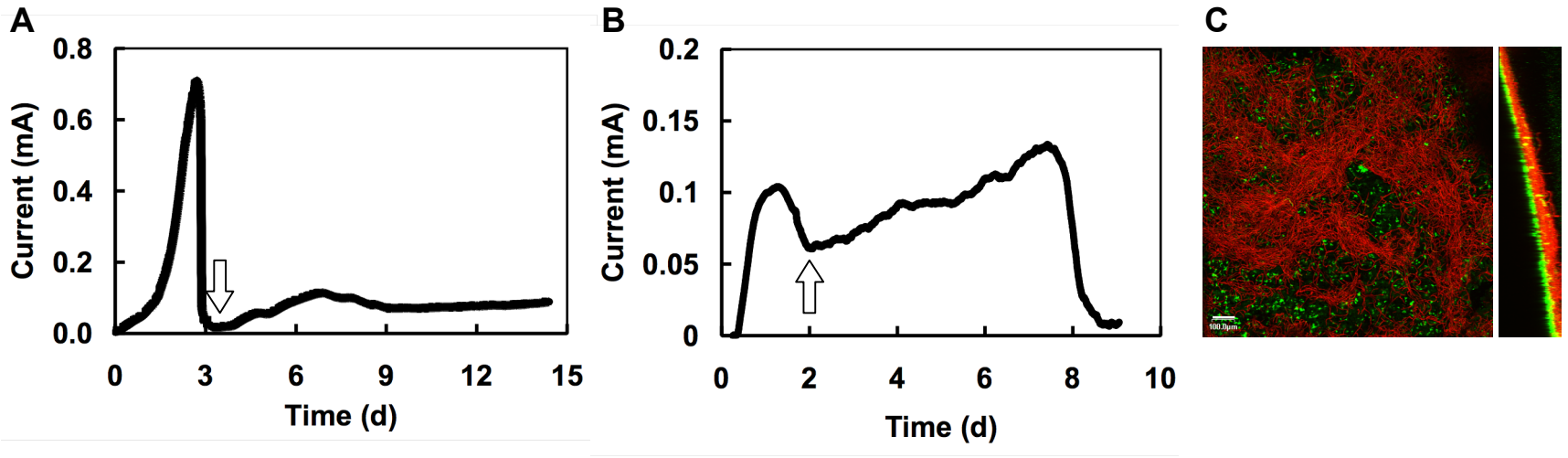

Fig. A.1: Anaerobic MEC cocultures with WT *G. sulfurreducens* and *A. variabilis* AVM13. (A-B) Current production in sequentially-inoculated MECs with nitrogen supplementation (A) and under nitrogen-fixing conditions (B). *G. sulfurreducens* was inoculated first and supplemented with 1 mM acetate, the anode media was then exchanged (arrow) for fresh DB medium containing with 5 mM fructose and 10 μM DCMU and inoculated with *A. variabilis* AVM13. (C) CLSM micrograph projection of anode electrode biofilm and corresponding *y* projection (right). *G. sulfurreducens* cells stained green and *A. variabilis* cells stained red. Scale bar, 100 μm.

The MEC experiment with nitrogen supplementation was repeated in the absence of DCMU to allow *A. variabilis* to carry out oxygenic photosynthesis. For these experiments, we first grew anode biofilms of *G. sulfurreducens* of different thicknesses using 1 mM or 3 mM acetate. Although more current was produced by the thicker biofilms fed with 3 mM acetate, the addition of *A. variabilis* prevented current production in the two MECs (Fig. A.2). This suggests that the O_2 produced during photosynthesis (24 ± 3 mM) was either toxic to the *G. sulfurreducens* biofilm or was used by the *G. sulfurreducens* as an electron acceptor thereby diverting electrons away from the anode electrode, as was found previously for *G. sulfurreducens* grown in batch culture with fumarate (11).

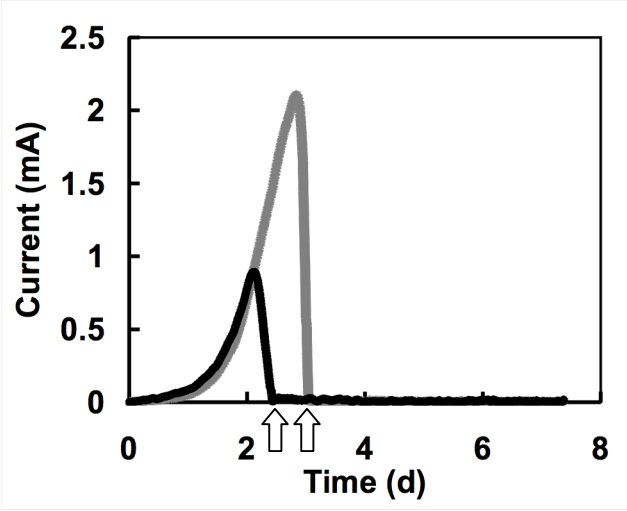

Fig. A.2: Aerobic MEC cocultures with WT *G. sulfurreducens* and *A. variabilis* AVM13 with nitrogen supplementation. *G. sulfurreducens* was inoculated first and supplemented with 1 mM (black line) or 3 mM (gray line) acetate. Once the acetate was depleted and current declined, the anode media was replaced (arrows) with fresh DB medium containing NH_4Cl and inoculated with *A. variabilis* AVM13.

Isolation of transposon-insertion mutants under oxygenated conditions. Because WT *G. sulfurreducens* was unable to produce current in aerobic MECs with *A. variabilis*, oxygen-tolerant (oxt) mutants of *G. sulfurreducens* were identified in a screening of a mutant library generated via Tn5 transposon mutagenesis. For this screening, the electrocompetent cells that were transformed with the Tn5 construct were recovered overnight and then transferred to oxygenated soft agar medium, which selected for the growth of oxygen-tolerant clones as isolated colonies (Fig. A.3A). The site of the transposon insertion was identified for 11 mutants (oxt1-11) by rescue cloning of the Tn5 insert and sequencing of the transposon flanking region (Table A.1). Surprisingly, the oxt1 mutant carried the Tn5 insertion in the gene encoding the cytochrome c551 peroxidase gene, which has previously been implicated in protecting *G. sulfurreducens* from oxidative damage by reducing hydrogen peroxide to water (9). Annotation of the genome of *G. sulfurreducens* identified many genes that are predicted to encode for proteins involved in oxidative stress responses such as rubredoxin-oxygen oxidoreductase, flavodoxins, catalase, superoxide dismutase and peroxidases (14), it is therefore likely that there is redundancy in the cell response for oxygen tolerance and feedback mechanisms to regulate the expression of some of the components in response to specific sources of oxidative stress (i.e., O_2 versus H_2O_2). Another mutant (oxt2) carried the Tn5 insertion in the Glutamyl-tRNA reductase gene, which is responsible for catalyzing the initial step of tetrapyrrole biosynthesis including porphyrins such as heme (17), suggesting a shift in heme synthesis pathways or reduction of heme synthesis for O_2 tolerance. Mutant oxt7 had the insertion in a cytochrome *c* family protein, which could function in a number of different electron

transfer reactions in the cell. The oxt10 mutant had the Tn5 insertion in the putative C subunit of the SbcCD nuclease. In *E. coli* the SbcCD nuclease cleaves DNA hairpins, which can inhibit DNA replication (4). The oxt9 mutant had the Tn5 insertion in the glycine cleavage system H protein, which is responsible for glycine degradation (16). The remaining mutants had the Tn5 insertion in hypothetical or conserved hypothetical proteins. Further characterization of the interrupted genes is warranted.

Table A.1: Tn5 transposon-insertion mutants isolated under oxygenated conditions.

Mutant	GSU locus [a]	Annotation [b]	Coordinate [c]
oxt1	0466	Cytochrome c551 peroxidase (ccpA-1)	496353-496354
oxt2	3284	Glutamyl-tRNA reductase (hemA)	3603990-3603991
oxt3	2093	ABC transporter, ATP-binding protein	2300780-2300781
oxt4	1572	ribD domain protein	1725150-1725151
oxt5	0710	Hypothetical protein	759621-759622
oxt6	3173	Conserved hypothetical protein	3482511-3482512
oxt7	2912	Cytochrome *c* family protein	3206886-3206887
oxt8	2224	Response regulator	2439568-2439569
oxt9	0376	Glycine cleavage system H protein (gcvH-1)	410932-410933
oxt10	1725	Nuclease SbcCD, C subunit, putative	1889544-1889545
oxt11	3289	Conserved hypothetical protein	3608610-3608611

[a] GSU locus containing the transposon insertion.

[b] Annotation assigned by the Comprehensive Microbial Resources available through the J. Craig Venter Institute (http://cmr.jcvi.org/).

[c] Genomic coordinate for the transposon insertion.

Survival in atmospheric oxygen and growth with O_2 as the sole electron acceptor. Previous experiments with WT *G. sulfurreducens* (11) showed that they were able to survive O_2 exposure for up to 24 h. I repeated their experiment with the WT and oxt strains, challenging the cells in oxygenated media for 36 h before transferring the cells to anaerobic medium and monitoring their growth (Fig. A.3B). Cells that were not exposed to O_2 were also grown as a control (Fig. A.3B). The growth rates of the unchallenged cultures were very similar for the WT and all of the oxt mutants (5.9 ± 0.2 d^{-1}). All the strains survived a 36 h challenge with O_2 and were able to grow when transferred to anaerobic medium. Surprisingly, during the 36 h oxygen challenge, the WT strain grew in the oxygenated medium to an OD_{600} of 0.7 while the oxt strains did not grow above OD_{600} ~0.02. This suggested that the WT strain was either more tolerant to the O_2 than the oxt strains and/or able to use the O_2 as an electron acceptor. Consistent with an increased tolerance, the growth of WT in the anaerobic recovery tubes was faster (6.4 ± 0.1 d^{-1}) than the average growth rate of the oxt strains (5.9 ± 0.3 d^{-1}), and the WT grew to a higher OD_{600} (1.23 ± 0.02) than the oxt strains (1.02 ± 0.03) (Fig. A.3B).

Genome annotation of *G. sulfurreducens* revealed a gene encoding cytochrome *c* oxidase, which is responsible for consuming O_2 as a terminal electron acceptor (14). Later experiments (11) demonstrated the ability of *G. sulfurreducens* to couple growth with O_2 reduction as the sole electron acceptor under microaerophilic conditions (i.e.

10% O_2). I repeated this experiment to determine if the oxt strains could reduce O_2 as an electron acceptor. The WT and oxt strains were grown with limiting fumarate until the fumarate was depleted and growth stopped (an average OD_{600} of 0.53 ± 0.03). 10% O_2 was then introduced into the headspace of the tubes and additional growth was monitored (Fig. A.3C). The WT strain was the only culture that was able to grow with O_2 as sole electron acceptor as indicated by the additional growth of the culture to an OD_{600} of 0.68 ± 0.01, while the oxt strains did not grow above an average OD_{600} of 0.57, indicating that the oxt strains cannot divert electrons to O_2. The inability of the oxt strains to use O_2 as an electron acceptor has advantages for use in aerobic MECs with *Anabaena* because the electrons will not be diverted away from the anode electrode.

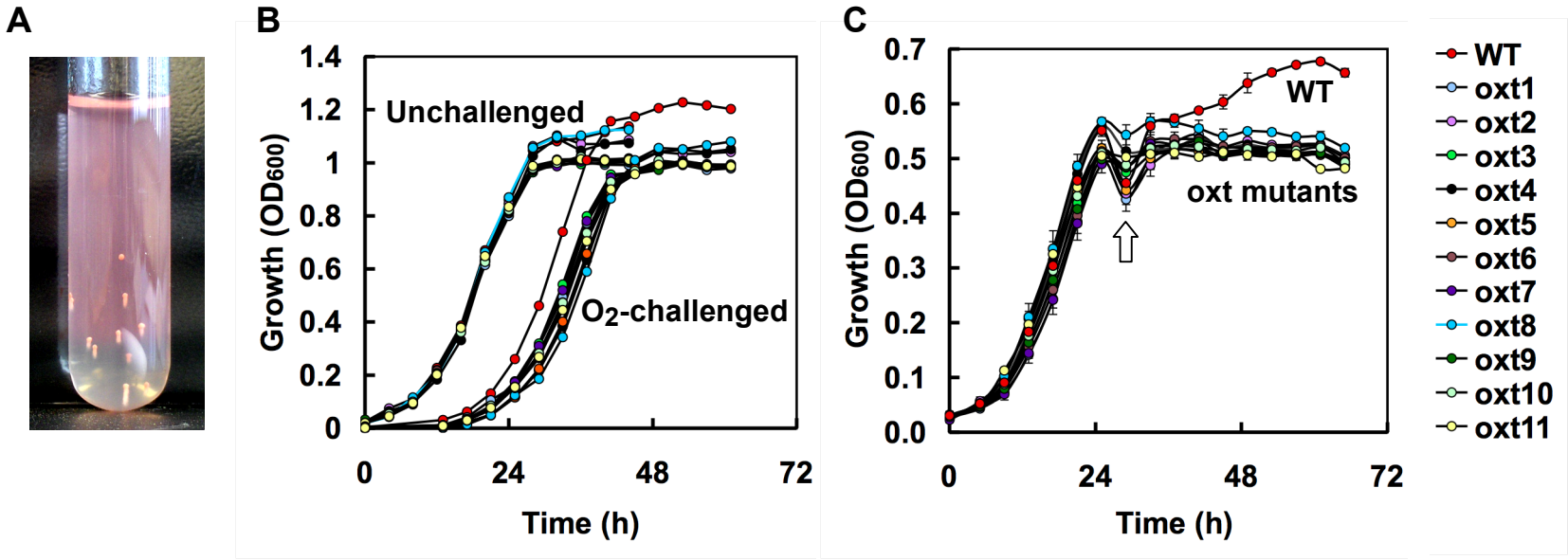

Fig. A.3: Selection and characterization of oxt mutants in oxygenated conditions. (A) Recovery of colonies of Tn5 mutants in tubes with soft agar containing KM^{50} and resazurin, and exposed to air from the headspace of the tube. Mutant colonies were selected from the oxygenated region of the agar as indicated by the color change of resazurin from clear to pink. (B) Growth of WT and oxt strains of *G. sulfurreducens* in anaerobic medium following 0 h (Unchallenged) or 36 h of oxygen exposure (O_2-challenged). (C) Growth of WT and oxt strains in media with limiting fumarate as the electron acceptor. When fumarate was depleted, 10% O_2 was added to the headspace of the culture tubes (arrow). Further growth of the WT strain resulted from the use of O_2 as an electron acceptor.

Growth with insoluble Fe(III) oxides. In order for the oxt mutants to grow and produce current in MECs, they must be able to reduce extracellular insoluble electron acceptors. We therefore tested the strains for growth on Fe(III) oxides. 1 mM NTA was added to the cultures during the first transfer into Fe(III) oxide medium to promote growth. Oxt2, oxt5 and oxt7 did not grow on Fe(III) oxides with 1 mM NTA, and oxt1, oxt4 and oxt8 did not grow in subsequent transfers in which NTA was omitted. Oxt3, oxt6, oxt9, oxt10 and oxt11 all grew well in Fe(III) oxide medium during several transfers without NTA supplementation. After 4 transfers, oxt10 reduced Fe(III) faster (1.4 mM/d) than WT (1.0 mM/d), and was therefore chosen for further investigations in MECs.

Oxt10 in aerobic MECs. MECs were set up as described previously with 1 mM acetate provided as the electron donor and inoculated with *G.sulfurreducens* WT or oxt10 strains. The initial rate of current production in the anaerobic MECs was 1.9-fold higher for oxt10 (0.045 mA/hr) compared with WT (0.024 mA/hr), consistent with its robust growth with Fe(III) oxides. The current production increased as the cells grew on the anode electrode. At approximately 0.7 mA of current production, 20 ml of filter-sterilized air was injected into the anode headspace. The current immediately decreased in both MECs as a result of the O_2 exposure, and the rate of current decrease was calculated. The current production by oxt10 decreased at a slower rate (0.12 mA/h) compared with WT (0.24 mA/h) over a period of ca. 3 h, suggesting that oxt10 dissipated its electrons to O_2 less readily than WT. Following the 3 h exposure to O_2, the anode headspace was sparged with N_2:CO_2 to remove the O_2. The time it took for the current to return to original levels was longer for WT (ca. 10 h) than for oxt10 (ca.

2 h). While current production by oxt10 was negatively affected by the presence of O_2, it was not as sensitive to the O_2 intrusion as the WT strain.

The oxt10 strain was then tested in MECs in coculture with *A. variabilis* AVM13 under aerobic, nitrogen-fixing conditions. Oxt10 was pre-grown with 1 mM and 3 mM acetate until the acetate was depleted and current had declined. The media was exchanged for fresh HEPES-buffered DB medium (NH_4Cl was omitted) and *A. variabilis* was inoculated into the anode chamber. However, current production by the oxt10 mutant did not resume under these conditions, presumably because the amount of O_2 produced by *Anabaena* was ca. 2.5-fold greater than atmospheric O_2 concentrations.

While the oxt10 mutant was shown to perform better than WT in microaerobic MECs, it is clear that further strain improvements of *G. sulfurreducens* are necessary for successful interspecies H_2 transfer with *A. variabilis* in aerobic MECs. One possible strain improvement would be the targeted mutation of the cytochrome *c* oxidase gene in the oxt10 background to prevent the use of O_2 as an electron acceptor. Another improvement would be adaptive evolution of the oxt10 strain for additional O_2 tolerance. Alternatively, the O_2 production by *A. variabilis* could be decreased by controlling the amount of illumination of the MECs thereby decreasing the rate of photosynthesis.

REFERENCES

REFERENCES

1. **Allen, M. B., and D. I. Arnon.** 1955. Studies on nitrogen-fixing blue-green algae: Growth and nitrogen fixation by *Anabaena Cylindrica* Lemm. Plant Physiol. **30:**366-72.

2. **Bond, D. R., and D. R. Lovley.** 2003. Electricity production by *Geobacter sulfurreducens* attached to electrodes. Appl. Environ. Microbiol. **69:**1548-55.

3. **Cologgi, D. L., S. Lampa-Pastirk, A. M. Speers, S. D. Kelly, and G. Reguera.** 2011. Extracellular reduction of uranium via *Geobacter* conductive pili as a protective cellular mechanism. Proc. Natl. Acad. Sci. USA **108:**15248-52.

4. **Connelly, J. C., L. A. Kirkham, and D. R. F. Leach.** 1998. The SbcCD nuclease of *Escherichia coli* is a structural maintenance of chromosomes (SMC) family protein that cleaves hairpin DNA. Proc. Natl. Acad. Sci. USA **95:**7969-7974.

5. **Coppi, M. V., C. Leang, S. J. Sandler, and D. R. Lovley.** 2001. Development of a genetic system for *Geobacter sulfurreducens*. Appl. Environ. Microbiol. **67:**3180-7.

6. **Edwards, P. P., V. L. Kuznetsov, and W. I. David.** 2007. Hydrogen energy. Philos. Transact. A Math Phys. Eng. Sci. **365:**1043-56.

7. **Hallenbeck, P. C.** 2012. Hydrogen production by cyanobacteria, p. 15-28. *In* P. C. Hallenbeck (ed.), Microbial Technologies in Advanced Biofuels Production. Springer, New York.

8. **Happe, T., K. Schutz, and H. Bohme.** 2000. Transcriptional and mutational analysis of the uptake hydrogenase of the filamentous cyanobacterium *Anabaena variabilis* ATCC 29413. J. Bacteriol. **182:**1624-31.

9. **Hoffmann, M., J. Seidel, and O. Einsle.** 2009. CcpA from *Geobacter sulfurreducens* is a basic di-heme cytochrome *c* peroxidase. J. Mol. Biol. **393:**951-965.

10. **Kirby, J. R.** 2007. In vivo mutagenesis using EZ-*Tn5*. Methods Enzymol. **421:**17-21.

11. **Lin, W. C., M. V. Coppi, and D. R. Lovley.** 2004. *Geobacter sulfurreducens* can grow with oxygen as a terminal electron acceptor. Appl. Environ. Microbiol. **70:**2525-8.

12. **Lovley, D. R., and E. J. Phillips.** 1986. Organic matter mineralization with reduction of ferric iron in anaerobic sediments. Appl. Environ. Microbiol. **51:**683-689.

13. **Lovley, D. R., and E. J. Phillips.** 1987. Rapid assay for microbially reducible ferric iron in aquatic sediments. Appl. Environ. Microbiol. **53:**1536-1540.

14. **Methé, B. A., K. E. Nelson, J. A. Eisen, I. T. Paulsen, W. Nelson, J. F. Heidelberg, D. Wu, M. Wu, N. Ward, M. J. Beanan, R. J. Dodson, R. Madupu, L. M. Brinkac, S. C. Daugherty, R. T. DeBoy, A. S. Durkin, M. Gwinn, J. F. Kolonay, S. A. Sullivan, D. H. Haft, J. Selengut, T. M. Davidsen, N. Zafar, O. White, B. Tran, C. Romero, H. A. Forberger, J. Weidman, H. Khouri, T. V. Feldblyum, T. R. Utterback, S. E. Van Aken, D. R. Lovley, and C. M. Fraser.** 2003. Genome of *Geobacter sulfurreducens*: metal reduction in subsurface environments. Science **302:**1967-1969.

15. **Nevin, K. P., P. Zhang, A. E. Franks, T. L. Woodard, and D. R. Lovley.** 2011. Anaerobes unleashed: Aerobic fuel cells of *Geobacter sulfurreducens*. J. Power Sources **196:**7514-7518.

16. **Okamura-Ikeda, K., Y. Ohmura, K. Fujiwara, and Y. Motokawa.** 1993. Cloning and nucleotide sequence of the gcv operon encoding the *Escherichia coli* glycine-cleavage system. Eur. J. Biochem. **216:**539-548.

17. **Schauer, S., C. Lüer, and J. R. Moser.** 2003. Large scale production of biologically active *Escherichia coli* glutamyl-tRNA reductase from inclusion bodies. Protein Expres. Purif. **31:**271-275.

18. **Seibert, M., P. W. King, M. C. Posewitz, A. Melis, and M. L. Ghirardi.** 2008. Photosynthetic water-splitting for hydrogen production, p. 273-291. *In* J. Wall (ed.), Bioenergy. ASM Press, Washington, D.C.

19. **Speers, A. M., and G. Reguera.** 2012. Consolidated bioprocessing of AFEX-pretreated corn stover to ethanol and hydrogen in a microbial electrolysis cell. Environ. Sci. Technol. **46:**7875–7881.

20. **Speers, A. M., and G. Reguera.** 2012. Electron donors supporting growth and electroactivity of *Geobacter sulfurreducens* anode biofilms. Appl. Environ. Microbiol. **78:**437-44.

21. **Thiel, T.** 1993. Characterization of genes for an alternative nitrogenase in the cyanobacterium *Anabaena variabilis*. J. Bacteriol. **175:**6276-86.

22. **Thiel, T., and B. Pratte.** 2001. Effect on heterocyst differentiation of nitrogen fixation in vegetative cells of the cyanobacterium *Anabaena variabilis* ATCC 29413. J. Bacteriol. **183:**280-6.

23. **Tsygankov, A. A.** 2007. Nitrogen-fixing cyanobacteria: A review. Appl. Biochem. Microbiol. **43:**250-259.

24. **Wolk, C. P., A. Ernst, J. Elhai, and D. A. Bryant.** 1994. Heterocyst metabolism and development, p. 769-823. *In* D. A. Bryant (ed.), The Molecular Biology of Cyanobacteria, vol. 1. Springer, Netherlands, Kluwer Academic Publishers.